United States
Environmental Protection
Agency

Great Lakes
National Program Office
77 West Jackson Boulevard
Chicago, Illinois 60604

EPA 905-R-95-007
April 1995

EPA

# Assessment and Remediation of Contaminated Sediments (ARCS) Program

## Application of Mass Balance Modeling To Assess Remediation Options For the Buffalo River

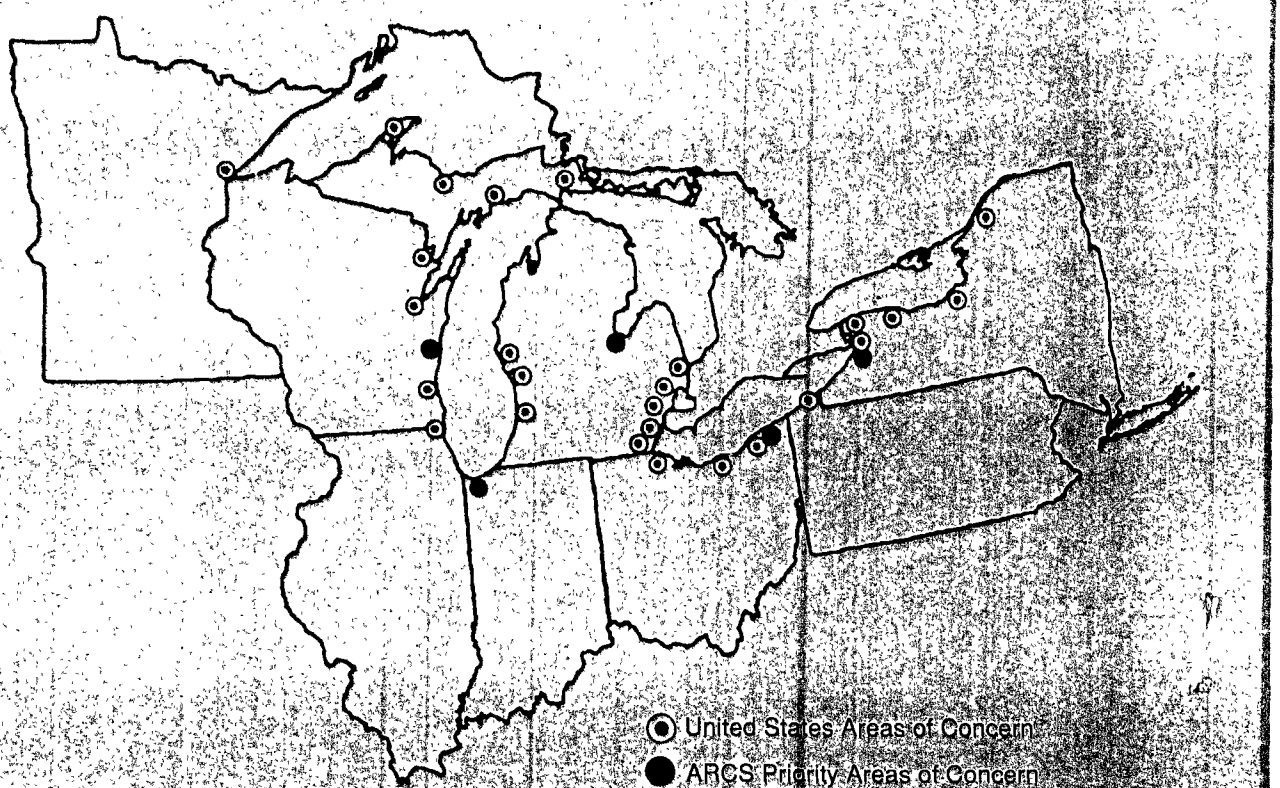

# APPLICATION OF MASS BALANCE MODELING TO ASSESS REMEDIATION OPTIONS FOR THE BUFFALO RIVER

by

Joseph V. DePinto, Michael Morgante, Joseph Zaraszczak,
Tricia Bajak and Joseph F. Atkinson

Great Lakes Program
Department of Civil Engineering
State University of New York at Buffalo
Buffalo, New York 14260

Grant No. X995915-01-0
Project Officer
Marc L. Tuchman
Great Lakes National Program Office
United States Environmental Protection Agency
Chicago, Illinois 60604

## DISCLAIMER

The information in this document has been funded wholly or in part by the United States Environmental Protection Agency under Grant No. X995915-01-0 to the University at Buffalo. It has been subject to the Agency's peer and administrative review, and it has been approved for publications as an EPA document. Mention of trade names or commercial products does not constitute endorsement or recommendation for use by the U.S. Environmental Protection Agency.

## ACKNOWLEDGEMENTS

The authors would like to thank all members of the ARCS/RAM work group for their ongoing peer review during the course of this project and for their review of this report. We would especially like to thank the ARCS/RAM work group chair, Marc L Tuchman, Environmental Scientist, EPA Great Lakes National Program Office, for his assistance and patience in the completion of this work.

Of course, this work would not have been possible without the efforts of all those individuals who collected and analyzed water and sediment samples from the Buffalo River, including Harrish Sikka, Jill Singer, and Kim Irvine from Buffalo State College and scientists from the EPA, Large Lakes and Rivers Research Branch, ERL-Duluth, Grosse Ile, Michigan. Special thanks to Mark Velleux (ASCI), Joe Gailani (CSC), and John Connolly (HydroQual, Inc.) for consultation on various aspects of this study. Finally, we would like to acknowledge the assistance of Scott Rybarczyk, Great Lakes Prgram student assistant, in the preparation of this manuscript.

## TABLE OF CONTENTS

## LIST OF FIGURES

## LIST OF TABLES

## SUMMARY

The Buffalo River (Buffalo, New York) is one of 43 Great Lakes Areas of Concern identified by the International Joint Commission. It was also chosen for study under EPA's Assessment and Remediation of Contaminated Sediments (ARCS) program. As part of the ARCS studies in the Buffalo River, the Risk Assessment and Modeling (RAM) subgroup, supported a study to develop and field test a management mass balance modeling framework that could be used to assess the load/response relationship (on both long and short time scales) for a series of contaminants of concern. The results of this study, which was conducted by the Great Lakes Program at the University at Buffalo, are presented in two EPA reports. The first report, entitled "Model Data Requirements and Mass Loading Estimates for the Buffalo River Mass Balance Study (Atkinson, *et al.* 1994)," compiled and analyzed data from previous studies and from the ARCS program in order to provide loading and parameterization input for the mass balance model application presented in this report.

The model code employed for this study was a modified version of WASP4/TOXI4 (Freeman, *et al.* 1992) designed specifically for application in river systems where sediment-water exchange of solids and associated contaminants has a potential impact on contaminant exposure and export. The model permitted the calculation of the time-variable concentrations of solids and contaminants in the water column and bottom sediments of the river as a function of external loadings and forcing functions for the system. The application of this framework to the Buffalo River included configuration, parameterization, and calibration of the model to data from river, followed by application of the model to help us gain a better understanding of the effects of contaminated sediments on exposure and effects of contaminants in Areas of Concern and to evaluate a number of remediation options for the Buffalo River. Loading data were compiled for eleven contaminants in the first report, but only five of the most significant contaminants were modeled: total PCBs, benzo[a]anthracene, benzo[a]pyrene, lead, and copper. In addition to this physical-chemical transport and fate modeling, this report also contains the results of our application of a PCB bioaccumulation model for carp (adaptation of FDCHN4 (Connolly, *et al.* 1992)) to the Buffalo River. In addition to evaluating remediation alternatives, the results of both models were used for a comparative human

health ri. assessment for this site also being conducted under the ARCS program.

Five basic remediation alternatives were evaluated with the above modeling framework:

1. No Action - This scenario evaluated the river's response over a ten year period with existing external loading conditions and continued navigational dredging.
2. Discontinued dredging above Hamburg Cove - This scenario examined the impacts of discontinuing navigational dredging upstream of Hamburg Cove (approximately half way from the mouth of the river to the upstream boundary of the modeled domain), thus permitting this portion of the river to fill with "clean" sediments from upstream.
3. Environmental Dredging - This scenario examined the impact of nearshore dredging along the entire length of the river within the designated AOC area. This option would remove several "hot spots" along the banks.

In order to determine the importance of resuspension on water column contamination, scenarios 1 and 2 were also evaluated with no external loadings. Everything else was kept the same, so any contamination of the water column would be strictly from sediment resuspension. These two scenarios were designated as:

4. No Action - No Loading.
5. Hamburg Cove - No Loading.

In conducting this remediation assessment, we discovered that the geometry and hydraulics of the Buffalo River are such that sediment resuspension only contributes a significant amount of contaminants to the water column during major high flow events. Furthermore, that resuspension contribution virtually all comes from the dredged channel of the river. On days of average or low flow, resuspension of contaminated sediments was not a significant factor in water column concentrations. The primary source of water column exposure and subsequent export to Lake Erie was determined to be loading from upstream of the modeled section of the river. This rather surprising result is reflective of the fact that significant decreases in point and combined sewer overflow loadings of contaminants to the river have already occurred.

Because of these modeling results, we concluded that sediment remediation would not have a significant impact on reducing water column contaminant exposure. However, both the mass balance modeling and the carp bioaccumulation modeling indicated that sediment remediation would

be a potentially important action for reducing direct sediment exposure, especially in "hot spots". The contaminant body burdens of bottom-dwelling and bottom-feeding organisms, such as carp, will improve in response to sediment remediation actions.

# SECTION 1

# INTRODUCTION

## 1.1 PROJECT BACKGROUND

The Buffalo River is located in the City of Buffalo, Erie County, in Western New York State. Three main tributaries, Buffalo Creek, Cazenovia Creek and Cayuga Creek, converge to form the river. From that point, the river meanders about 8.8 kilometers (5.5 miles) towards the west and discharges into Lake Erie near the head of the Niagara River. Figure 1-1 shows a map of the region.

The Buffalo River watershed is 78 square kilometers (30 square miles) in area, located west of South Buffalo and Lackawanna, NY. The drainage area of the entire river watershed (including tributaries) is 1155 square kilometers (446 square miles). The three tributaries drain primarily agricultural and wooded sections of land as well as several small residential communities. The lower river watershed drains a heavily industrialized section of south Buffalo. This area was once booming with grain mills, chemical and oil refineries and coke and steel mills, many of which are no longer in operation. In addition to the historical discharge of pollutants from these facilities, combined sewer overflows (CSOs) and inactive hazardous waste sites remain as potential sources of river contamination. Thirty-eight CSOs discharge to the river or lower Cazenovia Creek during periods of high runoff. These represent potential sources of organic and inorganic toxic contamination as well as BOD. Inactive hazardous waste sites are documented in 19 locations within or adjacent to the Buffalo River. Metals and cyanides have been detected in 12 of the sites, while the potential for off-site migration has been confirmed or indicated at 4 of these sites.

Extensive contamination of the bottom sediments has occurred due to the historical and present discharge of pollutants into the Buffalo River. Although present point source loadings have been reduced significantly from historic levels, possible contamination of the water column exists from resuspension of these heavily polluted bottom sediments. The U.S. Army Corps of Engineers maintains a navigational channel at a depth of 6.7 meters (22 feet) below lake level

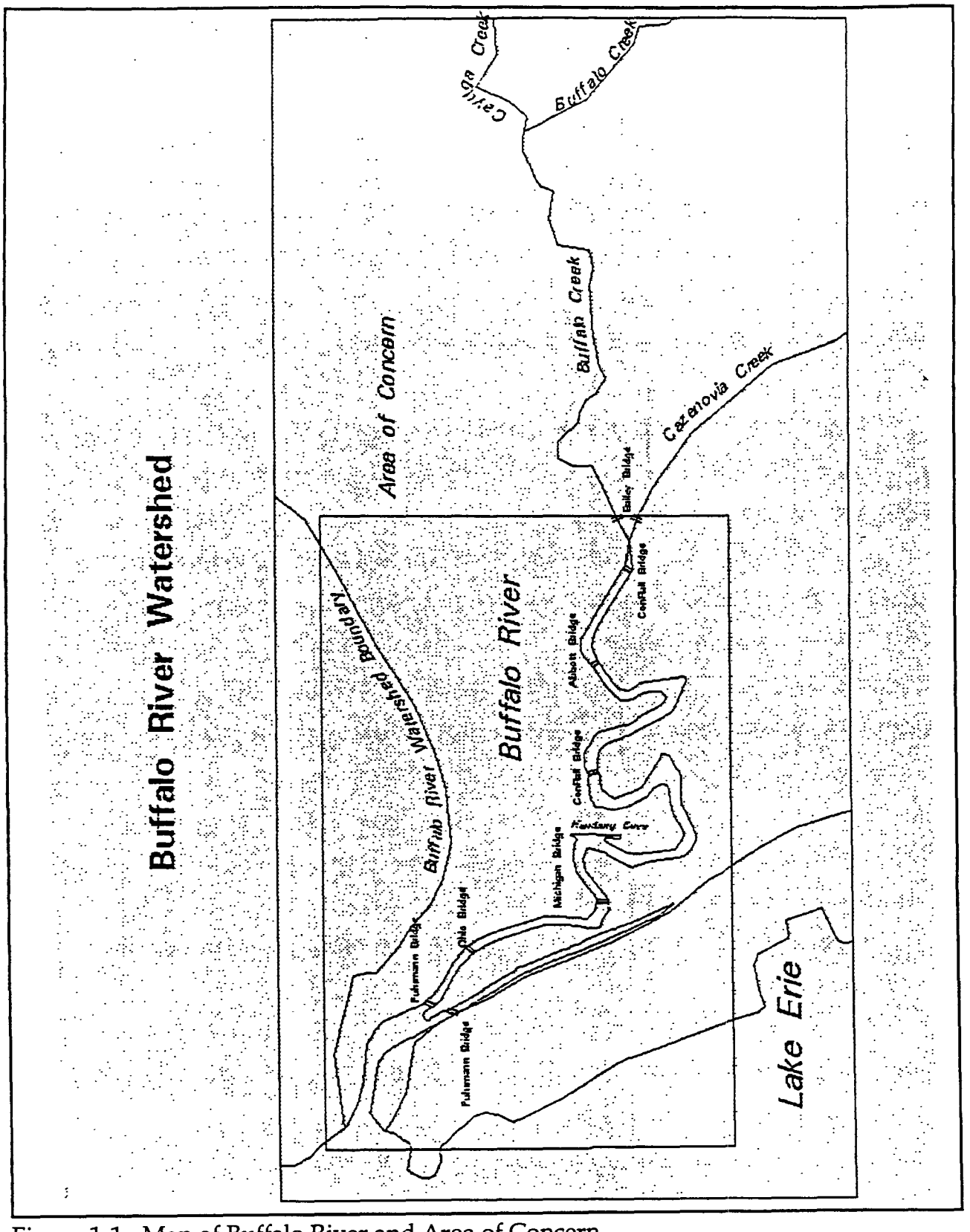


Figure 1-1. Map of Buffalo River and Area of Concern

through a regular program of navigational dredging in the lower 8.0 kilometers (5 miles). Due to dredging and a low gradient in the region, the river assumes an estuarine character. Also, because of the seasonal lag between river and lake temperatures, thermal stratification of the river occurs seasonally. Navigational dredging also prevents a natural armoring effect from taking place and may represent a short-term introduction of contaminants into the water column during the dredging process.

Contaminated bottom sediments have become of special concern for water resource management. Ecosystem and human health problems may exist since these "in-place pollutants" represent a potential source of acute and chronic toxicity. Unlike many of the more conventional pollutants, hydrophobic organic chemicals tend to have a strong affinity for particulate matter in aquatic systems. Thus, depending on the chemical properties and characteristics of the receiving water, much of the introduced contaminants are sorbed by biotic and abiotic suspended matter and settle from the water column, accumulating in bottom sediments. This long-term accumulation in bottom sediments was once considered a safe repository of these relatively insoluble substances. However, recent studies have demonstrated that, when external loads to a water body have been eliminated, the recovery of the system is not governed by washout from the water column. There is a much slower response controlling the long-term recovery of the system that is governed by the interaction of contaminated bottom sediments with the overlying water.

In 1985, the International Joint Commission listed the Buffalo River as one of 43 Areas of Concern (AOC) in the Great Lakes basin that exhibited significant environmental degradation and severe impairment of beneficial uses. Contaminated sediments were considered to be a major factor in these degraded conditions. There are goals to develop the river and its banks for greater public access and other uses, including fish propagation. However, in-place pollutants represent a serious potential obstacle for development and use of the river.

A demonstration program known as ARCS (Assessment and Remediation of Contaminated Sediments) was set up by the U.S. Environmental Protection Agency through its Great Lakes National Program Office to examine the impact of in-place pollutants in Great Lakes Areas of Concern (GLNPO, 1991). The ARCS program was designed to develop and test

methods for the assessment of the relative importance of sediment contamination and for the selection and demonstration of treatment technologies on a site-specific basis. With the understanding that addressing the many site-specific issues associated with contaminated sediments was a complex task, the designers of the ARCS program established, as one of four work groups a Risk Assessment/Modeling (RAM) Work Group. One of the objectives of this ARCS/RAM work group was to develop a management mass balance modeling framework that could be used to assess load/response relationships (on both long and short time scales) for Great Lakes AOCs. The modeling framework would be field tested by application to the Buffalo River AOC. The specific objectives of this report were to develop water quality mass balance and bioaccumulation models for the Buffalo River by simulating a time-history of contaminant concentrations in the water column, sediments and biota of the river as a function of source inputs. These field tested models would then be useful in evaluating the system response to a variety of possible remediation/regulatory actions for the Buffalo River AOC. Ultimately, it is desired within the RAM Work Group to develop and apply an "integrated exposure-risk model" to estimate the risk imposed on wildlife and humans through exposure to contaminant concentrations.

As shown in Figure 1-2, the overall modeling framework consists of the following:

1. loading submodel - that comp...es the spatial and temporal distribution of external inputs of contaminants to the river from both point and non-point sources.
2. hydrodynamic transport submodel - calibration with a tracer (conductivity)
3. sediment transport submodel - includes time- and space-variable settling, resuspension, and bottom sediment accumulation/erosion of different particle types.
4. physical-chemical toxics submodel - incorporates the above two submodels into a framework that includes the processes affecting the contaminant fluxes and reactions in the water column and sediments.
5. food chain bioaccumulation submodel - uses output of the integrated contaminant model to calculate the body burdens in various trophic levels of the food chain.
6. risk analysis submodel - for humans and key biota in the system as a function of the output from the previous two submodels.

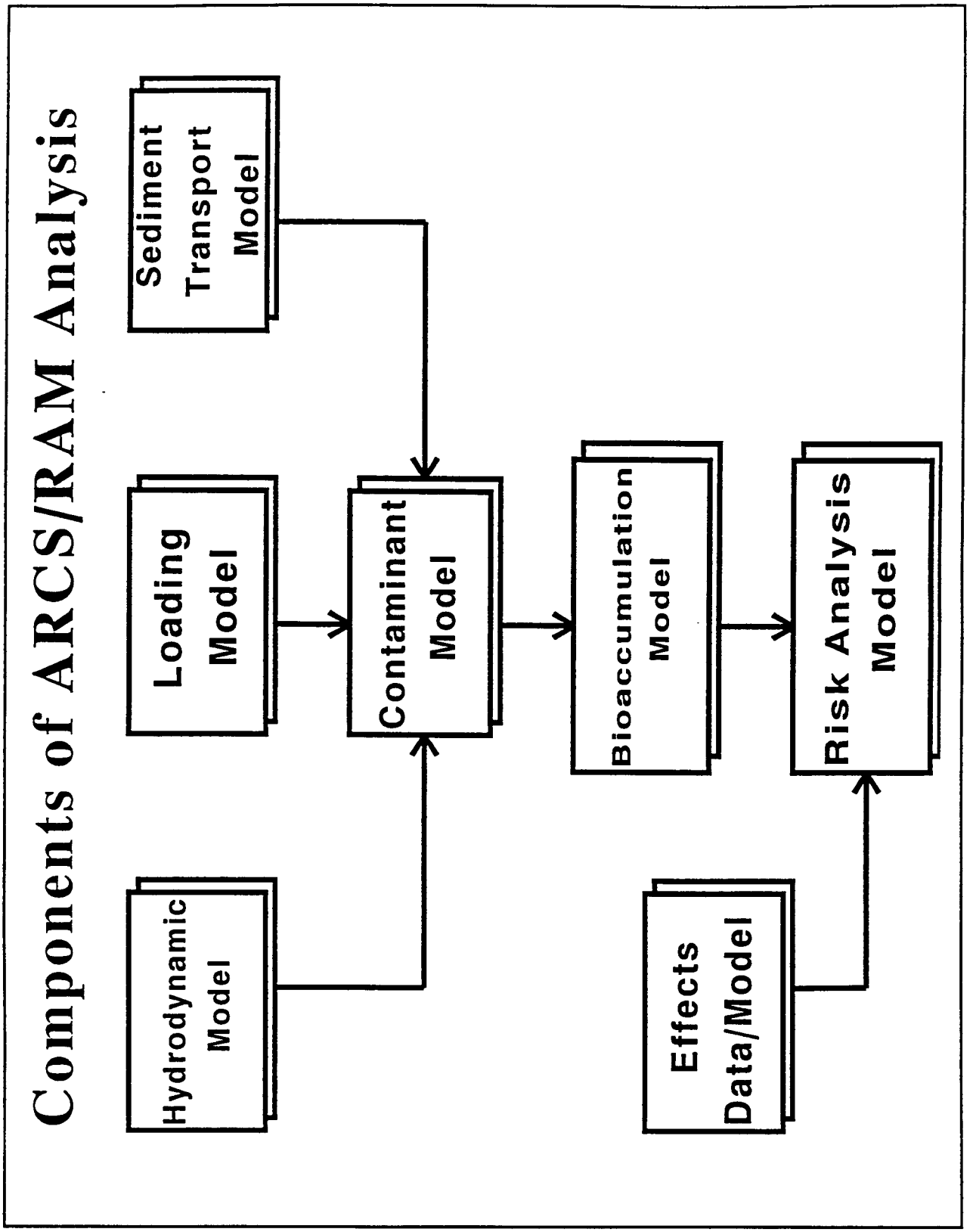


Figure 1-2. Overall modeling framework for the ARCS/RAM project

## 1.2 SCOPE OF WORK

This report contains a discussion and results of submodels 2 through 5. Much of this work is based on submodel 1 (Loading), which is presented along with a data summary in Model Data Requirements and Mass Loading Estimates for the Buffalo River Mass Balance Study (ARCS/RAM Program) (Atkinson et al., 1993). The modeling results presented in this report draw heavily on the results of the aforementioned report. Together they comprise an overall analysis of remediation options for the Buffalo River.

The procedure followed to meet the specific objectives mentioned above included:

1. Organization and reduction of data.
2. Model configuration of the Buffalo River (segmentation).
3. Comparison of model output to field data (calibration).
4. Application to various management scenarios (predictive 10-year simulations).
    a. No Action
    b. Hamburg Cove
    c. Environmental Dredging
    d. No Action with No Loading
    e. Hamburg Cove with No Loading
    f. Zero Initial Conditions
    g. Flow Switching
5. Interpretation of toxics model output.
6. Preparation of bioaccumulation model input.
7. Simulation of bioaccumulation model.

Data were obtained for a wide range of organic chemicals, pesticides, and heavy metals. The contaminants that were modeled included total PCBs, 2 PAHs (Benzo[a]anthracene, Benzo[a]pyrene) and two metals (lead, copper).

# SECTION 2

# MODEL DEVELOPMENT

## 2.1 OVERVIEW

The water quality model for the Buffalo River AOC is dependent on the following submodels: loading submodel, water transport submodel, and sediment transport submodel.

Loading Submodel

The external loading to the Buffalo River AOC was developed in a collaborative effort by the University at Buffalo and the State University College at Buffalo. Loading data were gathered and analyzed for use in conducting a mass-balance modeling effort on the Buffalo River. Loading estimates from upstream inputs, CSOs, industries and groundwater sources are available in the Buffalo River loading report (Atkinson, et al. 1993).

Water Transport Submodel

The hydraulics (advective and dispersive transport) of the Buffalo River, which are necessary to develop sediment and contaminant transport models, were derived from modeling a tracer (conductivity). A 1.5 year period was calibrated with sample conductivity data taken throughout the time interval (October 17, 1990 to April 30, 1992) at 6 locations. Dispersion coefficients were adjusted seasonally and spatially along the river for model calibration.

Sediment Transport Submodel

Sediment transport in the Buffalo River was computed via a model developed by Lick and co-workers for use in this phase of the ARCS program. The basic framework of the model is reported in Gailani et al. (1991) and Ziegler et al. (1992). This approach was applied to the Fox River, Wisconsin by Endicott et al. (1991). A similar approach was used for the Buffalo River model which will be discussed later on in this report.

The water quality model was calibrated over a 1.5 year period (October 18, 1990 to April 30, 1992). Solids (TSS) and contaminants (PCBs, benzo[a]anthracene, lead, copper, and benzo[a]pyrene) data taken during the period at six locations were compared to the model output for calibration purposes.

## 2.2 Computational Framework of Buffalo River Contaminant Model

A modified version of the Water Quality Analysis Program, WASP4, (Ambrose et al., 1987; Freeman and Endicott, 1990; Freeman et al., 1992) was used for the contaminant mass balance model. WASP4 is a general water quality modeling framework based on the principles of mass conservation. It has been widely used for the analysis of contaminants in surface waters.

The application of WASP4 to an aquatic system requires discretization of the water body into a series of control volumes (finite segments). The WASP framework accounts for the entry, accumulation, transformation and export of each state variable in every segment. Coupled mass balance partial differential equations (one for each state variable within each finite segment) are solved simultaneously by the program using Euler's method to integrate a series of ordinary differential equations (Ambrose, 1987). Temporal and spatial concentration distributions of each state variable within the system are provided as model output. Export (between segments) and mass budgets for each state variable are also valuable outputs from the WASP framework.

TOXI4 is a kinetic module contained in the WASP4 framework designed to compute exposure concentrations of organic chemicals and heavy metals. A modified version of this framework was used for the Buffalo River AOC allowing the simulation of up to three chemicals and a single solids type (Freeman et al., 1992). Several components can be modeled within this module: (1)The impacts of sorption, (2)transport of "dissolved" phases of the chemicals (volatilization-absorption atmospheric exchange and sediment-water diffusive exchange) and (3)in-situ transformations (such as hydrolysis, photolysis, oxidation, ionization, and biodegradation). The transformation processes required in the framework depend on the contaminants chosen for simulation.

Parameterization and segmentation must be completed before TOXI4 can be used to

perform dynamic mass balance modeling. Parameter values which must be specified include: transport and fate processes, forcing functions, and simulation control parameters. Limitation of the integration time step is necessary to ensure numerical stability in this framework. Parameter and data requirements and integration and simulation options are contained in the WASP4 user's guide (Ambrose et al., 1987).

## 2.3 Conceptual Framework of Buffalo River Contaminant Model

The conceptual framework of the Buffalo River contaminant model is presented in Figure 2-1. The transport and fate processes included are:

1. Input of TSS and contaminants via various external loadings.
2. Advection and dispersion in the water column.
3. Settling, resuspension and burial.
4. Porewater transport.
5. Air-water exchange.
6. Partitioning of contaminants between water and TSS.

Dynamic mass balance equations for each of the model state variables were developed based on these processes. These partial differential equations are functions of both time and space, and they represent interactions between segments. In order to simplify these equations to the forms shown below, the following assumptions were made:

1. Water column volumes are constant with respect to time ($\delta V/\delta t = 0$).
2. Surficial sediments do not move horizontally (no bed load).
3. Contaminant partitioning to solids is rapid compared to other processes (local equilibrium).

4. There is no differentiation among sorbent types; in other words, there is only one solids type which comprise all particulate matter in the system.

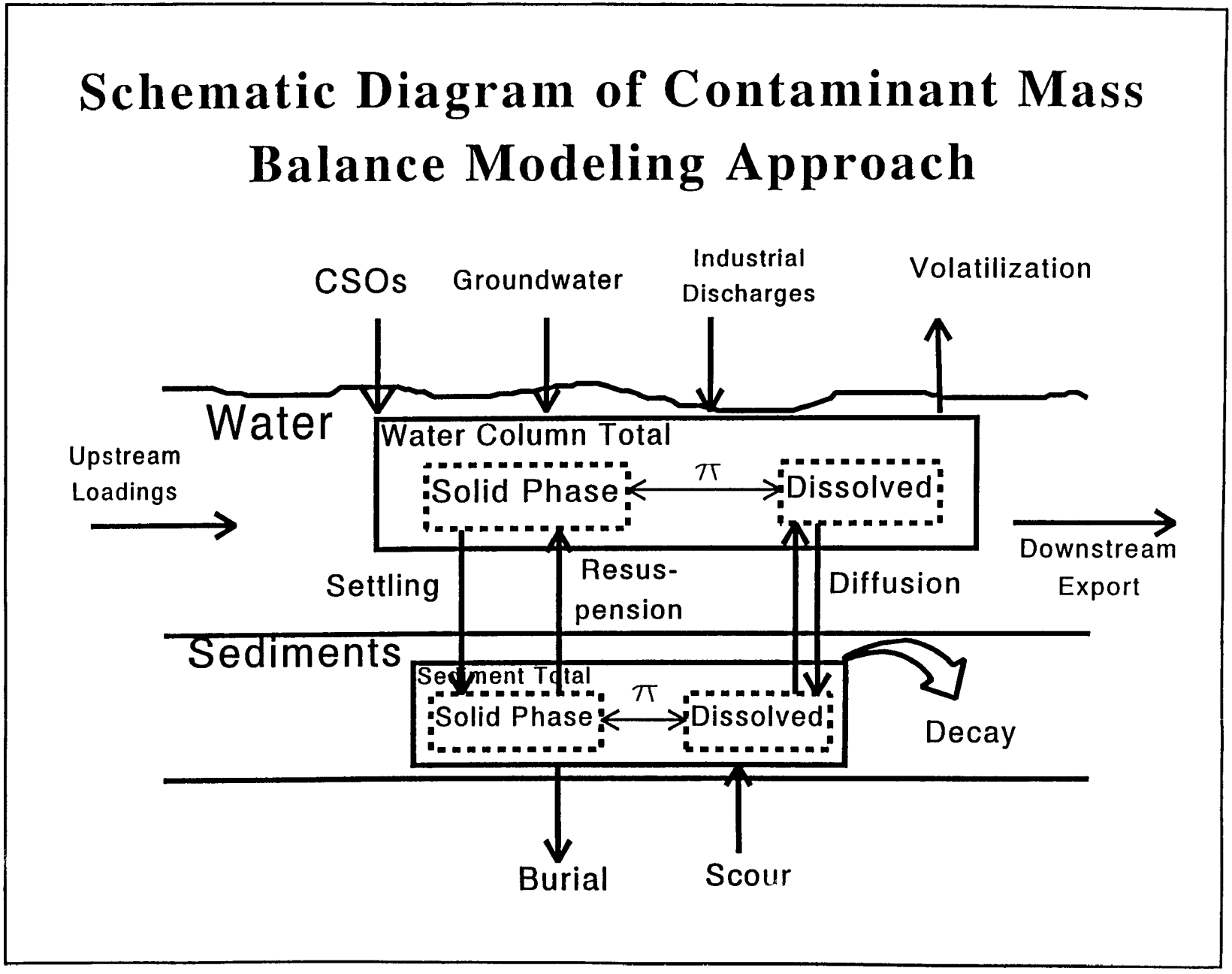


Figure 2-1. Conceptual framework of Buffalo River model

The fate and transport mass balance equations that were performed on individual segments within the WASP framework are:

Total Conservative Tracer in the Water Column (Conductivity)

$$\frac{d[C_T]}{dt} = \frac{Q_I}{V_W} C_{Twi-1} - \frac{Q_{out}}{V_W} C_{Twi} + \frac{E_b}{V_W}(C_{Twi-1} - C_{Twi}) + W_i \qquad (2\text{-}1)$$

Total Suspended Solids in the Water Column (TSS)

$$\frac{d[m_W]}{dt} = \frac{Q_I}{V_W} m_{wi-1} - \frac{Q_{out}}{V_W} m_{wi} - v_s \frac{A_S}{V_W} m_{wi} + v_r \frac{A_S}{V_S} m_S + W_i \qquad (2\text{-}2)$$

Total Chemical in Water Column (PCBs, B[a]a, B[a]p, Lead, Copper)

$$\frac{d[C_{Tw}]}{dt} = \frac{Q_I}{V_W} C_{Twi-1} - \frac{Q_{out}}{V_W} C_{Twi} + \frac{E_b}{V_W}(C_{Twi-1} - C_{Twi}) \qquad (2\text{-}3)$$

$$- v_s \frac{A_s}{V_W} f_{pw} C_{Twi} + v_r \frac{A_s}{V_s} f_{ps} C_{Ts} - K_V \frac{A_s}{V_W}\left[f_{dw} C_{Twi} - \frac{C_a RT}{K_H}\right] + W_i$$

Total Solids in the Sediments (TSS)

$$\frac{d[m_S]}{dt} = v_s \frac{A_s}{V_W} m_w - v_r \frac{A_s}{V_S} m_s - v_b \frac{A_s}{V_S} m_s \qquad (2\text{-}4)$$

Total Chemical in Sediments (PCBs, B[a]a, B[a]p, Lead, Copper)

$$\frac{d[C_{TS}]}{dt} = v_s \frac{A_S}{V_W} f_{pw} C_{Twi} - v_r \frac{A_S}{V_S} f_{ps} C_{TS} - v_b \frac{A_S}{V_S} f_{ps} C_{TS} \qquad (2\text{-}5)$$

where:

$C_{Tw}$ , $C_{Ts}$ = Contaminant concentration in the water column and sediments ($M/L^3$)

$m_W$ , $m_S$ = Solids concentration in the water column and sediments ($M/L^3$)

$Q_I$ , $Q_{out}$ = Water inflow and outflow ($L^3/T$)

$v_s$, $v_r$, $v_b$ = Settling, resuspension, and burial velocities (L/T)

$f_d$ , $f_p$ = Contaminant fractions dissolved and particulate (L/T)

$V_W$ , $V_S$ = Volume of the water and sediments ($L^3$)

$E_b$ = Bulk dispersion coefficient ($L^3/T$)

$A_s$ = Surface area ($L^2$)

$K_V$ = Volatilization coefficient (L/T)

$C_a$ = Contaminant concentration in air ($M/L^3$)

$K_H$ = Henry's Law Constant (atm * $m^3$ / mol)

R = Universal gas constant (atm * $m^3$ / mol * T)

T = Temperature (absolute)

W = Sum of all external loadings (M/T)

## 2.4 Segmentation for Buffalo River Model

The Buffalo River model system contained 157 segments in the water column and sediments combined. The water column was divided into 31 segments in one layer (See Figure 2-2). The sizes of the segments were based on relative advection and dispersion patterns in order to keep the concentration gradient insignificant for each control volume and to satisfy numerical stability criteria (Thomann and Mueller, 1987). Segment 31 represents the entire Buffalo Ship Canal which is a small factor in the Buffalo River hydrodynamic flow routing scheme. Segment 30 represents the boundary with Lake Erie. Table 2-1 contains the morphometry for each water column segment.

The remaining 126 segments are accounted for in three layers of sediments. A surficial sediment layer (depth of 10 cm) and a subsurface sediment layer (depth of 50.5 cm) contained two segments for each water column segment (62 segments in each layer). A bottom subsurface sediment layer (depth of 200 cm) contained only two segments (see Figure 2-3).

The top two sediment layers were divided into depositional and erosional areas. Net deposition occurs in the nearshore areas while net erosion generally occurs in the mid-channel region of the Buffalo River. Upon consulting sounding maps (USACE, 1988), it was found that the nearshore gradient (banks) of the Buffalo River is fairly steep. Depositional areas were

Table 2-1. Water Column Morphometry

| WC Seg.# | Volume ($m^3$) | Surf. Area ($m^2$) | Avg. Depth (m) | Adjac. W.C. Seg. # | Interface Area W.C. ($m^2$) | Deposit. Sediment segs. # | Interface Area Sed ($m^2$) | Erosion. Sediment segs. # | Interface Area Sed ($m^2$) |
|---|---|---|---|---|---|---|---|---|---|
| 1 | 1.38e5 | 1.80e4 | 7.68 | 2 | 5.21e2 | 32, 94 | 3.16e3 | 33, 95 | 1.49e4 |
| 2 | 1.45e5 | 1.57e4 | 9.24 | 3 | 9.17e2 | 34, 96 | 3.06e3 | 35, 97 | 1.26e4 |
| 3 | 1.52e5 | 1.46e4 | 1.04e1 | 4 | 6.71e2 | 36, 98 | 2.87e3 | 37, 99 | 1.18e4 |
| 4 | 1.50e5 | 1.58e4 | 9.5 | 5 | 7.46e2 | 38, 100 | 2.71e3 | 39, 101 | 1.31e4 |
| 5 | 2.59e5 | 2.22e4 | 1.17e1 | 6 | 1.16e3 | 40, 102 | 2.62e3 | 41, 103 | 1.95e4 |
| 6 | 3.31e5 | 3.24e4 | 1.02e1 | 7 | 1.24e3 | 42, 104 | 2.68e3 | 43, 105 | 2.97e4 |
| 7 | 1.56e5 | 1.91e4 | 8.16 | 8 | 6.67e2 | 44, 106 | 2.78e3 | 45, 107 | 1.63e4 |
| 8 | 1.66e5 | 1.75e4 | 9.48 | 9 | 1.06e3 | 46, 108 | 2.78e3 | 47, 109 | 1.47e4 |
| 9 | 2.21e5 | 2.04e4 | 1.08e1 | 10 | 1.08e3 | 48, 110 | 2.78e3 | 49, 111 | 1.76e4 |
| 10 | 2.65e5 | 2.31e4 | 1.14e1 | 11 | 1.17e3 | 50, 112 | 2.78e3 | 51, 113 | 2.03e4 |
| 11 | 2.11e5 | 1.96e4 | 1.08e1 | 12 | 1.12e3 | 52, 114 | 2.78e3 | 53, 115 | 1.67e4 |
| 12 | 3.05e5 | 3.47e4 | 8.78 | 13 | 9.43e2 | 54, 116 | 2.78e3 | 55, 117 | 3.20e4 |
| 13 | 1.73e5 | 2.06e4 | 8.41 | 14 | 7.94e2 | 56, 118 | 2.78e3 | 57, 119 | 1.78e4 |
| 14 | 1.99e5 | 1.94e4 | 1.03e1 | 15 | 1.07e3 | 58, 120 | 2.78e3 | 59, 121 | 1.66e4 |
| 15 | 1.55e5 | 1.64e4 | 9.47 | 16 | 7.04e2 | 60, 122 | 2.78e3 | 61, 123 | 1.36e4 |
| 16 | 1.24e5 | 1.41e4 | 8.79 | 17 | 8.13e2 | 62, 124 | 2.78e3 | 63, 125 | 1.13e4 |
| 17 | 1.79e5 | 2.06e4 | 8.69 | 18 | 1.00e3 | 64, 126 | 2.78e3 | 65, 127 | 1.78e4 |
| 18 | 2.14e5 | 2.53e4 | 8.45 | 19 | 5.71e2 | 66, 128 | 2.78e3 | 67, 129 | 2.25e4 |
| 19 | 1.62e5 | 1.97e4 | 8.23 | 20 | 6.10e2 | 68, 130 | 2.78e3 | 69, 131 | 1.69e4 |
| 20 | 2.32e5 | 2.18e4 | 1.07e1 | 21 | 7.19e2 | 70, 132 | 2.78e3 | 71, 133 | 1.90e4 |
| 21 | 1.19e5 | 1.52e4 | 7.84 | 22 | 5.13e2 | 72, 134 | 2.78e3 | 73, 135 | 1.24e4 |
| 22 | 1.22e5 | 1.68e4 | 7.23 | 23 | 4.81e2 | 74, 136 | 2.78e3 | 75, 137 | 1.40e4 |
| 23 | 1.41e5 | 1.67e4 | 8.43 | 24 | 5.81e2 | 76, 138 | 2.78e3 | 77, 139 | 1.39e4 |
| 24 | 9.32e5 | 1.20e4 | 7.74 | 25 | 4.52e2 | 78, 140 | 2.78e3 | 79, 141 | 9.26e3 |
| 25 | 1.45e5 | 1.62e4 | 8.95 | 26 | 7.35e2 | 80, 142 | 2.50e3 | 81, 143 | 1.39e4 |
| 26 | 2.48e5 | 3.29e4 | 7.56 | 27 | 1.68e3 | 82, 144 | 1.86e3 | 83, 145 | 3.10e4 |
| 27 | 2.50e5 | 3.53e4 | 7.1 | 28 | 1.60e3 | 84, 146 | 1.68e3 | 85, 147 | 3.36e4 |
| 28 | 2.63e5 | 3.41e4 | 7.71 | 29 | 8.47e2 | 86, 148 | 2.04e3 | 87, 149 | 3.21e4 |
| 29 | 1.77e5 | 2.55e4 | 6.91 | 30 | 7.30e2 | 88, 150 | 2.50e3 | 89, 151 | 2.30e4 |
| 30 | 3.79e5 | 4.41e4 | 8.58 | Lake | 4.00e2 | 90, 152 | 2.65e3 | 91, 153 | 4.15e4 |
| 31 | 9.99e5 | 6.23e4 | 1.60e1 | 26 | 1.25e3 | 92, 154 | 2.22e4 | 93, 155 | 4.01e4 |

chosen as 0.46 meters (15 feet) off each shore for the entire river area modeled, with erosional areas encompassing the remaining width of the river. One depositional and one erosional segment are contained in the top two sediment layers for each water column segment. The bottom subsurface segments include a net depositional segment and a net erosional segment for the entire river length. This bottom layer serves as a deep sediment boundary for the model.

Lengths and widths of water column segments were approximated from maps. Water column volumes, surface areas, depths and cross-sectional areas were generated through the use of a program written in the ARC macro language (AML) contained in the ARC/INFO package (Guan, 1993). A programming module within AML called the Triangular Irregular Network (TIN) was applied which calculates the various morphometry values given the characteristics of the Buffalo River.

Sediment morphometry was influenced by the water column segments. The sediment segment surface areas and widths (combined depositional and erosional) were taken to be the same as the overlying water column segment. The depths for sediment layers were based on the available sediment core data. The finest resolution in the core data (surficial) was 24 inches (60.5 cm). This was too great a depth to accurately describe resuspension in the system. An arbitrary 10 cm upper sediment layer was created so the model could better describe contaminant transport in sediments. The additional 50.5 cm became the subsurficial sediment depth. The same initial conditions were applied to both layers. The bottom layer allowed for use of the deepest measurements taken in the core sampling. Sediment segment volumes were obtained from the product of surface area and layer depth.

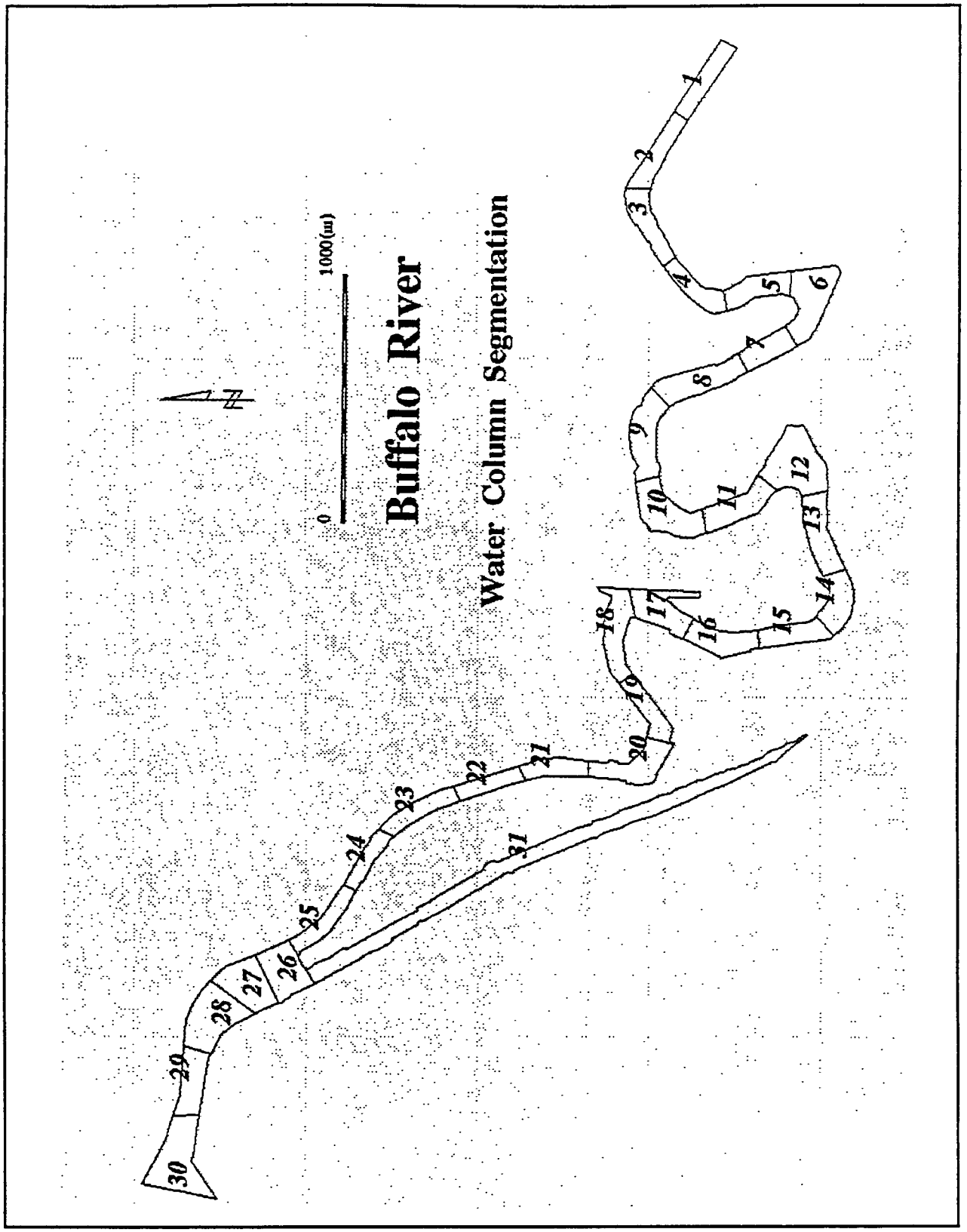


Figure 2-2. Water column segmentation

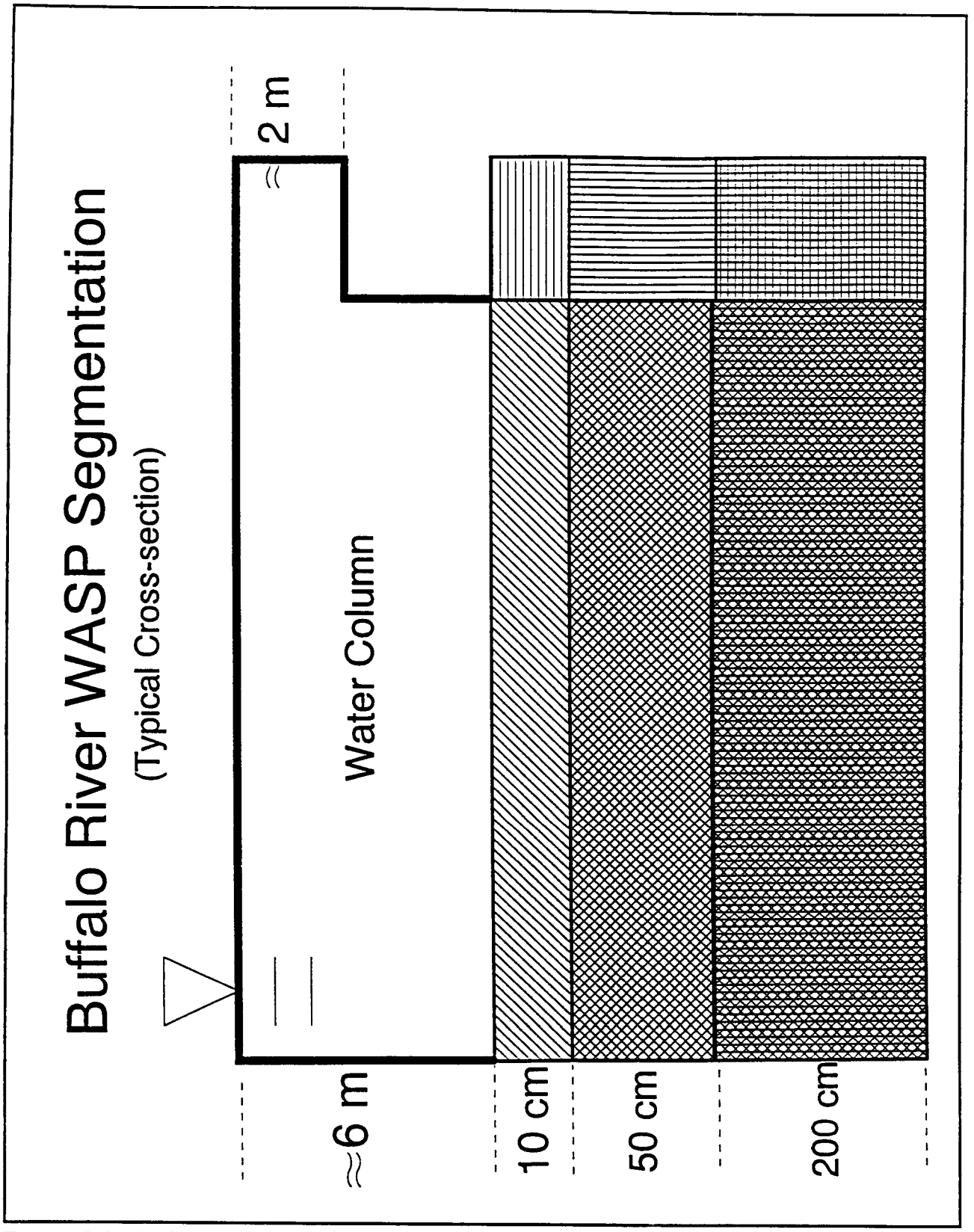


Figure 2-3. Sediment segmentation diagram

# SECTION 3

# DATA DEVELOPMENT

## 3.1 MODEL INPUT DATA

**Input set requirements for Buffalo River model**

The WASP framework requires specific input data and parameters. The requirements depend on the nature of simulation. For this contaminant model, the following items were necessary in the input data sets: time step, segment morphometry, dispersion coefficients, flows, settling and resuspension rates, boundary conditions, loadings, partitioning parameters ($K_{oc}$, $K_d$), volatilization parameters ($H_c$), various time functions (temperature, $f_{oc}$, DOC, wind), and initial conditions. The values used in the model, including where and/or how they were obtained, are included in this chapter. Segment morphometry was already discussed in Section 2. Dispersion coefficients were calibrated with conductivity modeling and the values are included in Section 4. Loadings were discussed in detail in the loading report, and they are mentioned generally in this chapter. Burial rates do not to need to be specified since they are computed directly in WASP based on settling and resuspension rates. The sediment-diffusion rate ($K_D$) and volatilization rate ($K_V$) are computed internally as well.

**Time Step**

Since the WASP framework uses a first-order Euler method for numerical integration, it is essential to apply a time step which avoids numerical instability. The time step is limited by the hydraulic residence time of the smallest water column segment volume. This value still did not meet model stability needs. The value was lowered until stability (based on model output) was achieved at a time step of 0.0032 days (roughly 5 minutes). The time step was kept uniform through the periods of simulation.

**Flows**

Values for Buffalo River and industrial flows are required as input in this model. Except

during very low flow periods, CSO and groundwater flows are insignificant relative to the upstream flow, but were still included as input to the system. Actual Buffalo River flows were used for the calibration runs from October 18, 1990 to April 30, 1992. For the 10-year predictive runs, actual mean daily flows from the 1970s were used (see Figure 3-1). The 70's flow data were selected over actual flows from other decades since a good number of flow events occurred and the overall decade average was consistent with the historical average (20 cms). Significant events (flows greater than 400 cms) occurred on 5 days in the decade. Industrial Cooling water discharge to the river from PVS Chemical (0.35cms) and Buffalo Color (0.44cms) were included in the model (Atkinson et al., 1993). These industrial flows are usually minor, but they can provide a significant contribution to river flow during summer low flow periods.

**Settling Rates**

Input values for settling rates were computed using the methods of Gailani and Lick. Their work, conducted as part of the Green Bay Mass Balance Study, included the development of a solids transport submodel for the Lower Fox River (Gailani et al.,1991). The submodel was used for a WASP application on the Fox River by Endicott et al. (1991). A weighted-average function based on particle size distribution was used to estimate TSS settling rates. Two major assumptions of the Gailani and Lick method are that particle distributions can be represented by three size fractions (fine, medium, and coarse) and that particle size distribution is a function of flow (Gailani et al. 1991). This second assumption necessitated the division of the modeled river into three reaches. The upstream reach contained the greatest amount of coarse-sized particle settling, while the midstream and downstream reaches contained less coarse settling but greater amounts of medium and fine-sized settling. The overall daily settling rates were based on a size-fraction weighted average of the particle class settling rates for each particle type.

The following particle size fractionation relationships were used for the Buffalo River (Gailani, personal communication).

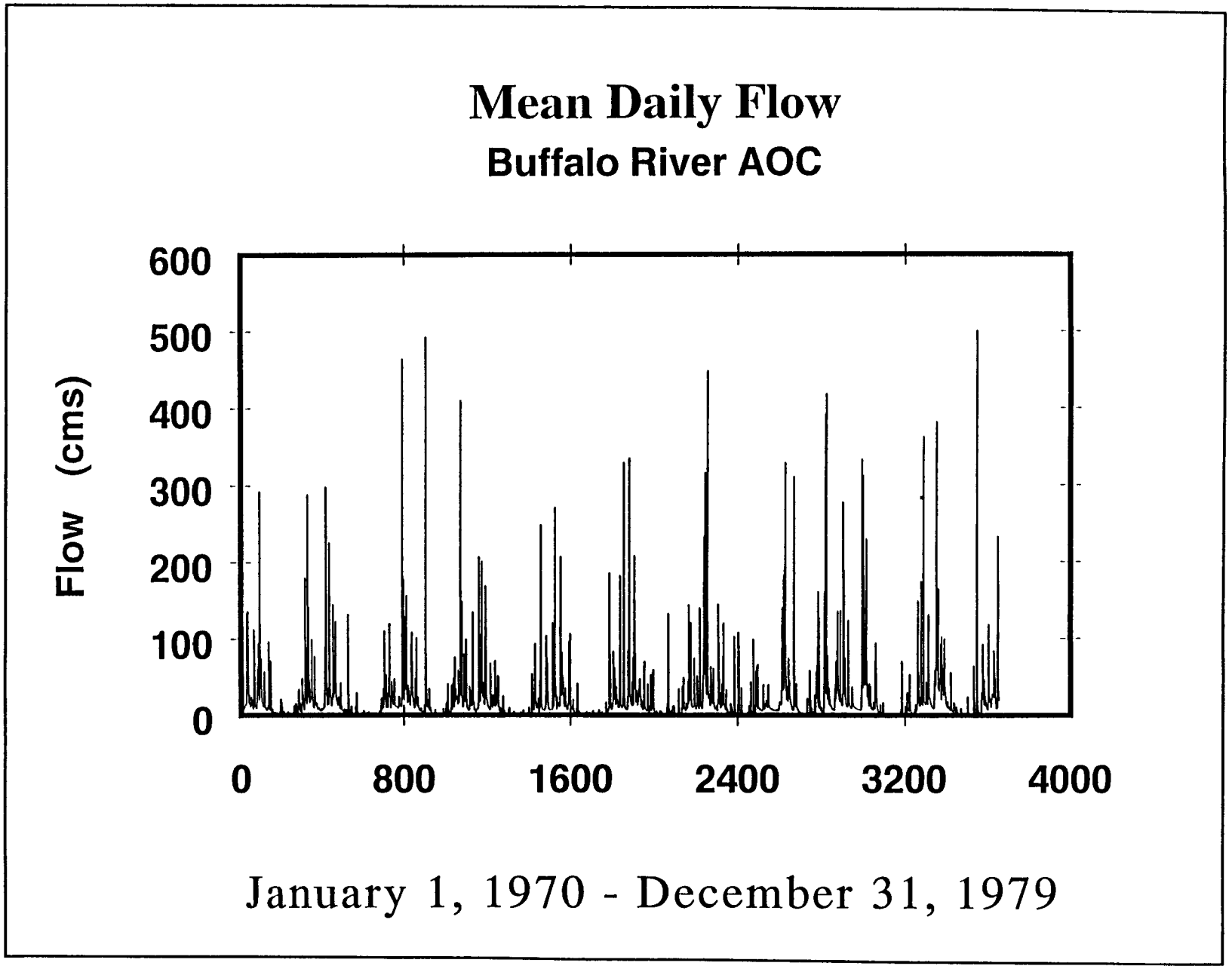


Figure 3-1. Actual Buffalo River flows for the 1970s

| | |
|---|---|
| For Q ≤ 400 cms (non-event) | Fine Fraction = 0.6<br>Medium Fraction = 0.4<br>Coarse Fraction = 0 |
| For Q ≥ 400 cms (event)<br>and Q ≥ 100 cms (after event) | Fine Fraction = 0.3<br>Medium Fraction = 0.2<br>Coarse Fraction = 0.5 |
| For Q≤ 100 cms<br>(after event until Q = 20 cms) | Fine Fraction = 0.3<br>Medium Fraction = 1-(Fine+Coarse)<br>Coarse Fraction = (0.5*Q)/100 |

The segments used for the various Buffalo River reaches are listed in Table 5-1 with the typical event settling velocity. The settling rate during a non-event period for every river reach was 1.20e-5 m/s.

Table 3-1. Settling Rates for Buffalo River Events

| River Reach | Segment Range | Event Settling Rate (m/s) |
|---|---|---|
| Upstream | 1-6 | 1.56e-4 |
| Midstream | 7-17 | 8.10e-5 |
| Downstream | 18-31 | 5.60e-5 |

**Resuspension Rates**

Estimation of resuspension velocities were also based on the methods of Gailani and Lick (Gailani et al., 1991) which were applied to WASP by Endicott et al. (1991). In their model, resuspension is a function of shear stress in the river. Shear stress is a function of water velocity in the river. The amount of sediment entrained as a function of shear stress exerted at the sediment-water interface is approximated by (Gailani, et al. 1991):

$$\epsilon = \frac{a_0}{t_d^n}\left[\frac{\tau - \tau_c}{\tau_c}\right]^m \qquad \text{for } \tau > \tau_c \qquad (3\text{-}1)$$

$$\epsilon = 0 \qquad \text{for } \tau \leq \tau_c \qquad (3\text{-}2)$$

$$\tau = 0.003(v_A)^2 = 0.003\left(\frac{Q}{A_x}\right)^2 \qquad (3\text{-}3)$$

where:

$\epsilon$ = Amount of sediment resuspended per unit surface area ($M/L^2 = g/cm^2$)

$a_0$ = Empirical sediment entrainment constant

$t_d$ = Time after deposition (T = days)

$\tau$ = Shear stress exerted at the sediment-water interface ($dynes/cm^2$)

$\tau_c$ = Critical shear stress for entrainment ($dynes/cm^2$)

n = Empirical sediment deposition exponent ≈ 2

m = Empirical sediment entrainment exponent ≈ 3

$v_A$ = Advective velocity (L/T = cm/sec)

Q = Flow ($L^3/T = cm^3/sec$)

$A_x$ = Cross-sectional area ($L^2 = cm^2$)

The resuspension velocity is calculated using the amount of entrained sediments according to the following equation:

$$v_r = \frac{\epsilon}{\rho_b t_c} \qquad (3\text{-}4)$$

where:

$v_r$ = Resuspension velocity (L/T)

$\rho_b$ = Bulk density of surficial sediments ($M/L^3$)

$t_e$ = Time to entrain sediments (T)

Since resuspension is a function of water velocity, it varies spatially throughout the river. It was assumed that event-driven resuspension takes place in the erosional zones, which occur in the swifter mid-channel area of the river. Based on flow data, daily resuspension velocities were computed for the erosional surficial sediment segments. Critical shear is typically reached only on days with high flow. A small "background" resuspension velocity was added since resuspension rates are approximately zero (and not zero) when shear stress is less than critical stress. For erosional segments, this background resuspension velocity was 1.25e-11 m/s. An even smaller background resuspension velocity (6.26e-12 m/s) was applied to the depositional segments.

Water column concentration peaks occur on high flow days due to greater loadings during events and resuspension of in-place pollutants into the water column. Resuspension is a factor in water column contamination only on and around high flow events. Figure 3-2 shows flow and resuspension fluxes over a small period of 20 days, including one major and one minor high-flow event. Resuspension is significant only during the high flow events as seen in this figure. During non-event periods, resuspension is not significant.

## Boundary Conditions

Upstream boundary conditions for contaminants and TSS were governed by upstream loading estimates. A discussion on downstream boundary conditions along with a data summary are included in the Buffalo River loading report (Atkinson et al., 1993). Average values were computed from various samples of Lake Erie TDS, TSS and contaminant data. The downstream boundary conditions were also used as boundary conditions for the Buffalo River Improvement Corporation (BRIC) since BRIC flow is lake water. Downstream boundary conditions used in the model are listed in Table 3-2.

The only boundary condition used for the deep sediment layer was a constant 3.75e+5

mg/L for TSS. This value was constant for TSS throughout the sediments (see Initial Conditions).

Table 3-2. Downstream Boundary Conditions

| Variable | Downstream Boundary Cond. [mg/L] |
|---|---|
| TDS | 175.4 |
| TSS | 11 |
| PCBs | 2.90e-6 |
| B[a]a | 2.00e-7 |
| Lead | 1.25e-3 |
| Copper | 1.50e-3 |
| B[a]p | 4.00e-7 |

**Loadings (Upstream, CSO, Industrial, Groundwater)**

For WASP input needs, conductivity data values [μS/cm] were converted to total dissolved solids (TDS) by the methods of Linsley & Franzini (1979):

$$TDS = 0.6 * \text{conductivity} \quad (3\text{-}5)$$

This allowed conductivity to be expressed in units of mg/L which are required in the WASP framework. Data from sample site 1 (upstream; segment 1) was used to generate an upstream TDS loading equation. A power equation of the form $TDS = aQ^b$ was assumed with TDS in mg/L and Q in cms. The coefficients a and b were determined using a best-fit linear equation [log TDS vs. log Q] with $r^2 = 0.863$ (see Figure 3-3). The resulting relationship was found for predicting TDS as a function of flow:

$$TDS = 256\ (Q)^{-0.209} \quad (3\text{-}6)$$

It was necessary to correct this equation due to statistical bias in regressions of log-transformed data (Newman, 1993). The general form of the regression model is:

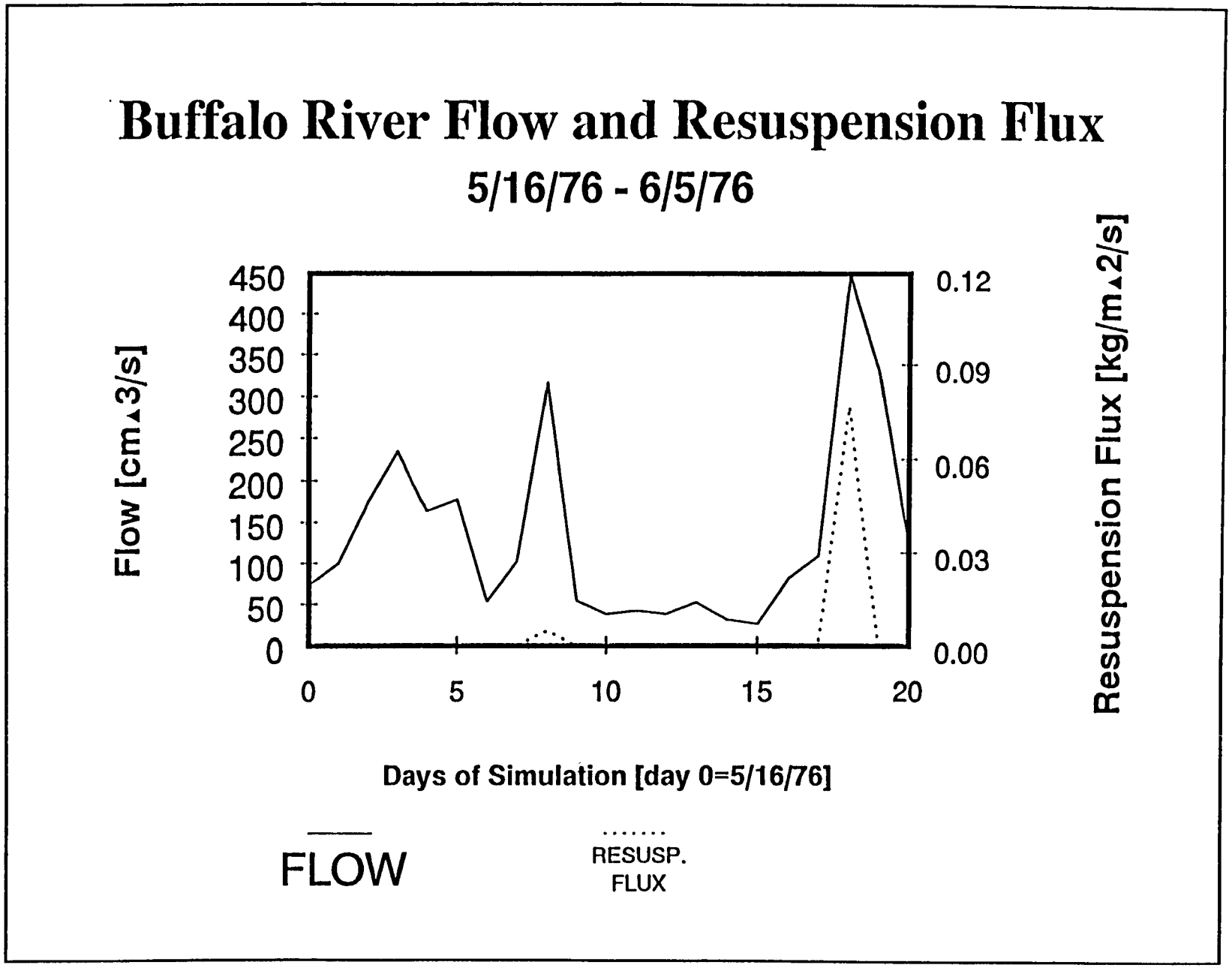


Figure 3-2. Buffalo River flow and resuspension flux during a small-scale period

$$\log TDS = B_0 + B_1 \log Q + \epsilon \quad (3-7)$$

where $B_0$ and $B_1$ are constants and $\epsilon$ is the error between the fitted line and the actual data. The error term is not included when this equation is back transformed to generate the power equation (under the assumption that there is zero error). The general power relation, including the error term is:

$$TDS = 10^{(B_0+\epsilon)} Q^{B_1} \quad (3-8)$$

where $10^{\epsilon}$ is the bias correction term. The bias correction was estimated based on a normal distribution of regression residuals from Havlicek and Crain (1989) and Newman (1993):

$$\epsilon = \frac{MSE}{2} \quad (3-9)$$

$$MSE = \frac{\sum_{i-1}^{N} \epsilon_i^2}{(N-2)} \quad (3-10)$$

where N is the number of observations.

A bias correction factor of 0.004 was found. The bias-corrected loading equation was:

$$TDS = 258\ (Q)^{-0.209} \quad (3-11)$$

Upstream contaminant and TSS loadings were generated based on the statistical regression equations discussed in the Buffalo River loading report (Atkinson et al., 1993). Although the equations were developed with limited data, the loading estimates are reasonable and appear to be genuine. The upstream loadings are largely determined by the river flow. Predicted upstream TSS loadings are compared to flow and actual sample data during the calibration period in figure 3-4. Figure 3-5 shows predicted upstream PCB loadings and the observed values in the calibration period. Combined sewer overflow (CSO) pollutant and solids loadings were based on the equations discussed in the Buffalo River loading report (Atkinson et al., 1993 and in Irvine et al., 1993; and Marshall, 1993). These equations were applied to daily rainfall data from the 1970s. CSO loads occurred when the rainfall exceeded the minimum

rainfall value ($I_{min}$) calculated for each outfall location. Three outfalls (57 and 58, 30, 42) produced a CSO loading for every precipitation event ($I_{min}$=0). CSO loadings from the other outfalls occurred only on days with significant rain. In general, CSO loadings were relatively small compared to the upstream loads.

Industrial load information was obtained from the Buffalo River loading report (Atkinson et al., 1993). Daily loads of 0.18 kg/d and 0.91 kg/d were used as input for lead and copper respectively. Groundwater loadings were very small. Daily loadings for b[a]a (6.11e-4 kg/d), copper (0.0649 kg/d), and lead (1.80e-3 kg/d) were entered as input.

**Partition Coefficients**

A full analysis of partitioning is included in the Buffalo River loading report (Atkinson et al., 1993). A two-phase approach was taken under the assumption of local equilibrium. Concentrations of dissolved organic carbon (DOC), particulate organic carbon (POC) and TSS were available from water quality data. Particulate ($C_p$) and dissolved ($C_d$) concentrations of the contaminants were also sampled. The fraction of organic carbon ($f_{oc}$) was found from the available data by dividing the concentration of POC by the TSS concentration.

$$f_{oc} = \frac{[POC]}{[TSS]} \tag{3-12}$$

where:

[POC] = concentration of POC (mg organic carbon/L)

[TSS] = concentration of TSS (mg dry weight solid/L)

Due to sparcity of data, average seasonal $f_{oc}$ values were entered as input. Values of $f_{oc}$ were set at 0.05 in the winter (on January 1) and 0.20 for the summer months (June 1 - August 30). The WASP framework would linearly interpolate between these values for winter and summer.

The field-observed partition coefficients for dry weight solids ($K'_d$) (L/kg d.w.) were calculated from:

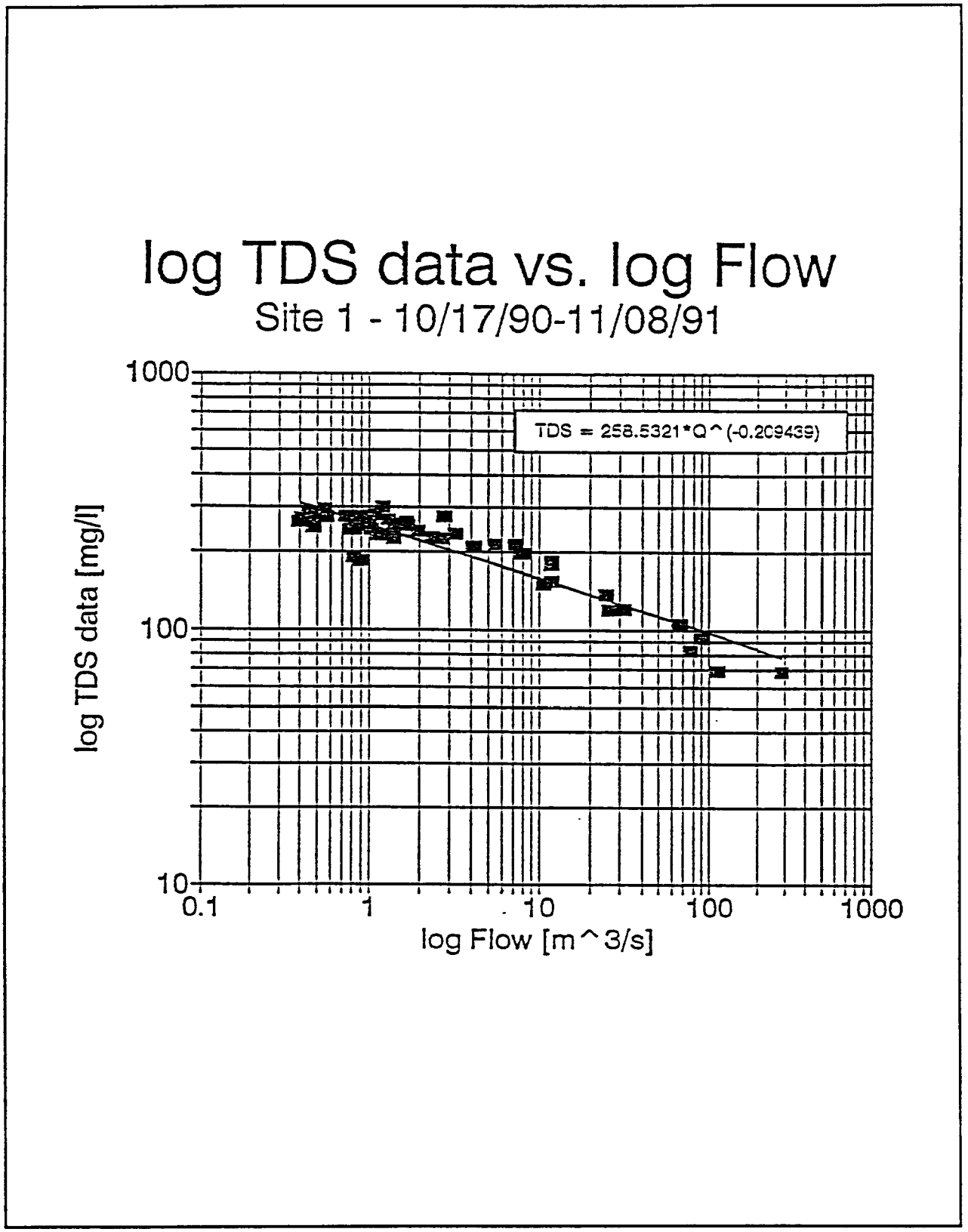


Figure 3-3. TDS loading regression

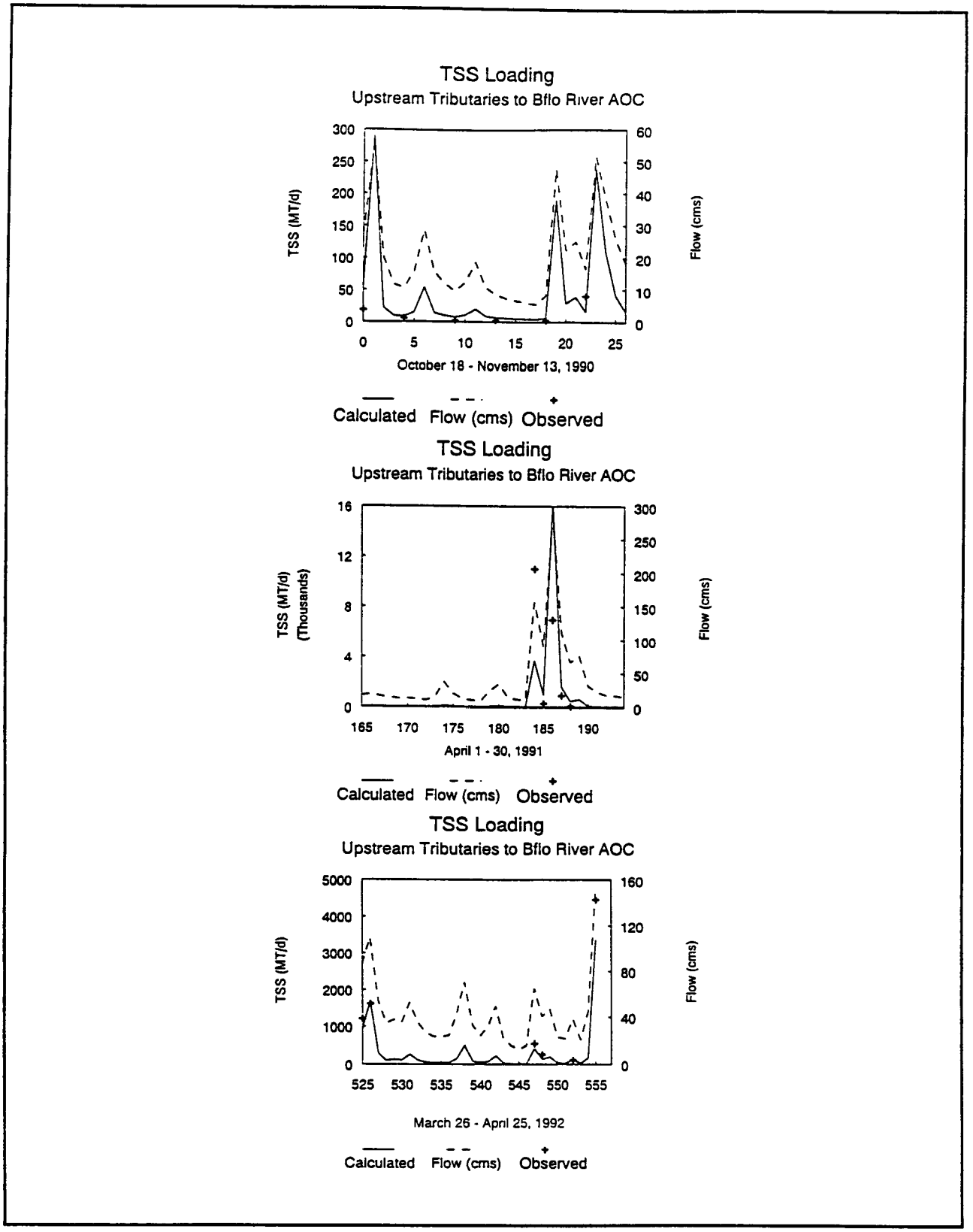


Figure 3-4. Predicted upstream TSS loadings vs. flow and actual data points

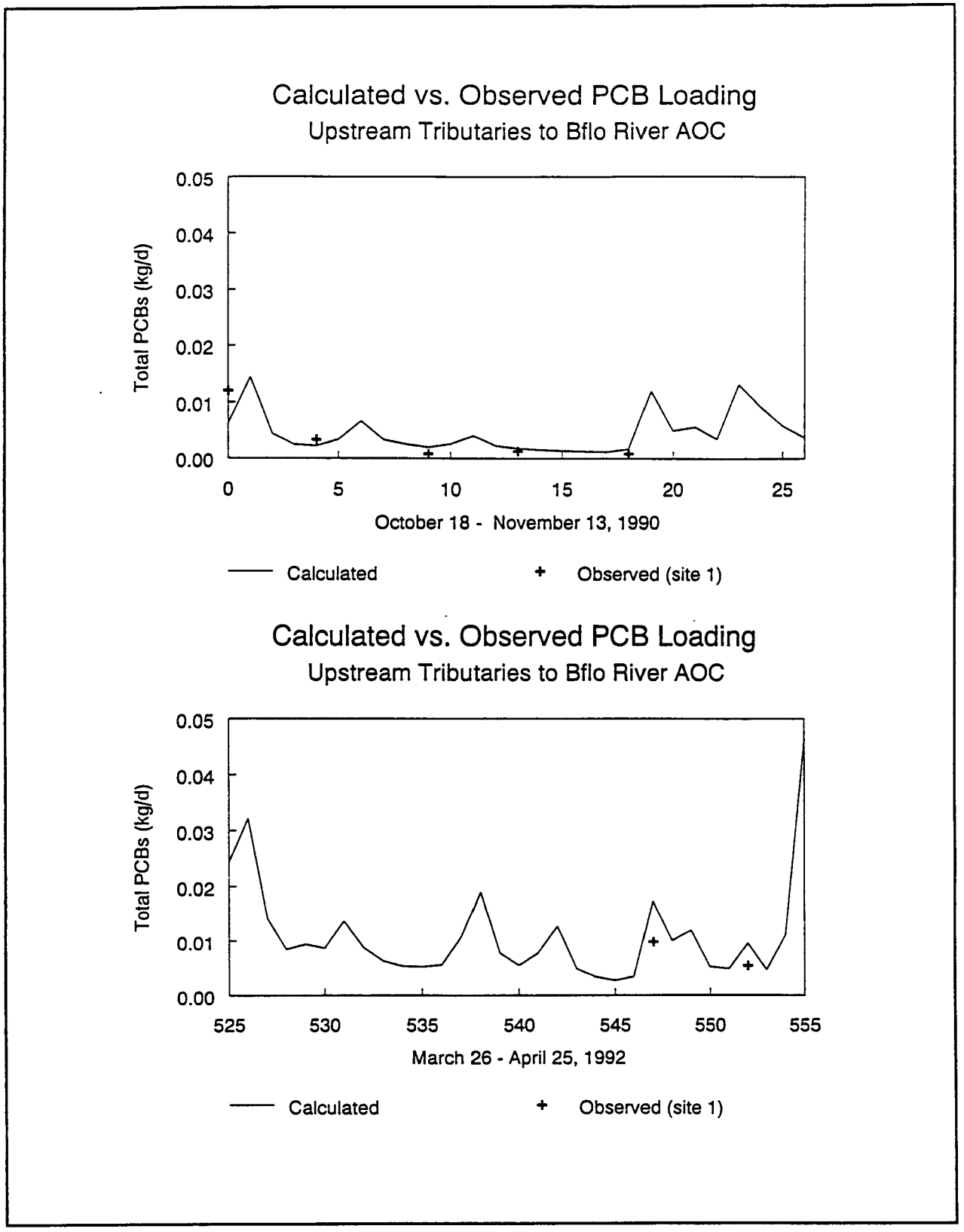


Figure 3-5. Predicted upstream PCB loadings and actual data points

The field-observed partition coefficients for dry weight solids ($K'_d$) (L/kg d.w.) were calculated from:

$$K_d = \frac{C_p}{[TSS]C_d} \tag{3-13}$$

For lead and copper, these values were used as input. For the organic chemicals, the field-observed partition coefficients were computed on an organic carbon basis ($K'_{oc}$) (L/kg org. carbon) using $f_{oc}$ calculated from data.

$$K_{oc} = \frac{K_d}{f_{oc}} \tag{3-14}$$

The partition coefficients (log $K_{oc}$ or log $K_d$) used as input for the model are listed in Table 3-3.

Table 3-3. Partition Coefficients for Contaminants

| Contaminant | log $K_{oc}$ (log $K_d$ for metals) |
|---|---|
| PCBs | 6.44 |
| B[a]a | 5.66 |
| B[a]p | 6.56 |
| Copper | 5.31 |
| Lead | 5.27 |

Spatial and temporal differences in the field-observed partition coefficients were analyzed in the loading report. However, these coefficients were kept constant for the entire time of simulation and for each segment. A strong correlation between the $K_{oc}$ values observed and values for the octanol-water partition coefficient ($K_{ow}$) obtained from literature was shown in the loading report.

The WASP framework internally computes an equilibrium partition coefficient ($K_p$) based on the field observed $K_{oc}$ and the time-series $f_{oc}$.

$$K_p = f_{oc} K_{oc} \quad (3\text{-}15)$$

The equilibrium partition coefficients for organic chemicals are influenced by the concentration of suspended materials. A particle-dependent partition coefficient ($K_{px}$)

$$K_{px} = \frac{K_p}{1 + \frac{[SPM]K_p}{\nu_x}} \quad (3\text{-}16)$$

is internally computed by the WASP framework.

where:

[SPM] = suspended particulate material concentration ($M/L^3$)

$\nu_x$ = particle interaction parameter.

The particle interaction parameter ($\nu_x$) values entered as input were either taken from similar values found in the Fox River (Endicott et al., 1991) or assumed to be large (i.e., not having a significant effect). For PCBs, a value of 9 was used. There was no evidence of this effect from data for b[a]a and b[a]p.

## Volatilization (Henry's Law Constants)

The volatilization rate ($K_V$) is internally computed in the WASP framework. The liquid and gas phase mass transfer rates are estimated from correlations. The liquid phase mass transfer rate was calculated using a modified form of the O'Connor-Dobbins reaeration correlation (O'Connor and Dobbins, 1958; Smith et al., 1981; Mills et al., 1982):

$$k_W = \left(\frac{D_W}{D_{O_2}}\right)^{0.5} \left[\frac{D_{O_2} U}{H}\right]^{0.5} = \left(\frac{M_{O_2}}{M_c}\right)^{0.25} \left[\frac{D_{O_2} U}{H}\right]^{0.5} \quad (3\text{-}17)$$

where:

$k_W$ = Water film mass transfer coefficient (L/T)

$D_W$ = Diffusivity of contaminant in water ($L^2/T$)

$D_{O2}$ = Diffusivity of oxygen in water ($L^2/T$)

U = Water velocity (L/T)

H = Depth of water column (L)

$M_{O2}$ = Molecular weight of oxygen (M)

$M_c$ = Molecular weight of contaminant (M)

Water column depth and contaminant molecular weight are required input parameters. The water velocity is internally computed by dividing the cross-sectional area for each segment by the flow. The ratio of the diffusivities is approximated from the molecular weight ratio.

The gas phase mass transfer rate was computed using the O'Connor-Rathbun correlation (O'Connor, 1988; Rathbun, 1990):

$$k_a = 0.001\left[\frac{D_a}{\nu_{air}}\right]^{0.667} U_{wind} \qquad (3\text{-}18)$$

where:

$k_a$ = air film mass transfer coefficient (L/T)

$D_a$ = diffusivity of contaminant in air ($L^2/T$)

$\nu_{air}$ = kinematic viscosity of air ($L^2/T$)

$U_{wind}$ = wind speed (L/T)

Wind is a required input parameter. Actual wind speeds collected from the Buffalo Greater International Airport for 1990 and 1991 were used in a repeated pattern. The kinematic viscosity of air ($\nu_{air}$) is internally computed in the framework based on air temperature. The diffusivity of the contaminant in air ($D_a$) is approximated in the framework from molecular weight.

The volatilization rate was based on these liquid and gas phase mass transfer coefficients:

$$\frac{1}{K_V} = \frac{1}{k_W} + \frac{RT}{k_a K_H} \qquad (3\text{-}19)$$

where:

$K_V$ = overall volatilization mass transfer coefficient (L/T)

R = universal gas constant ($L^3$-atm/°K-mol)

T = temperature (°K)

$K_H$ = Henry's Law Constant (atm $L^3$/mol)

Henry's Law Constants were taken from literature [see Buffalo River loading report (Atkinson et al., 1993)]. The values used are listed in Table 3-4.

Table 3-4. Henry's Law Constant for Organic State Variables

| Organic Chemical | Henry's Law Constant (atm $m^3$/mol) |
|---|---|
| PCBs | 3.86e-4 |
| B[a]a | 8.42e-8 |
| B[a]p | 4.90e-7 |

These values vary with water temperature. The following equation is used internally in WASP (Tateya et al., 1988):

$$\ln K_H = 18.53 - \frac{7868}{T} \qquad (3\text{-}20)$$

**Temperature**

Monthly temperature data from the Lake Erie boundary was used as input [see Buffalo River loading report (Atkinson et al., 1993)]. The values used are listed in Table 3-5 below. Stratification effects are known to occur in the Buffalo River (Atkinson and Blair, 1991), but the segmentation in the water column was kept as one-dimensional for this model. Thus, temperature was independent of depth and stratification.

The time for ice cover in the model was input as January 1 through March 31. This affected the reaeration across the air-water interface.

Table 3-5. Buffalo River Temperatures

| Month | Temperature (°C) |
|---|---|
| January | 0 |
| February | 1 |
| March | 1 |
| April | 8 |
| May | 17 |
| June | 21 |
| July | 22 |
| August | 19.5 |
| September | 15 |
| October | 9 |
| November | 4 |
| December | 1 |

**Initial Conditions**

The water column initial conditions were taken as the average of concentrations from six different sites collected on October 18, 1990. This was the initial time for the 1.5 year calibration runs and it was repeated for the 10-year predictive model input sets. The selection of water column initial conditions for a calibrated, predictive model is relatively arbitrary regarding the starting date since the concentrations quickly change.

Contaminant initial conditions for the sediment segments were selected from core sample data collected in the summer of 1990 [see Buffalo River loading report (Atkinson et al., 1993)]. The upper sediment layer in cores was a composite of the upper 24 inches (61 cm). Therefore, initial conditions for the top two sediment layers were the same since there were no finer-resolution core samples closer to the surface. The deep sediment layer initial conditions were found for each segment based on the core readings taken between 50 and 200 cm from the top.

The majority of the core samples were taken in nearshore areas, and there is comparable variability among depositional segment initial conditions. However, only two core samples were taken from the mid-channel region, and the average of these two readings served as the uniform initial conditions for erosional segments.

Initial conditions for TSS were uniform for each segment in all sediment layers. The bulk density for solids was used by multiplying 2.5e6 mg/L (1-porosity). A porosity of 0.15 was assumed and the initial TSS concentration was 3.75e5 mg/L.

## 3.2 DATA FOR MANAGEMENT APPLICATIONS

### Management Scenarios

Three primary remedial action scenarios were analyzed for the Buffalo River AOC using the modeling framework along with the input explained above. These management alternatives included:

1. No Action Scenario. This scenario focused on the system response over time under existing external loadings and continued navigational dredging. No additional actions on the river were simulated.
2. Hamburg Cove Scenario This scenario examined the impacts of discontinuing navigational dredging above Hamburg Cove, thus permitting this portion of the river to fill in with "clean" sediments from upstream. The potential for flooding exists as a result of this option.
3. Environmental Dredging Scenario. This scenario examines the impact of nearshore dredging along the entire river within the AOC. This option would remove several "hot spots" along the banks.

In order to determine the importance of resuspension on water column contamination, scenarios 1 and 2 were also evaluated with no external loadings. Everything else was kept the same, so any contamination of the water column would be strictly from sediment resuspension.

4. No Action - No Loading Scenario.
5. Hamburg Cove - No Loading Scenario.

Two additional scenarios were modeled to aid in the analysis of the other scenarios.

Although not practical management options, the results aided interpretation of the other remedial action scenarios.

6. Zero Initial Conditions Scenario. Similar to Scenario #3, the initial conditions in the top two layers of sediments (depositional and erosional) were set to zero. This effectively nullified currently contaminated sediments as a source of water column contamination. Thus, the sole impact would be from external loading.

7. Flow Switching Scenario. Two years of actual flow data were switched with each other to evaluate the effect on cumulative export and concentrations in the no action scenario. The flows from 1978-79, which contained several high flow events, were switched with those from 1970-71, which had no events, and vice versa. The results showed the importance of the sequence of high flow events in altering the final results.

**Navigational Dredging Approach**

Ten year predictive runs were chosen for model simulations of each scenario. During these runs, it was necessary to simulate navigational dredging, which is carried out regularly by the U.S. Army Corps of Engineers. A dredging schedule is not followed by the USACE as dredging is performed when an excess accumulation of solids exist. Since relatively minor amounts of solids typically accumulate in one year, it was decided that dredging would be implemented into the model simulations at the end of every two years. This necessitated the formation of five, two-year input sets for each scenario.

At the end of each two-year simulation, the net amount of solids (TSS) that had accumulated during the period was removed. The procedure for this "artificial" navigational dredging involved several steps. The total mass of TSS deposited in the two years was found by subtracting the mass resuspended from the mass settled. This net mass deposited [kg] was converted to the volume of TSS deposited [$m^3$] through division by the bulk density of solids in the sediments (3.75e5 $g/m^3$). The depth of solids deposited (cm) was then found by dividing the volume of TSS deposited by the surface area of the entire sediment-water interface (7.22e5 $m^2$). This depth was then dredged uniformly from the erosional sediment segments, and the sediment layers were then reinitialized as shown in Figure 3-6.

The WASP framework maintains constant segment volumes and depths in each of the three sediment layers. As shown in Figure 3-6, over the course of two years, 8 cm of solids accumulated on top of the original sediments. However, the model continuously treats the top 10 cm as sediment layer 1, the next 50.5 cm as layer 2 and the following 200 cm as the deep layer. The "artificial" dredging process removed the solids that had accumulated over each two-year period. The contaminant concentrations in the erosional sediment segments were than reinitialized corresponding with their removal. The given depth of solids was "removed" from the top of the sediments and the three layers were adjusted accordingly. A depth weighted average of concentrations was then used for reinitializing the sediment concentrations.

The layer 1 concentrations (from the last day of run 1) were multiplied by the ratio (difference between 10 cm and the depth dredged). These values were added to the product of layer 2 concentrations and the ratio: depth dredged/10 cm. The resulting values were the initial conditions in layer 1 segments for the next 2-year model run.

The new layer 2 initial conditions were found in a similar fashion. The layer 2 concentrations (from the last day of run 1) were multiplied by the ratio of the difference of 50.5 cm and the depth dredged to 50.5 cm. These values were added to the product of the layer 3 concentrations and the ratio of the depth dredged to 50.5 cm. The resulting values were the initial conditions in layer 2 segments for the next two-year model run.

The deep layer was not adjusted. The same concentrations from the last day of run 1 were used as the initial conditions for run 2. This assumed that contaminant concentrations below the 200 cm deep layer were the same as those in the deep layer. Deeper core records were not available beyond this depth throughout the river. In the 10-year modelling scenario, dredging did not reach the deep sediments directly.

Because the removal of the "cleaner" solids settled in 2 years, the reinitialized sediment contaminant concentrations increased. The greater the depth of solids dredged, the greater the increase in concentrations will be after reinitializing. The reinitialized sediment concentrations showed an increase in contaminant concentrations through the years as more contaminated sediments were exposed. In addition, water column contamination increased due to the resuspension of more contaminated sediments after dredging.

This method of dredging is purely for modeling purposes only. The effect of navigational dredging is merely simulated. The modeled dredging occurs instantaneously between the last day of run 1 and the first day of run 2.

Navigational dredging is an imprecise practice that is difficult to characterize physically. Translating all of the dredging phenomena into a modeling framework would be even more complex. A lack of full dredging records and data make application of a dredging approach into this model impossible without several assumptions. Since the approach used in this model is "artificial", several caveats are necessary.

The caveats include the fact that effects of sloughing were not accounted for in the dredging approach. After actual dredging, sediments that were stirred up from both outside and inside the dredging area often fill in over the dredged channel. Sloughing of nearshore sediments would include cleaner solids that have recently deposited. If these cleaner solids resettle on top of the post-dredging new sediment layer characterized with higher concentrations, the sediment exposure from dredging could be overpredicted by the approach used in this model. However there are no dredging records available that indicate how much the mid-channel sediment is affected by sloughing.

The dredging approach used in the management scenarios also implies that dredging is precise and accurate. Having several centimeters exactly removed from an actual dredging process is completely impractical. The machinery used for dredging tend to disturb the sediments below the desired dredging depth. Overdredging also frequently occurs to compensate for sloughing. These possible disturbances of deeper sediments (with higher concentrations) is not accounted for in this modeling framework. Resettling of spilled dredged materials is also not considered.

Finally, in this simulated dredging approach, it was assumed that a uniform depth of solids was dredged throughout the entire length and width of the channel in the erosional zones. In actual dredging processes, this is not likely to occur. Deposition of solids is certainly unlikely to occur in even amounts throughout the river. The sediment segments are viewed like "boxes" by the model and not like a true river cross-section.

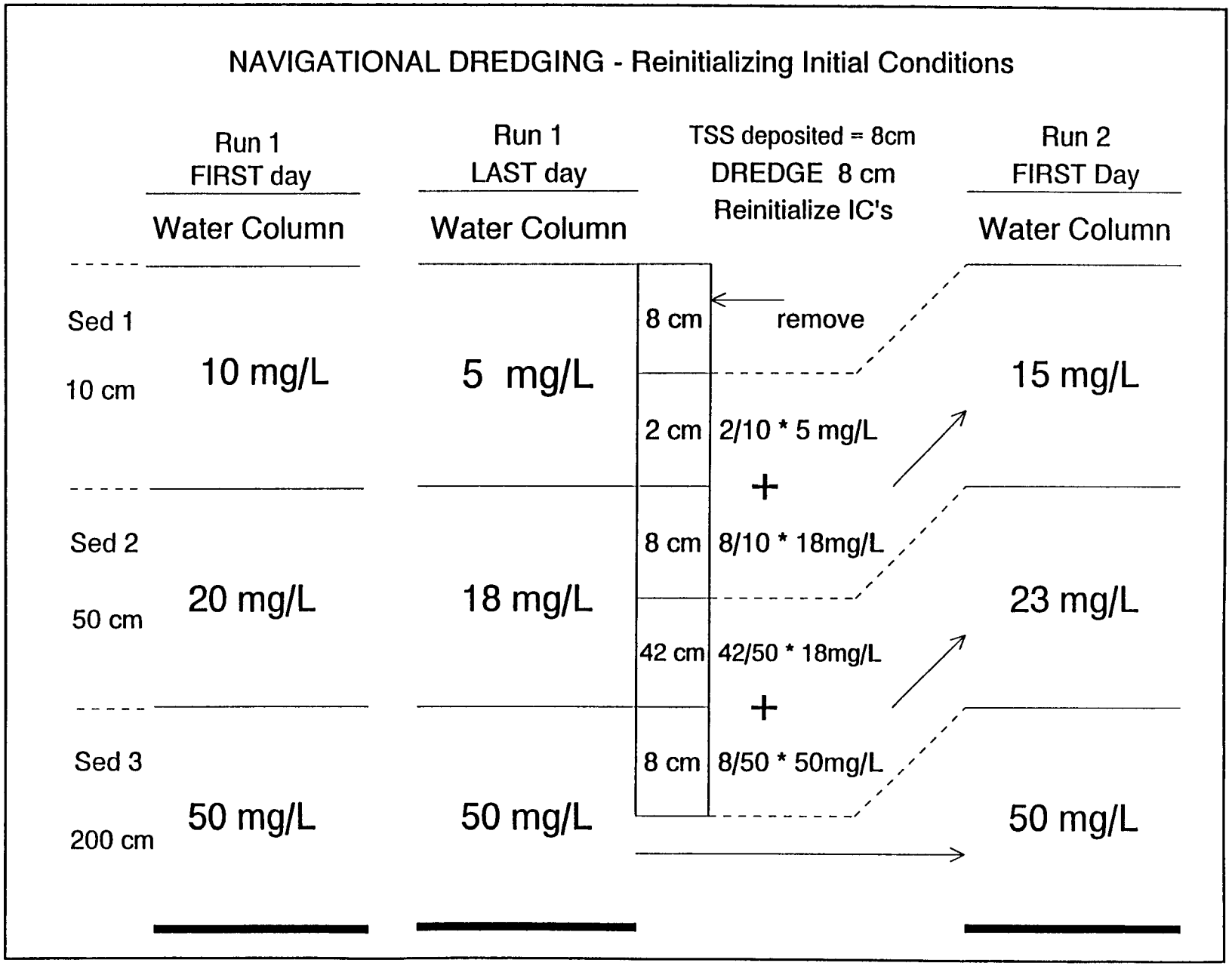


Figure 3-6. Navigational Dredging Approach

Although many of the complexities of dredging are not accounted for in the approach used in this model appication, it was a practical way of dealing with the effects of dredging. In effect, only a small depth of sediments are actually dredged. However, there is no question, based on core data collected in the river (Atkinson et al 1993), that deeper sediments are more highly contaminated than near surface sediments. Therefore, it is likely that the impact of the sediment resuspension on water column contamination may actually be overpredicted with this navigational dredging approach.

Since TSS loadings were constant for all scenarios except Flow Switching, the depths dredged were the same. Table 3-6 lists the depth [cm] of sediments dredged at the end of each two year period.

Table 3-6. 2-year accumulations of TSS

| Modeling Period (Flow years) | Accumulation in 2-yr period [cm] |
|---|---|
| 1970-71 | 4.42 |
| 1972-73 | 9.71 |
| 1974-75 | 5.17 |
| 1976-77 | 11.45 |
| 1978-79 (replaced 1970 in scen. 7) | 6.57 |

**Modeling Approach for Management Scenarios**

It was necessary to handle each scenario differently within the modeling framework and/or dredging procedure. The approaches taken to each scenario are listed below.

1. No Action. Full navigational dredging was applied every two years to the erosional sediment segments. The initial conditions for the water column and depositional sediment segments were the concentrations from the last day of the previous run.

2. Hamburg Cove. Navigational dredging was only applied in the erosional sediment segments

downstream of Hamburg Cove (water column segment 17). Erosional sediment segments between 33 and 63 (95 to 125 in the second layer sediments) were not dredged. The initial conditions for these segments were taken as the concentrations from the last day of the previous run.

3. Environmental Dredging. Nearshore, environmental dredging was simulated prior to the 10-year predictive run by setting the depositional sediment segment initial conditions to zero in the top 2 sediment layers. Full navigational dredging was carried out in the river.

4. No Action - No Loading. The same approach was taken as the No Action scenario except that all external loadings (upstream, CSO, industrial, groundwater) were set to zero.

5. Hamburg Cove - No Loading. The same approach was taken as the Hamburg Cove scenario except that all external loadings (upstream, CSO, industrial, groundwater) were set to zero.

6. Zero Initial Conditions. The initial conditions were set to zero in every segment (depositional and erosional) in the top two sediment layers. Full navigational dredging was applied.

7. Flow Switching. The same approach as the No Action scenario was followed except that flows and loads for the input sets of 1970-71 and 1978-79 were completely switched.

# SECTION 4

# CALIBRATION

## 4.1 WATER TRANSPORT MODEL TRACER CALIBRATION (TDS)

WASP4 was used to model the effects of advection (flow) and dispersion (mixing) in the water transport submodel. Since actual Buffalo River flows were used, calibration of advection was not necessary. Dispersion, or turbulent mixing, was calibrated using conductivity. Conductivity is a water quality parameter that characterizes the ability of a solution to conduct an electrical current. It behaves as a conservative material (or tracer) since it is only affected by advection and dispersion in the water column. A 1.5 year model simulation was run from October 17, 1990 through April 30, 1992.

The TDS model was calibrated strictly through the adjustment of the dispersion coefficient [$m^2/s$]. Dispersion coefficients vary temporally and spatially in the Buffalo River. They were found to be the greatest in the spring and fall. The impact of dispersion was insignificant during the ice cover period (January 1 - March 31) and also of lesser significance during a low flow period (May 6 - November 28). Dispersion has the greatest effect on the Buffalo River near Lake Erie. The further upstream stretches are not affected as much by mixing and seiche actions from the lake. The calibration results are listed in Table 4-1.

Table 4-1. TDS-Calibrated Dispersion Coefficients

| River stretch | segments | Jan 1 - Mar 31 | May 6- Nov 28 | rest of year |
|---|---|---|---|---|
| upstream | 1-6 | 0 | 0 | 5 |
| midstream | 7-17 | 0 | 5 | 15 |
| downstream | 18-31 | 0 | 10 | 25 |

Using the dispersion coefficients listed above, results were obtained which can be seen in figure 4-1. The model output compared well with field data in all three reaches of the river as

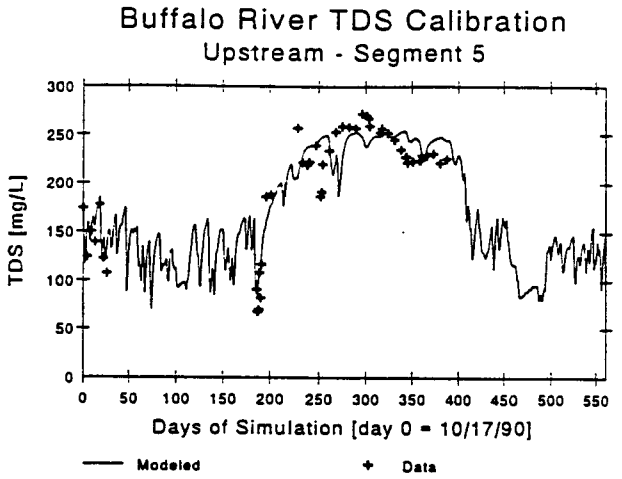


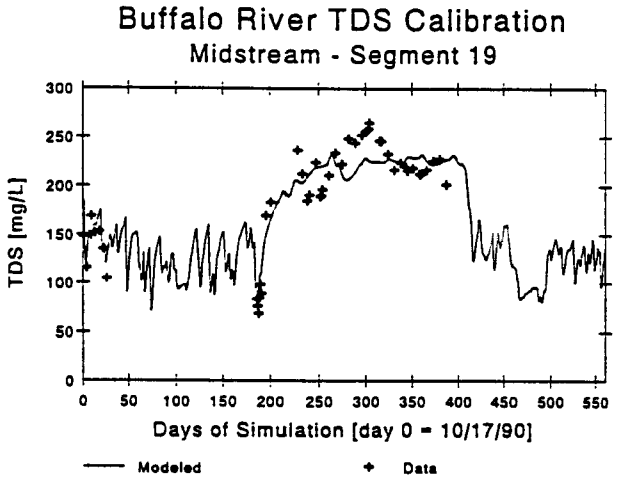


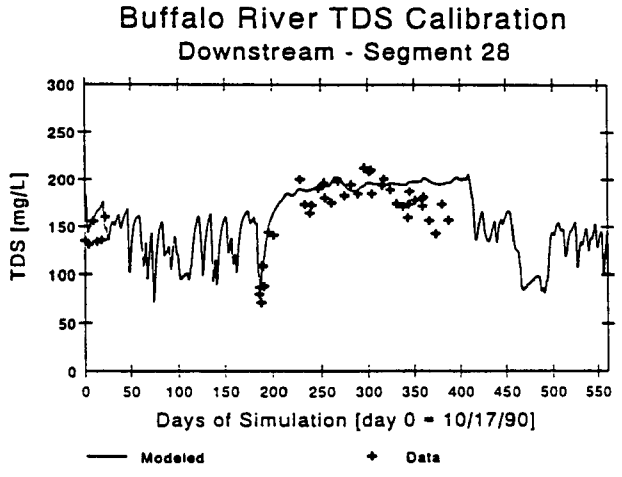


Figure 4-1. TDS Calibration for upstream, midstream, & downstream segments

seen in the figures. The water transport submodel was considered calibrated since the model output matched the field data rather well.

The temporal profiles of TDS are strongly influenced by flow. TDS concentrations are low during periods of high flow because of dilution. In periods of low flow, mainly during the summer months, the TDS concentrations show the influence of Lake Erie. TDS concentrations are steady around the boundary Lake concentration of 175.4 mg/L during low flow periods.

## 4.2 SEDIMENT TRANSPORT MODEL CALIBRATION (TSS)

The sediment transport submodel was calibrated using the WASP4 framework. Total suspended solids (TSS) were modeled for a 1.5 year period (October 18, 1990 - April 30, 1992). The solids dynamics formulations of Gailani / Lick were used to calibrate the model output to actual data. The approach used for the Fox River calibrations was applied to the Buffalo River (Endicott, et al. 1991). The resuspension formulations remained the same as in the Fox River study while the settling relationships were adjusted to the Buffalo River (see section 3.1). Using these formulations, settling rates and resuspension rates based on Buffalo River flow were entered as input into the model. The results came out satisfactory as seen in Figure 4-2. It was determined that no further adjustments were necessary since the data was matched as closely as possible.

It was difficult to calibrate for very high flow events since there was no applicable data. The TSS loading regressions were slightly biased by the lack of high-flow data points. This reduces the confidence of TSS loadings during high-flow events.

## 4.3 CONTAMINANT TRANSPORT MODEL (ORGANIC CHEMICALS, METALS)

With the water transport and sediment transport submodels already calibrated, only adjustment of partitioning remained for calibration of the contaminant transport model. Similar to the TSS modeling, a 1.5 year period (October 18, 1990 - April 30, 1992) was modeled using WASP. The field-observed partition coefficients ($K_{oc}$ or $K_d$ for metals) were entered as input along with $f_{oc}$ values calculated from sample data. The overall partition coefficients (PCBs, B[a]a, B[a]p) and distribution coefficients (Lead, Copper) were used for the entire 1.5 years.

Seasonal differences in these coefficients were found in the Buffalo River loading report (Atkinson et al., 1993) but the WASP framework did not allow temporal variation of partition coefficients. The fall data points were matched better with the model output using fall partition coefficients and likewise for spring. The overall values were the best for year-round conditions (see Table 3-3) and the model results came out good with their use.

The water column $f_{oc}$ values calculated from data were dropped in favor of a seasonal variation. A constant value of 0.20 was held from June 1-September 15 and dropped to 0.05 on January 1. Linearly-interpolated values were internally computed from January 1 through June 1 and September 15 through January 1 in the WASP model.

Acceptable data for lead and copper was limited leaving segment 19 as the only site for calibration with model output. The results can be seen in figure 4-2. Organic chemical model output was compared to data collected at 5 sites. The results for the midstream data site (segment 9) can be seen in figure 4-3. The model output matched fairly well with the sample data at each site. Similar to the TSS calibration, high flow periods were difficult to calibrate due to a lack of data during events. Since the contaminant transport model was parameterized as accurately as possible given the available data, it was deemed acceptable to run the management scenarios on a 10-year basis.

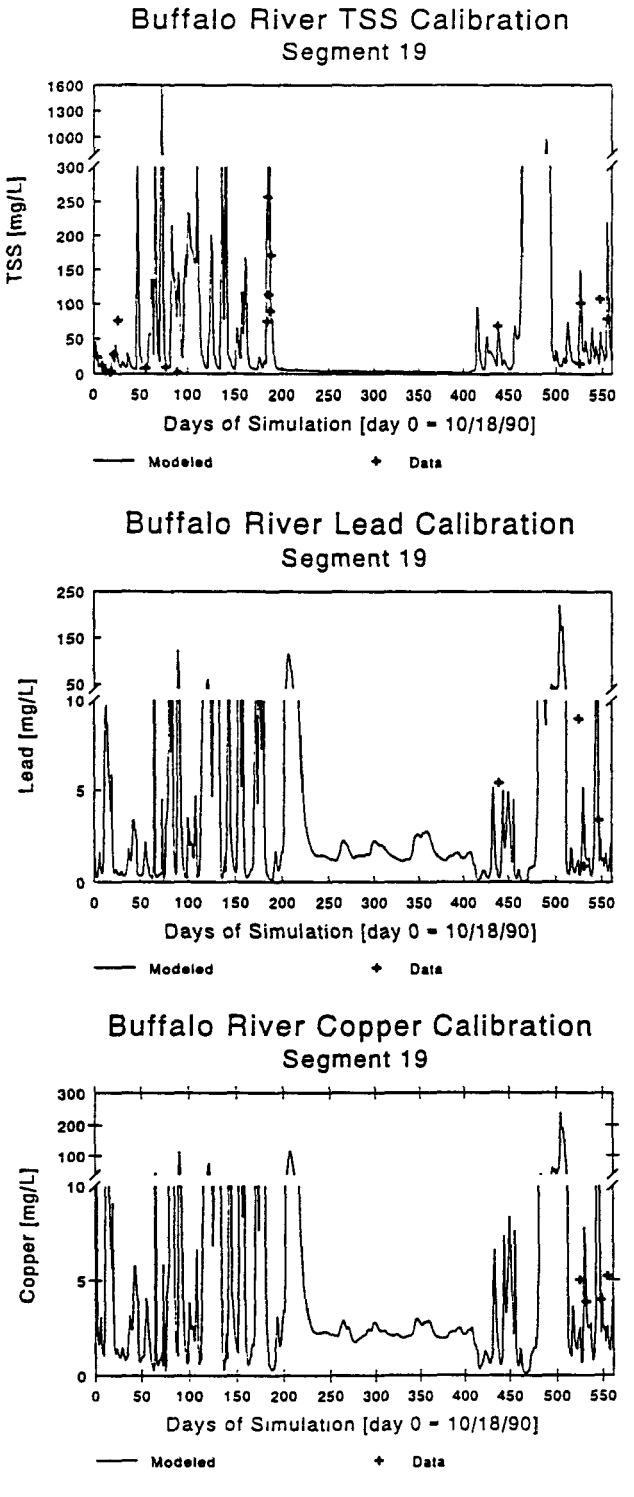


Figure 4-2. TSS and Metals calibration for midstream segment

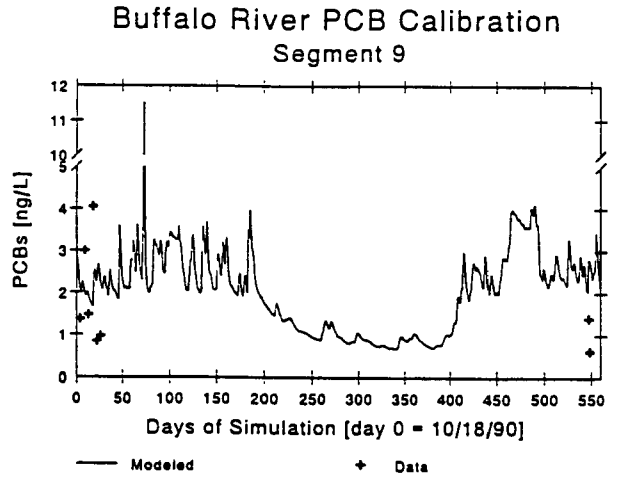


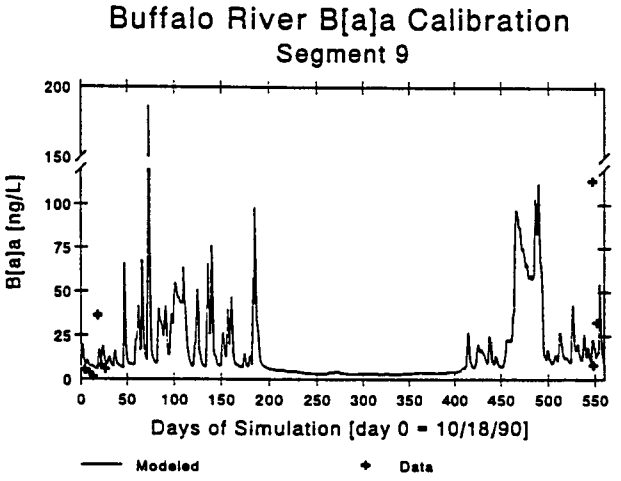


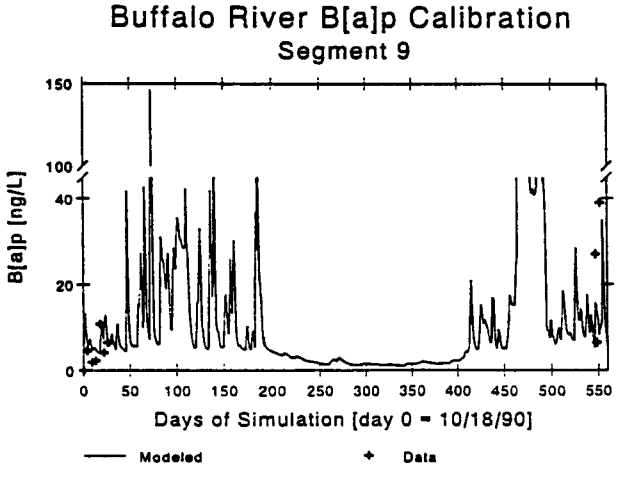


Figure 4-3. Calibration of organic chemicals at midstream segment

# SECTION 5

# MODEL APPLICATION

## 5.1 DIAGNOSTIC APPLICATIONS

One of the advantages of having a calibrated mass balance model for a system like the Buffalo River is that the model may be used as a diagnostic tool to develop a quantitative understanding of the dynamic behavior of the state variables and the relative significance of the processes at work in the system. In this subsection, we will use the Buffalo River model to investigate those model processes and associated parameters that affect the temporal and spatial variability of solids and toxic substances in the river water column and sediments. We will also identify those sources that are most responsible for the observed environmental exposure concentrations and mass fluxes.

**Water Column and Export Analysis**

Results from the no action scenario showed that downstream water column concentration peaks were greater than the upstream peaks. This results from the resuspension of contaminated sediments during high-flow events. Figure 5-1 shows the water column concentration of PCBs for an upstream segment and a downstream segment in the no action scenario over the full 10-year modeling period. Downstream locations have higher peak concentrations since resuspended contaminants from the full length of the river add to the concentration due to upstream loading. The upstream peaks are due almost exclusively to loading as significant resuspension occurred for only a limited length of the river (narrow channel from segments 20-25). Water column concentration peaks occur on high flow days due to greater loadings during events and resuspension of in-place pollutants into the water column. Resuspension is a factor in water column contamination only during high flow events ($Q > 350\ m^3/s$) as shown in figure 5-2.

Another noticeable difference between upstream and downstream water column concentrations occurs during low-flow periods. Note in Figure 5-1 that the downstream low-flow concentration levels are rather steady near the Lake Erie boundary at a value close to the

boundary condition. The upstream low-flow concentrations show more variation and dip to lower levels. Dispersion has a stronger effect on the downstream segments since they are closer to Lake Erie. Dispersion is not a significant factor in the upstream segments and it is not an important mass transport process at higher flows relative to advection.

The results from the model simulations show that significant export [kg] of solids and contaminants into Lake Erie occurs primarily during high flow days. Since greater loadings happen on days with higher flows, export levels increase through advection and dispersion of the large loadings. The contribution from resuspended contaminated sediments is significant to contaminant export during high-flow events as well.

The loading and export of TSS are shown on a daily basis over a 180-day period (including a major high flow event around day 155) in Figure 5-2. The daily TSS loadings are always greater than the TSS export. This demonstrates a net deposition of solids even during major resuspension events.

For PCBs and other contaminants, daily loadings are greater than daily exports except during big event periods. Figure 5-3 shows the loading and export over the same 180 day period shown in Figure 5-2. Unlike TSS, PCB export is greater than its upstream loading during the event period due to the net resuspension of contaminants
into the water column. This can only occur if the contaminant concentrations on the bottom sediments are greater than the concentrations on suspended sediments from upstream loadings.

In two-year model periods having numerous high flow events (1972-73, 1976-77, 1978-79), the loading mass fluxes for organic chemicals are less than the export mass fluxes. However, as seen in figure 5-4 for PCBs, the loading mass fluxes for two-year low flow periods (1970-71, 1974-75) are greater than the export mass fluxes for those times. Figure 5-4 also shows that the lead loading mass fluxes are greater than the export mass fluxes even in the high flow years. Resuspension is typically more significant for organic chemicals than metals due to greater variation between the concentrations on suspended sediments from upstream and bottom sediment concentration levels. The resuspension effect is accentuated in model periods with a greater number of high-flow events. This phenomena is discussed later in the Analysis of TSS and Contaminant Mass Fate portion of this section.

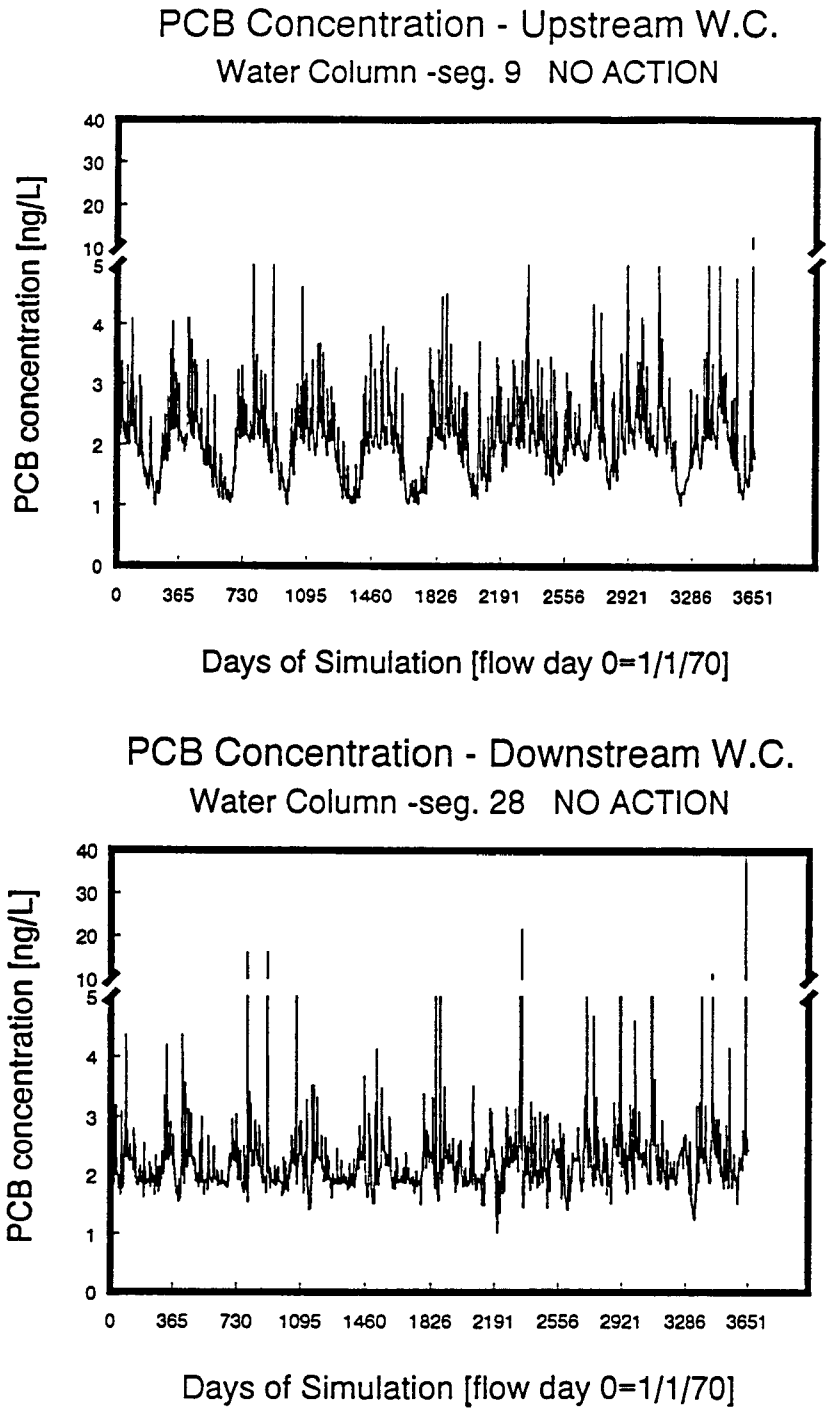


Figure 5-1. Ten year daily water column PCB concentrations for an upstream and downstream segment in the no action scenario.

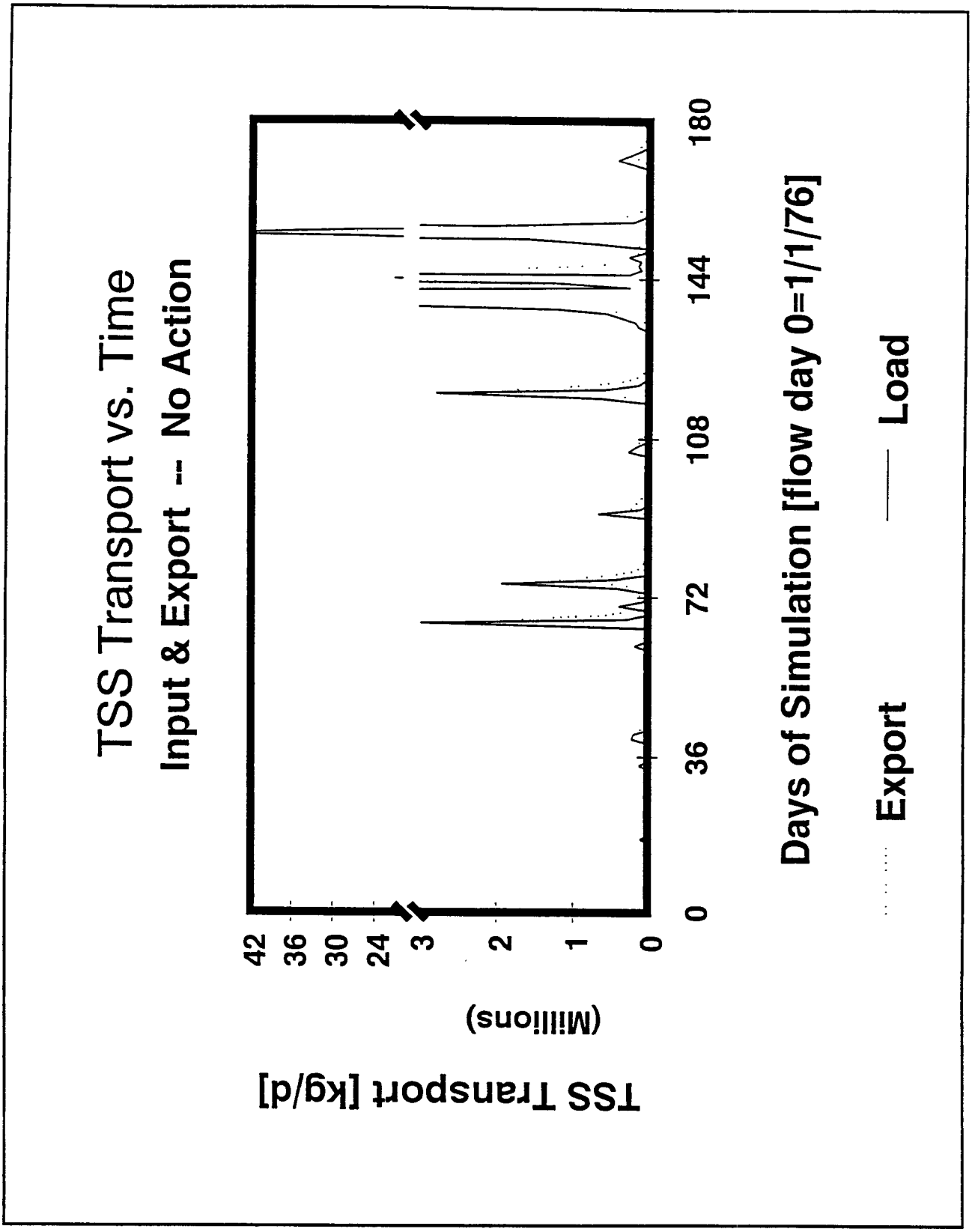


Figure 5-2. Comparison of daily TSS loading and export in the no action scenario

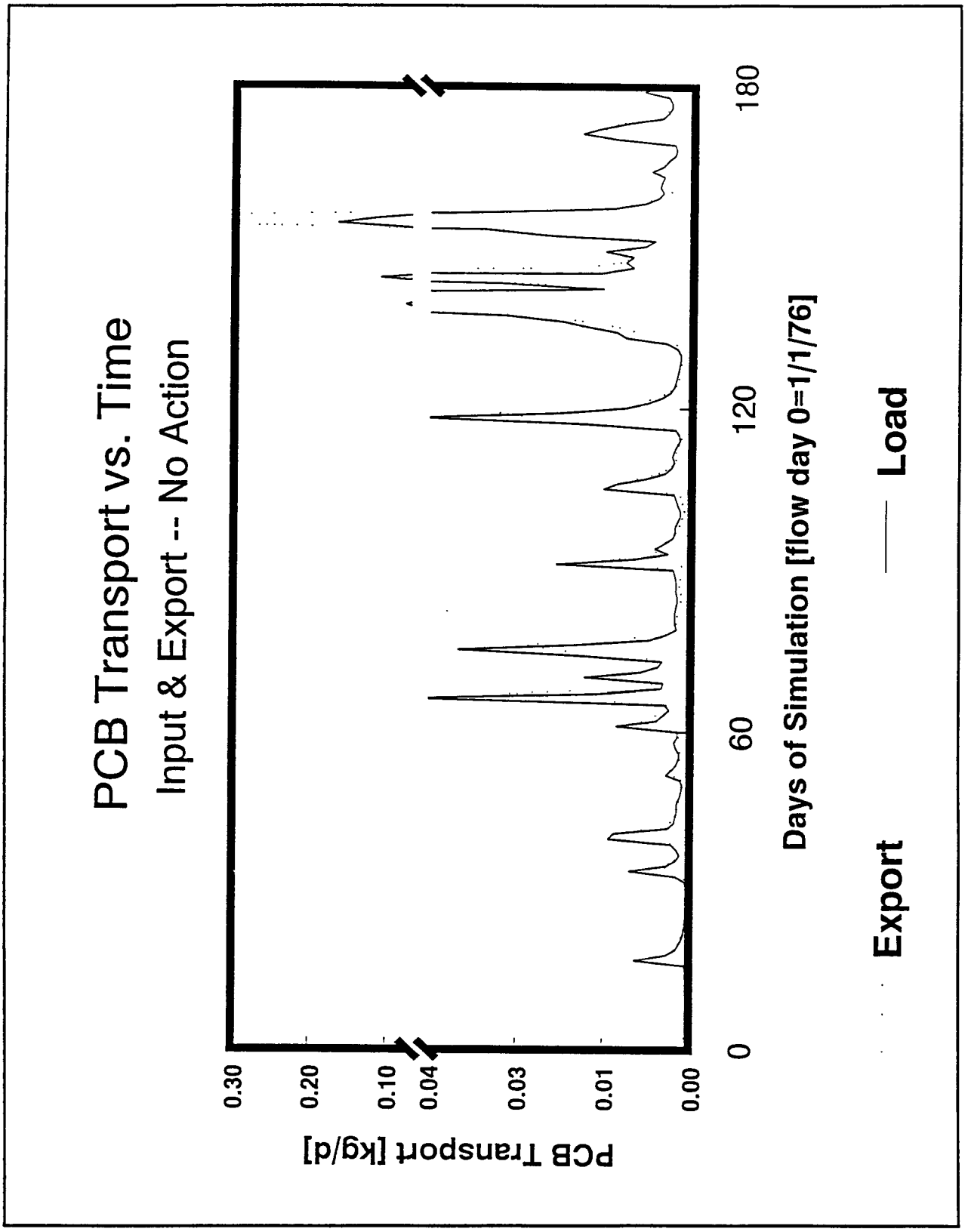


Figure 5-3. Comparison of daily PCB loading and export in the no action scenario

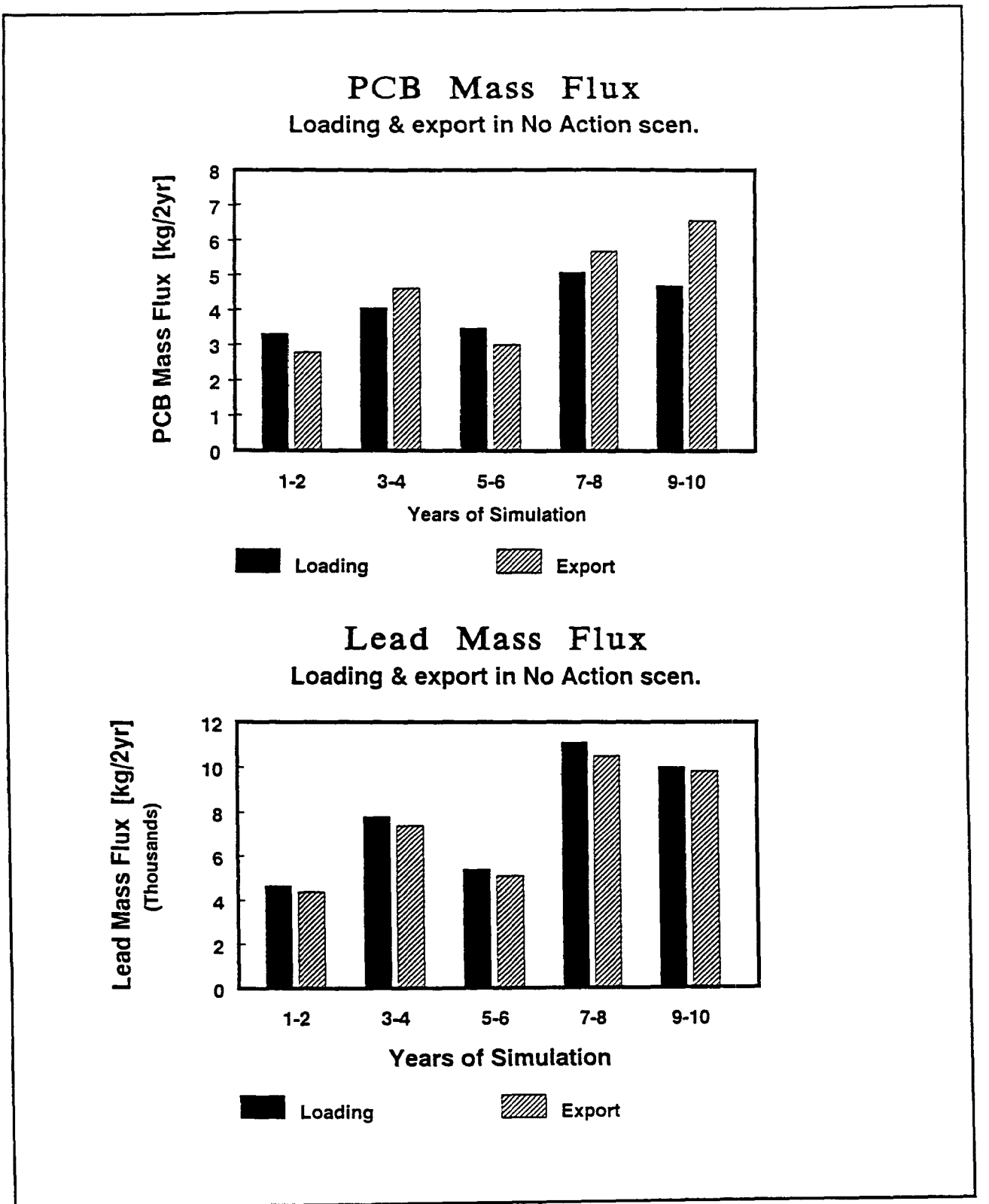


Figure 5-4. Loading and export during 2-year intervals for PCBs and lead in the no action scenario.

Contaminant export from event periods is a major component of the export flux during the two-year model periods in the no action scenario. Figure 5-5 shows that event export PCB flux makes up approximately half of the two-year cumulative export PCB flux in high flow years. The maximum 1-day PCB export for each model period is also shown in Figure 5-5. The PCB export contribution from one high flow day is nearly 1 kilogram during the last model period in the no action scenario. This shows the significance of events in the Buffalo River system, especially in high flow years.

**Sediment Analysis**

A 10-year profile of contaminant concentrations in the top (10 cm) layer of sediments for the no action scenario reveals a gradual decline in concentrations between dredging events (see Figure 5-6). The gradual decline between dredging events is due to continual deposition of "cleaner" (ie. lower PCB concentration) suspended sediments originating upstream of the modeled section of the river. Dredging brings about a virtually instantaneous rise in the sediment concentration levels. This occurs four times in the 10-year period since the dredging approach was implemented at the end of each 2-year model run. It was not necessary to dredge after the 10th year since the simulation time was completed. Higher contaminant concentrations exist deeper in the sediments. When the dredging approach was applied, cleaner sediments that had settled in the previous 2-year period were removed. Through re-initialization of the sediment concentration conditions, the concentration levels increased with the influence of the deeper sediments (see earlier dredging discussion in Section 3).

Sharp drops in the sediment concentration profile occur during high flow events. These drops are the result of resuspension of contaminated sediments into the water column and deposition of cleaner sediments from upstream. As discussed earlier, water column concentrations increased during high flow events in part because of resuspended contaminants which are transferred from the erosional sediments to the water column. Since there is a higher rate of sediment exchange with the water column and a net resuspension affect during high flow events, contaminant concentrations in the top erosional sediment layer decrease.

As seen in Figure 5-6, downstream erosional sediment concentration levels are only

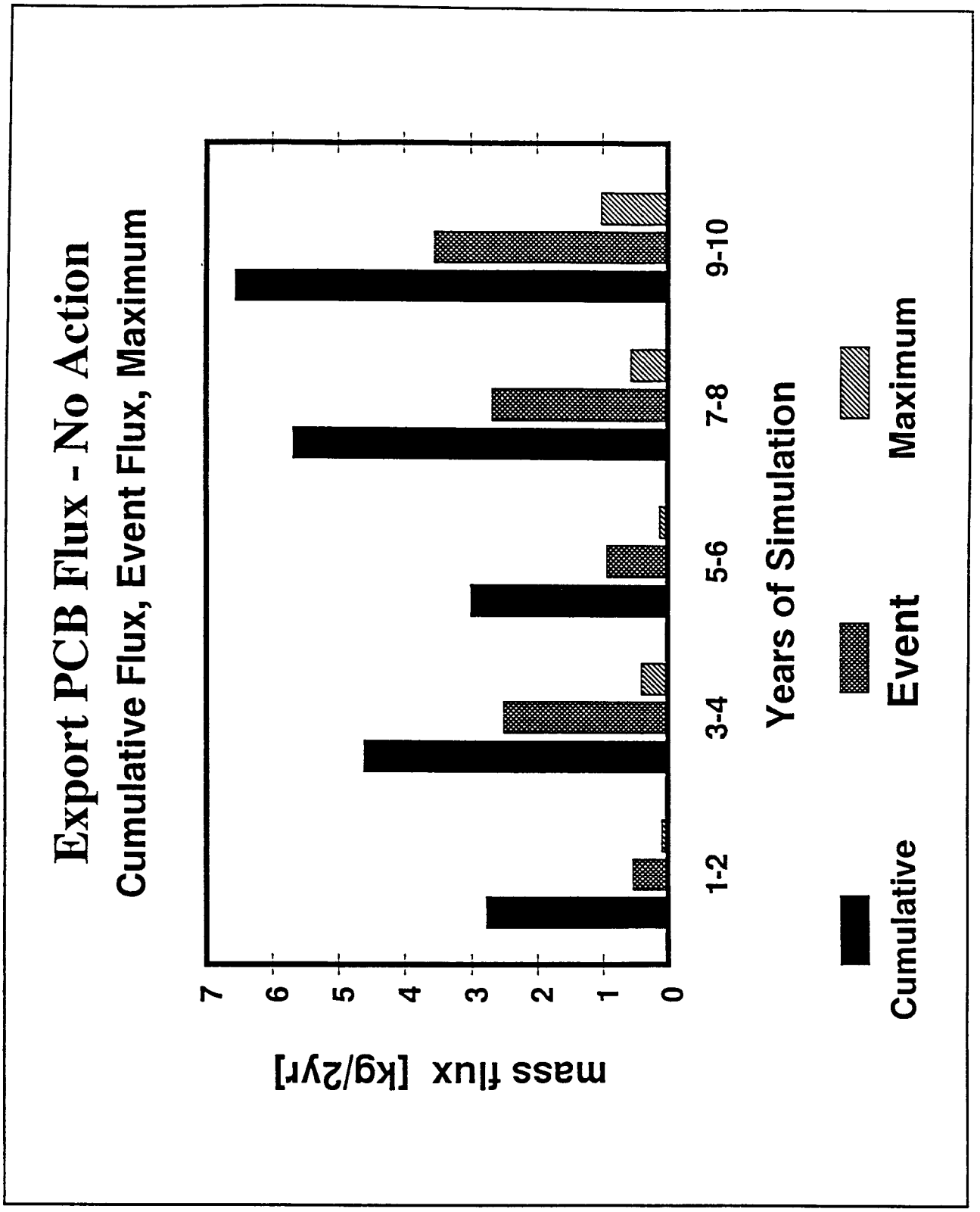


Figure 5-5. Two-year cumulative event period and maximum daily export PCB fluxes for the no action scenario

slightly greater than those upstream. This is due in part to the resettling of resuspended contaminants from upstream. There are also smaller settling rates in the downstream segments. On average, solids particles that settle downstream from loadings are finer than those settling upstream. There are greater contaminant concentrations on these smaller particles as discussed earlier in this chapter. This factors into slightly greater sediment concentrations downstream than those upstream.

The depositional sediment segments showed a gradual decline throughout the 10-year period in the no action scenario (see Figure 5-7). Similar to the erosional sediments, sharp drops occurred in the depositional sediment concentration profile during high flow events. Since resuspension rates were not increased during high flow periods in the depositional sediments, the decrease in concentrations was due to a net deposition of cleaner sediments. The nearshore areas were not included in the navigational dredging approach, so there are no sharp rises in the depositional sediment concentrations. As seen in Figure 5-7, the downstream initial concentration for PCBs is much higher than the value for the upstream segment. This is because the specific downstream segment chosen was a "hot spot". There is not necessarily a spatial trend of increasing concentrations heading downstream.

**Analysis of TSS and Contaminant Mass Fate**

The predicted mass fate of state variables was generated by WASP for each 2-year simulation. These mass budgets show various fate pathways for contaminant and TSS mass within the model boundaries during the 2-year period. Fate pathways in the model include loading, advection, dispersion, volatilization, settling, resuspension, burial, diffusion and scour. These pathways serve as net sources, net sinks or represent internal cycling of contaminant and TSS mass. The predicted mass fate of B[a]a and TSS in the Buffalo River are shown in figures 5-8 and 5-9 respectively for the no action scenario over selected 2-year periods. The sediment reservoir is the mass contained in the top two sediment layers.

For B[a]a, and other modeled contaminants, the volatilization and sediment diffusion (porewater transport) pathways are clearly insignificant. Approximately zero kilograms were cycled for each contaminant for every 2-year period in all scenarios. The remaining pathways

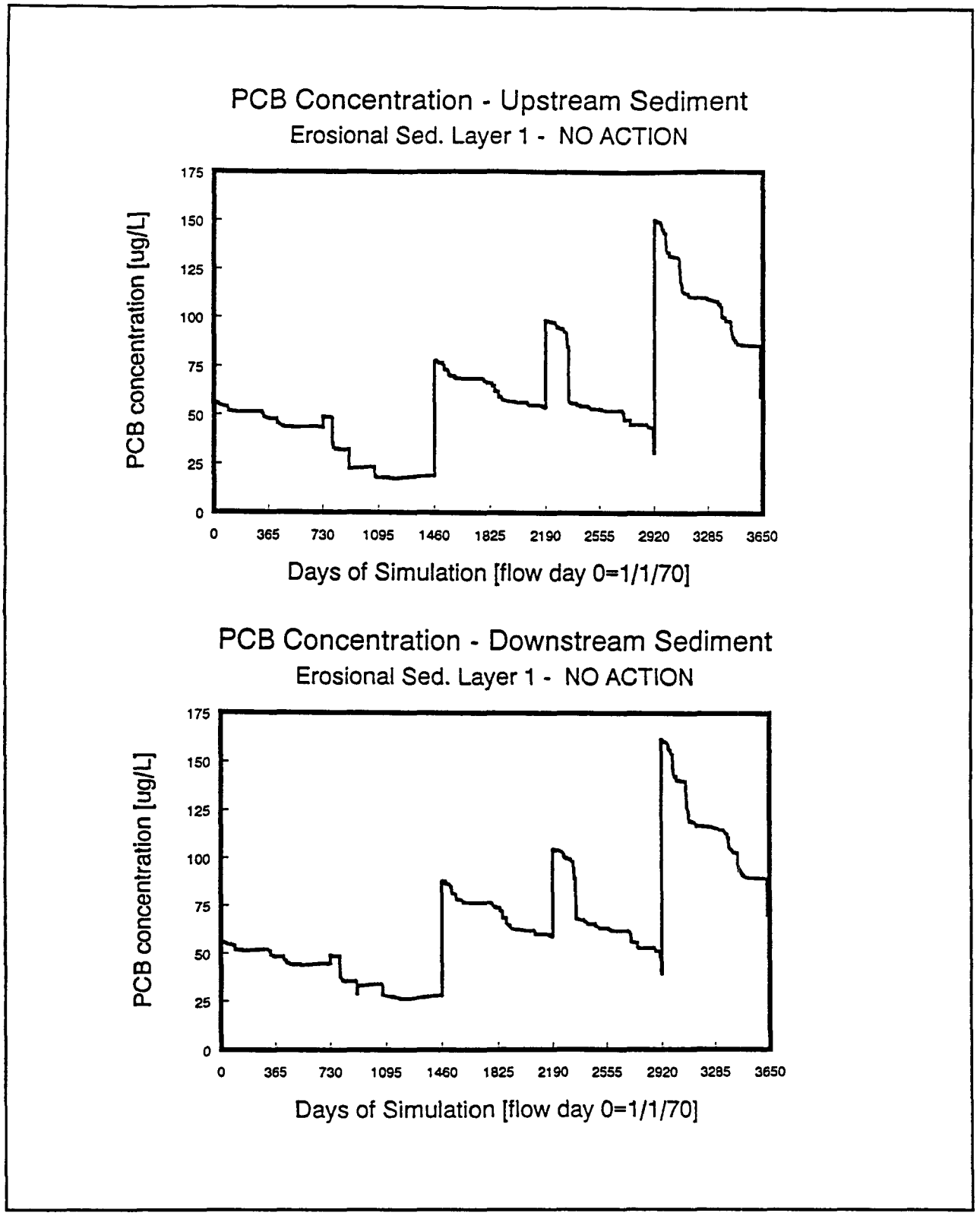


Figure 5-6. Ten year erosional sediment PCB concentrations for an upstream and downstream segment in the no action scenario

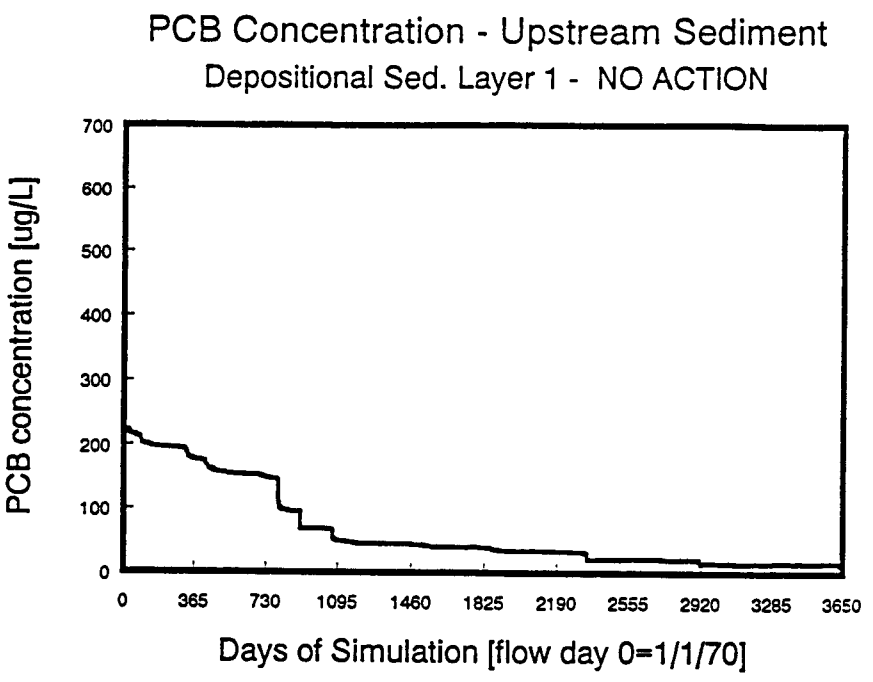


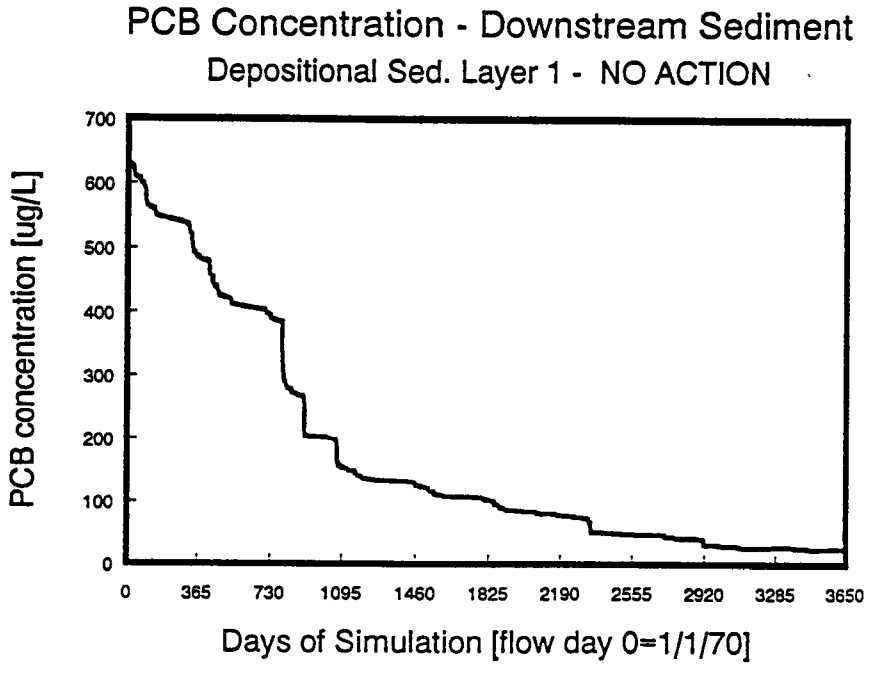


Figure 5-7. Ten year depositional sediment PCB concentrations for an upstream and downstream segment in the no action scenario.

were all significant in the sense that predicted non-zero values were obtained for mass fate.

Significant cycling occurred in the sediment through settling, burial, scour and resuspension. Settling and resuspension fluxes were greater for years with a greater number of high flow events. TSS settling greatly exceeded resuspension in each 2-year period. This deposition of settled solids was taken care of by the dredging approach for this model. The contaminant settling and resuspension were strongly influenced by the TSS fluxes.

Lead and copper were similar to TSS since settling exceeded resuspension each year in the no action scenario. For metals and TSS, the Buffalo River sediment always acted as a net sink in the 10-year period. However, the sediments acted as a net source in three out of five modeling periods for the organic chemicals. Each of these time periods included at least one major high flow event. Figure 5-10 shows settling, resuspension and net loss or net gain for TSS and lead for each 2-year period in the no action scenario. Figure 5-11 compares TSS and PCBs.

Flux calculations are useful in describing these sediment transport differences between organic chemicals and metals. The ratio of resuspension fluxes between contaminants and TSS is representative of the average contaminant concentration in the sediment. The following formula was used to compute these values for PCBs:

$$\frac{\text{kg PCB resusp}}{\text{kg TSS resusp}} * 10^6 \frac{\text{mg}}{\text{kg}} = \frac{\text{mg PCB}}{\text{kg TSS}} \qquad (5\text{-}1)$$

The ratio of settling fluxes between contaminant and TSS is representative of the average contaminant particulate concentration in the water column. The following formula was used to compute these values for PCBs:

$$\frac{\text{kg PCB settled}}{\text{kg TSS settled}} * 10^6 \frac{\text{mg}}{\text{kg}} = \frac{\text{mg PCB}}{\text{kg TSS}} \qquad (5\text{-}2)$$

Flux values were computed for one organic chemical (PCBs) and one metal (lead). A low flow period (1974-75) and a high flow period (1976-77) were selected for calculations.

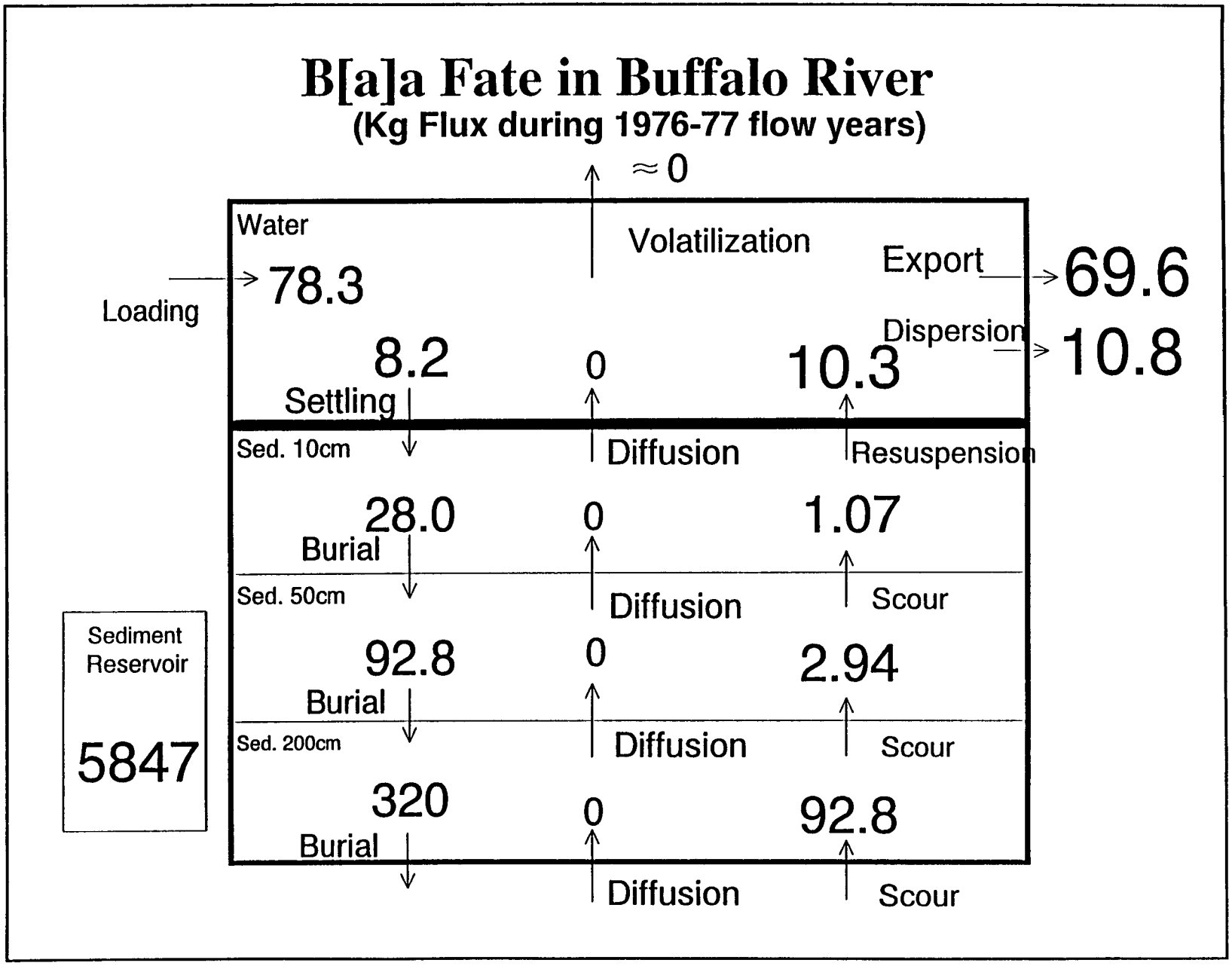


Figure 5-8. B[a]a fate for the no action scenario during 1976-77 flow years.

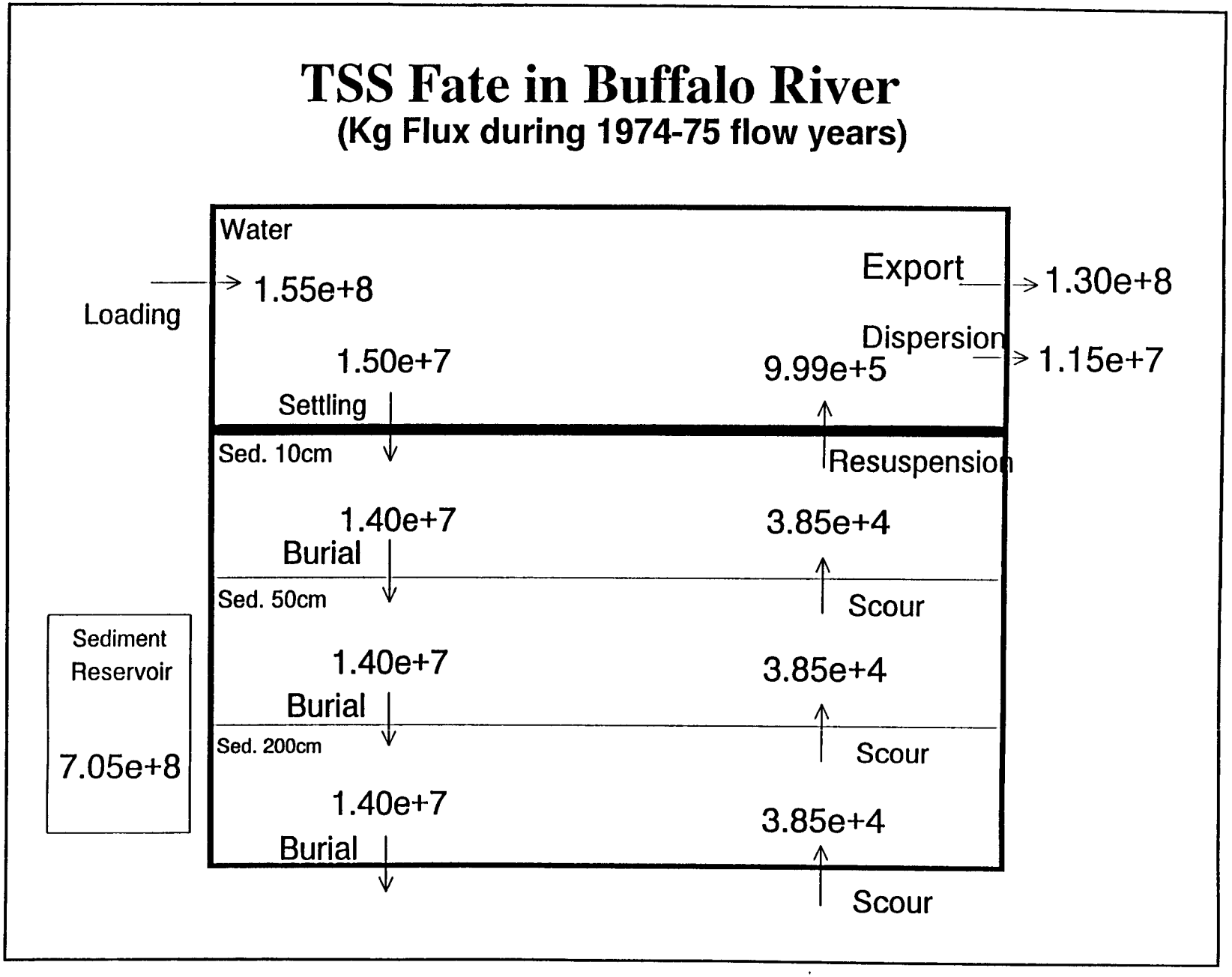


Figure 5-9. TSS fate for the no action scenario during 1974-75 flow years

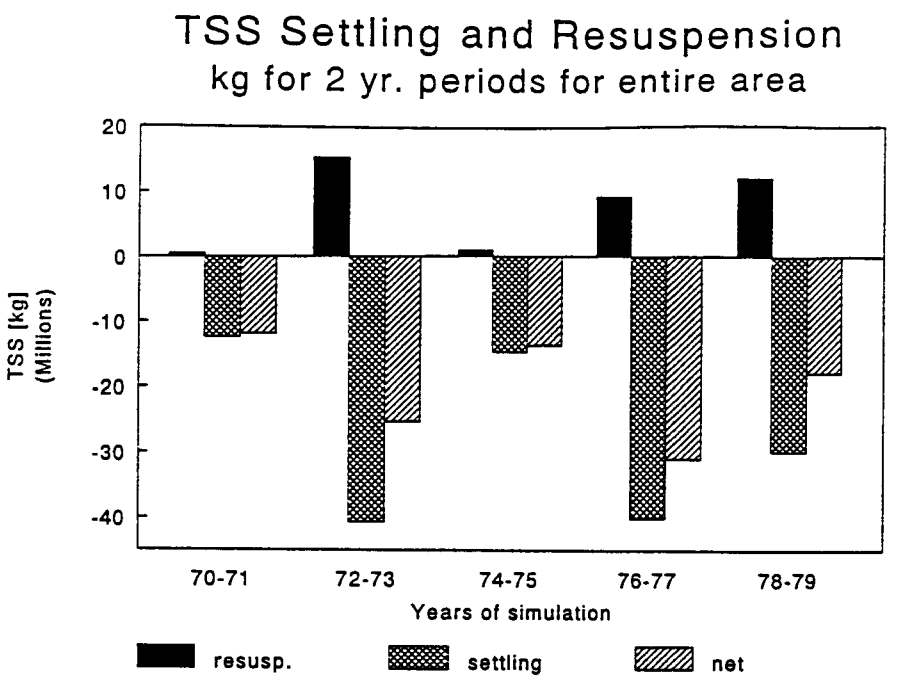


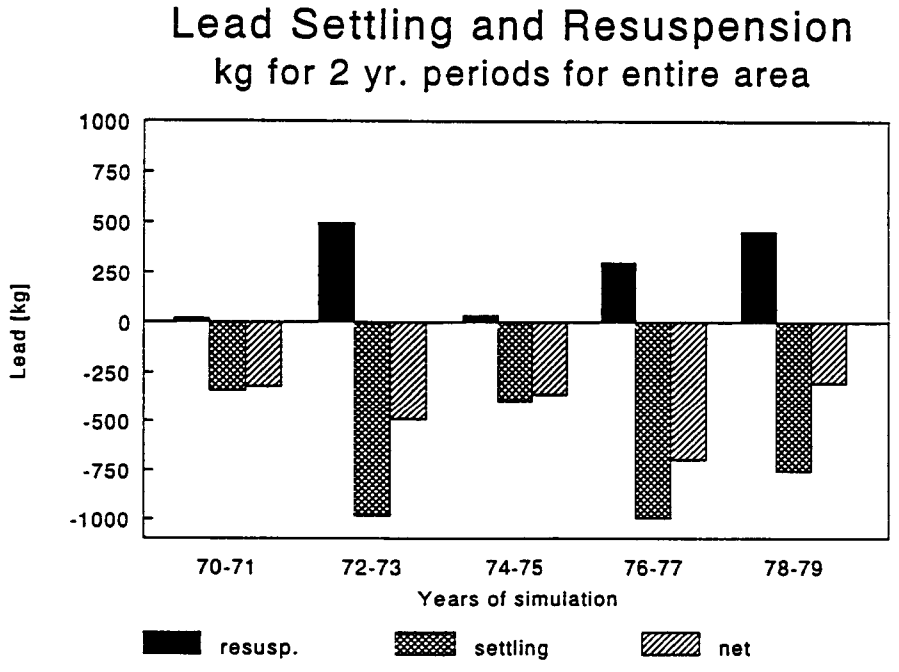


Figure 5-10. Comparison of 2-year TSS and Lead settling and resuspension for no action scenario.

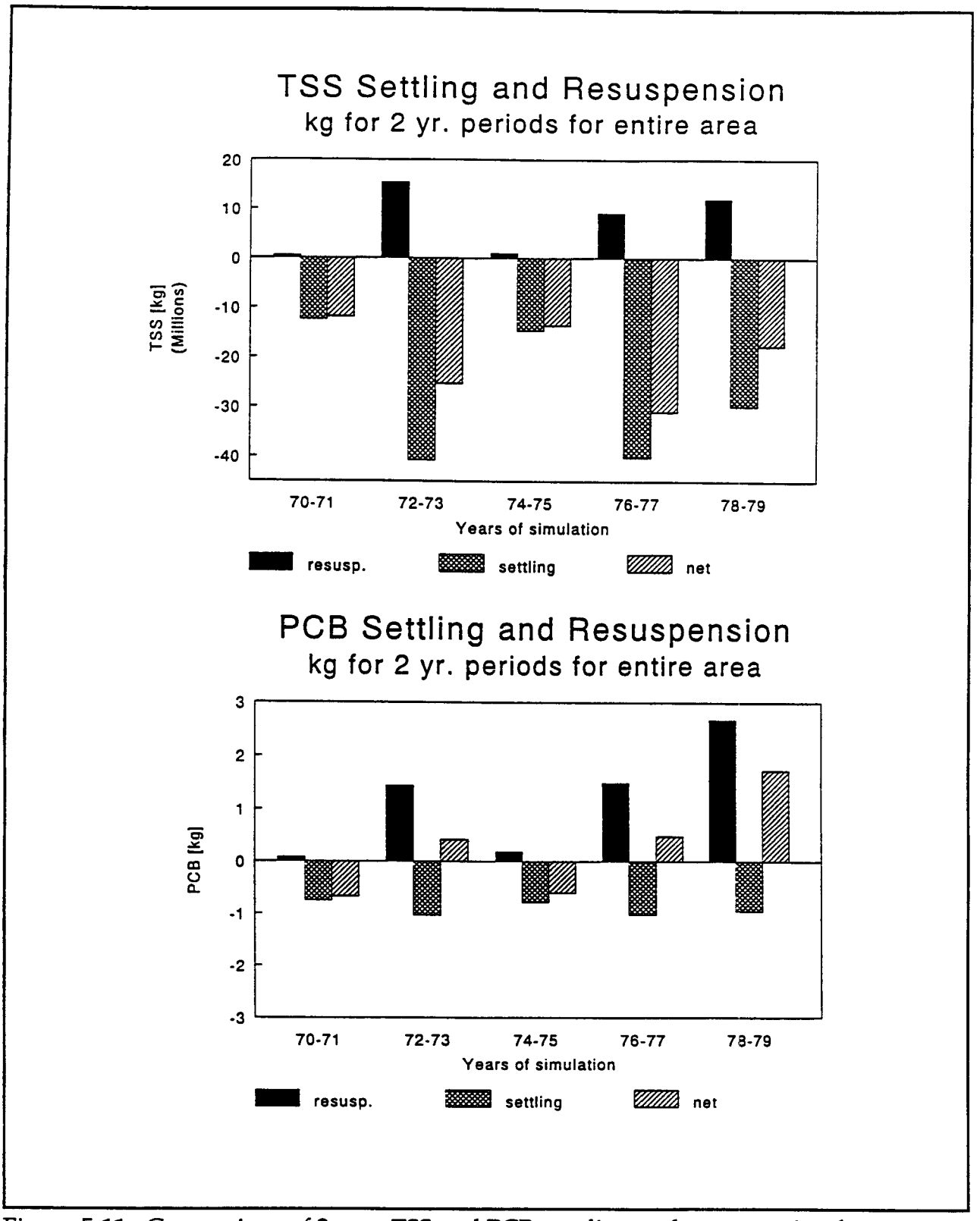


Figure 5-11. Comparison of 2-year TSS and PCBs settling and resuspension for no action scenario

Table 5-1 lists the representative values for the average mass-specific particulate concentrations in the sediment and the average mass-specific particulate concentrations in the water column based on the formulas listed above for the no action scenario.

Table 5-1. Representative average sediment and water column concentrations

| Flow Period | PCB sed. conc. [mg PCB/kg TSS] | PCB wat. col. conc. [mg PCB/kg TSS] | Lead sed. conc. [mg Pb/kg TSS] | Lead wat. col. conc. [mg Pb/kg TSS] |
|---|---|---|---|---|
| 1974-75 | 0.180 | 0.053 | 34.03 | 26.73 |
| 1976-77 | 0.164 | 0.025 | 32.82 | 24.86 |

The representative particulate concentrations in the water column were greater in the low flow period of 1974-75 than in the high flow period of 1976-77. This observation was consistent with the observed inverse relationship between PCB and TSS concentrations in the water column. TSS concentrations in the water column were greater in high flow years due to higher median particle size. Lesser amounts of mass-specific contaminant levels were carried on these larger particles [see Buffalo River loading report (Atkinson et al., 1993)].

The ratios of the average sediment concentrations and average particulate water column concentrations (table 5-2) indicate whether the sediments act as a net source or a net sink. The impact of a resuspension event is more significant when this ratio is larger since there is a greater difference between sediment and water concentrations. The ratios for PCBs and lead are listed in table 5-2 for the model periods of 1974-75 and 1976-77 in the no action scenario.

Table 5-2. Ratio of average sediment concentrations to average particulate water column concentrations for two year periods in the no action scenario.

| No Action Flow Period | PCBs (resusp:settling) sed conc: wc conc | Lead (resusp:settling) sed conc: wc conc |
|---|---|---|
| 1974-75 low | 3.4 | 1.3 |
| 1976-77 high | 6.6 | 1.3 |

The ratios for lead are the same for the two periods. Since the ratio is close to one there is relatively little difference between sediment and water concentrations for lead. Regardless of a high flow period, the sediment transport of lead will follow the TSS pattern and net settling will be greater than net resuspension. The concentration of lead in the sediment is not great enough to overcome the water column concentration and produce a greater net resuspension effect.

In the two year period that had several high flow events (1976-77), the average sediment PCB concentration is 6.6 times greater than the average particulate water column concentration. In this period, resuspension of PCBs (and other organics) is greater than the net settling. This effect occurs due to the significant difference in sediment versus suspended concentrations; the ratio is great enough to overcome even a large net deposition of solids. In the low flow period of 1974-75, sediment resuspention was small and the sediment to suspend PCB concentration was not great enough to generate a new source; therefore, there was a net loss of PCBs to the sediments.

Resuspension of contaminated sediments is not the primary source of water column contamination. Even when the sediments act as a net source of contaminants to the water column, upstream loading is a much greater source in the no action scenario. As seen in figure 5-8, B[a]a loading for the 1976-77 period was 78.3 kg whereas suspension only accounted for 10.3 kg of water column contamination. For each contaminant throughout the 10-year period, the loading pathway is much greater than the resuspension pathway in the no action scenario. Export and dispersion out of the water column are about equivalent to the loading. Over 2-year periods, mass budgets show that resuspension of in-place pollutants is not extremely significant. Upstream loading dominates and is clearly the primary source of water column contamination.

## 5.2 EVALUATION OF MANAGEMENT ALTERNATIVES

Results of the no action scenario were described in the previous section. The results from the other scenario runs are compared to the no action scenario in this section. Explanations of the management alternatives along with the modeling approaches used were presented in section 3.2. In this section, the various management alternatives are evaluated in terms of their impact on water column exposure and export as well as on sediment concentrations.

### Water column exposure and export

A plot of contaminant cumulative export [kg] over the entire 10-year period of simulation is useful in the analysis of export and for the comparison of management alternatives. Figures 5-12 through 5-16 show the 10-year contaminant cumulative export of PCBs, B[a]a, B[a]p, lead and copper, respectively, for the various scenarios. In general, the plots show a gradual increase in the cumulative export with several sharp increases. These sharp increases are the result of high flow events with high levels of export over a short period of time. This is further evidence that high flow events are significant to the export of contaminants in this system. Also, in all cases, the figures show that the no action and sediment remediation (Hamburg Cove and environmental dredging) scenarios have very similar cumulative export trends, whereas the two scenarios without contaminant loading are much lower.

As seen in figures 5-12 to 5-16, the contaminant cumulative exports for the Hamburg Cove scenario are slightly lower than those for the no action scenario. Water column contaminant concentrations are slightly lower during events in the Hamburg Cove scenario as well (see figure 5-17). These slightly lower water column concentrations occur because resuspension in the upstream portion of the river contributes less contaminants to the water column in the absence of navigational dredging. This happens because cleaner sediments fill in upstream areas during the absence of navigational dredging.

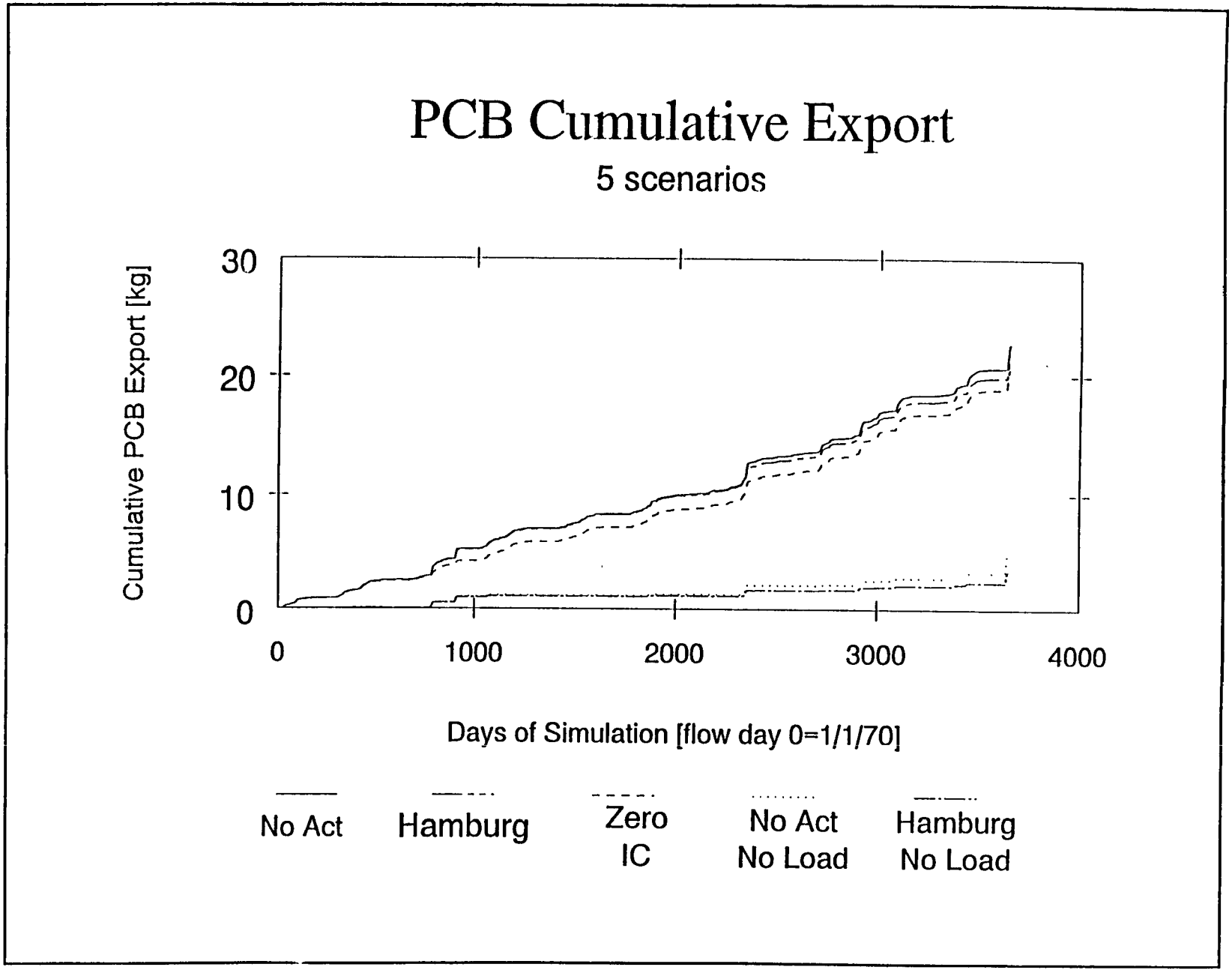


Figure 5-12. Ten-year PCB cumulative export for 5 scenarios

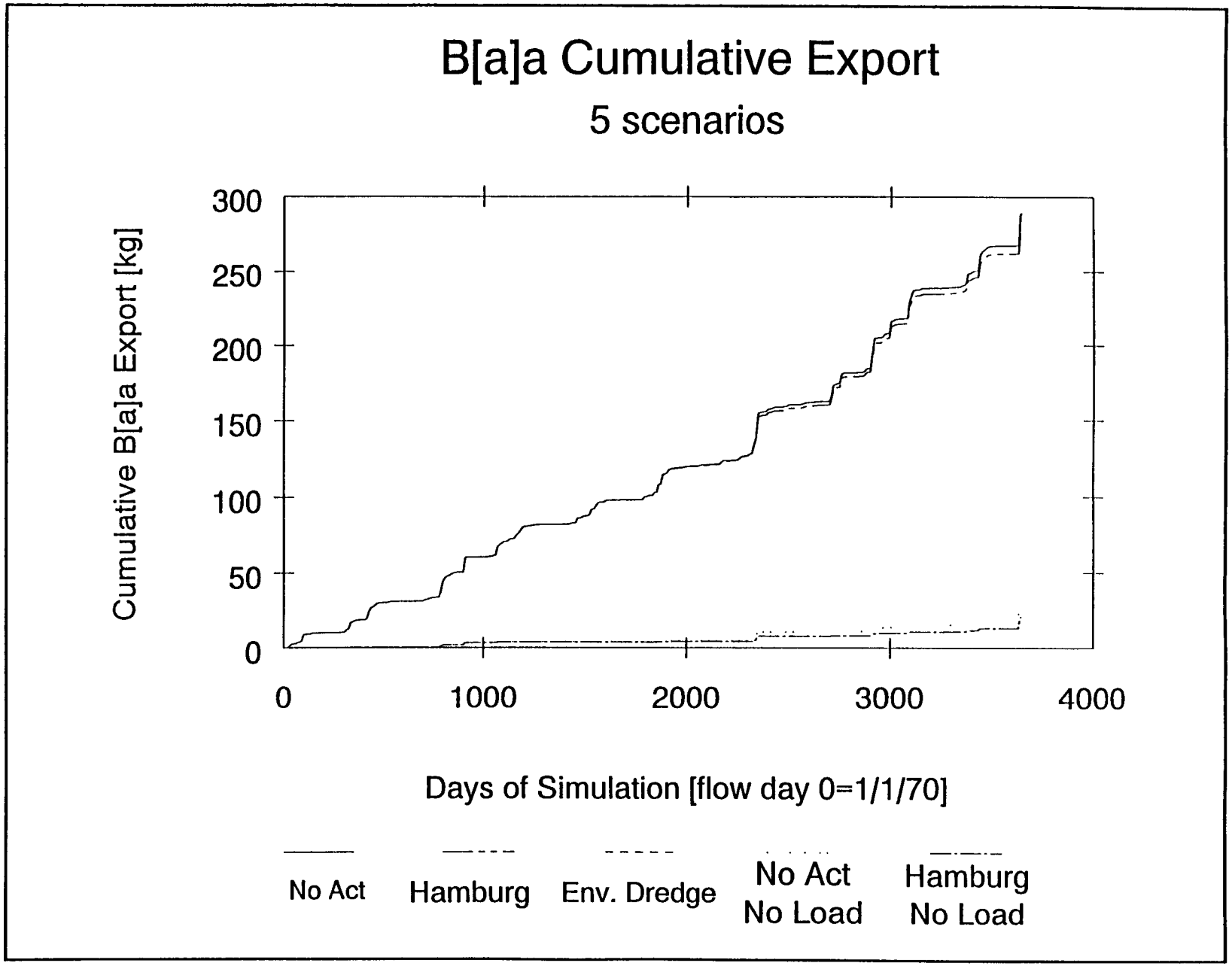


Figure 5-13. Ten-year B[a]a cumulative export for 5 scenarios

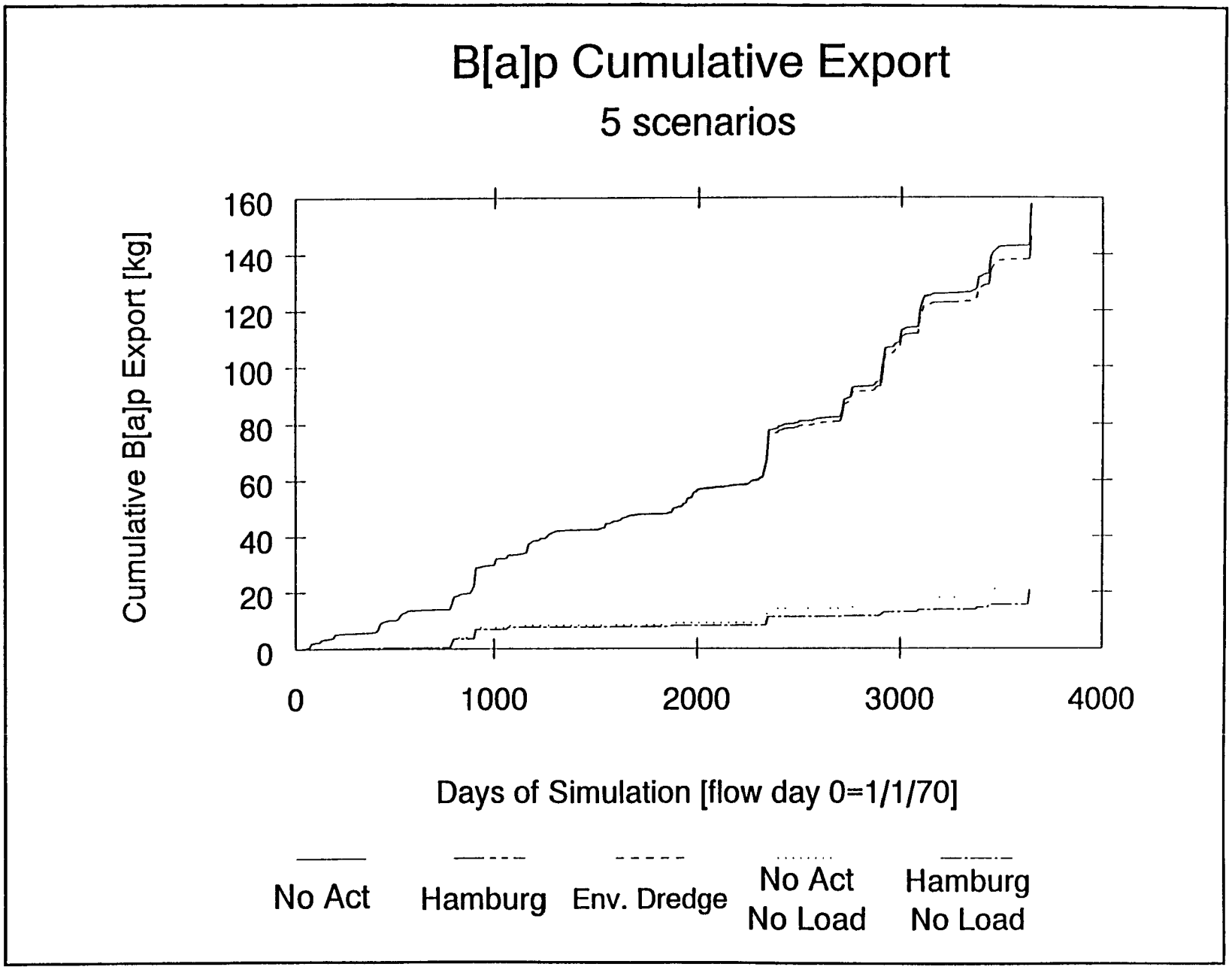


Figure 5-14. Ten-year B[a]p cumulative export for 5 scenarios

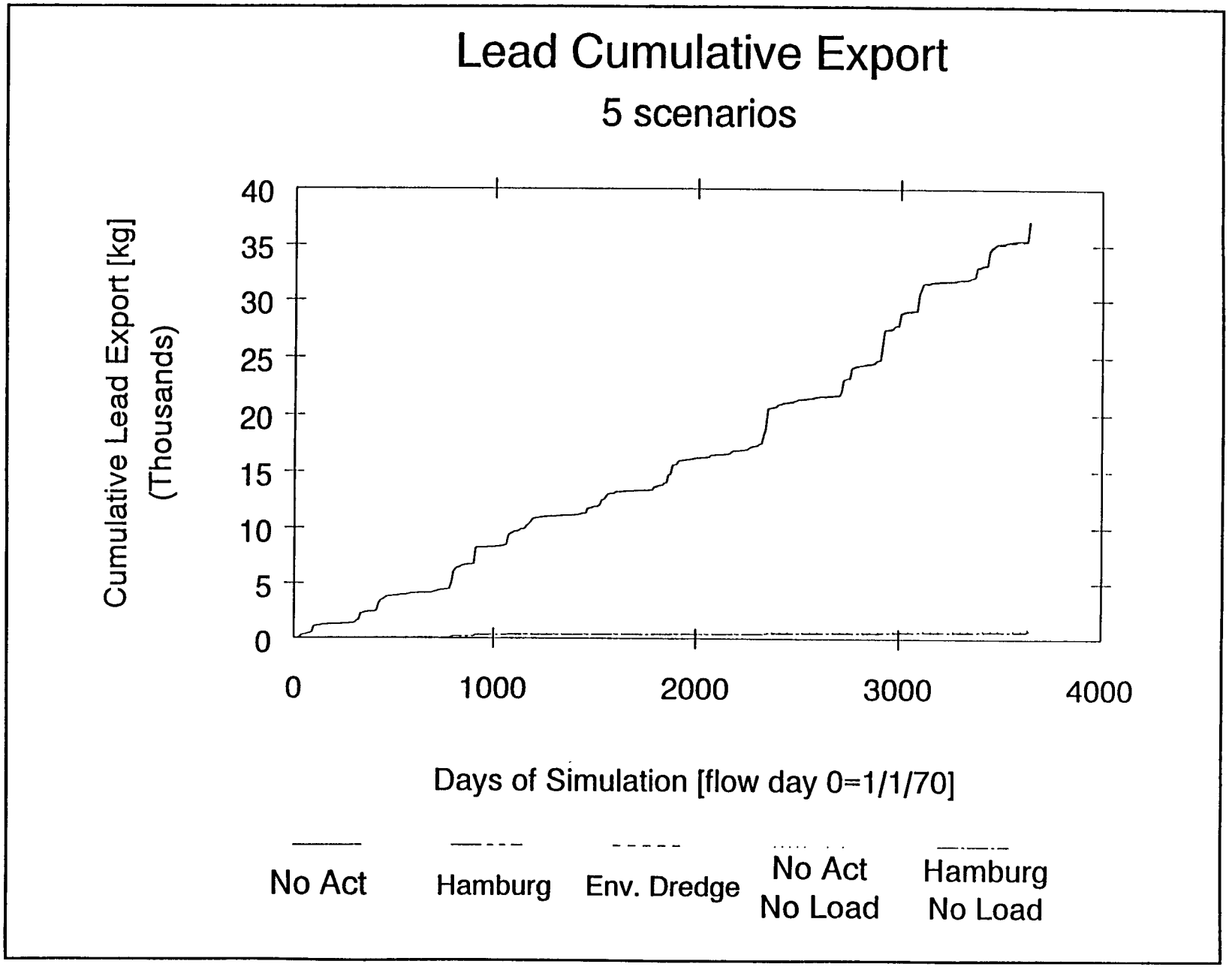


Figure 5-15. Ten-year lead cumulative export for 5 scenarios

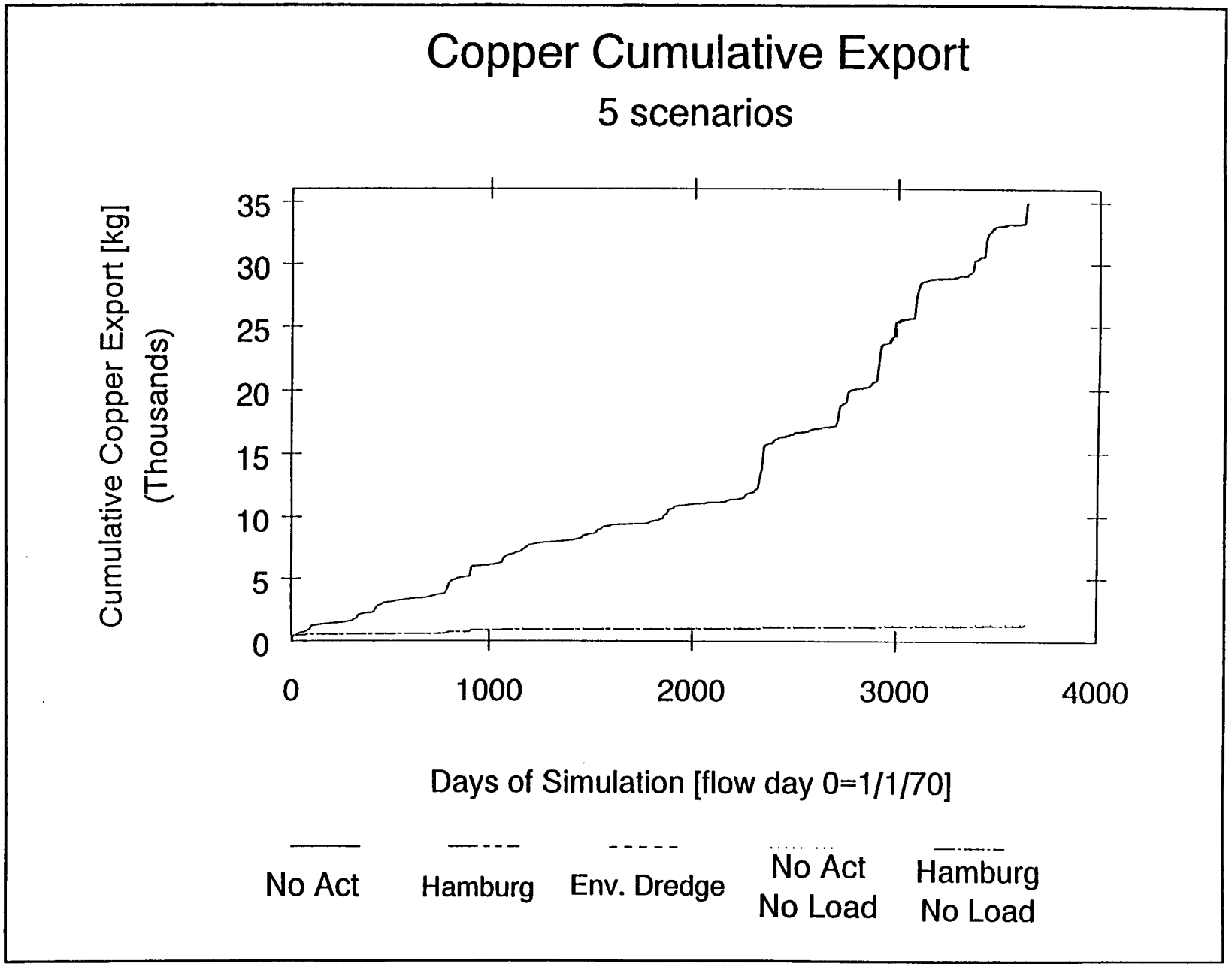


Figure 5-16. Ten-year copper cumulative export for 5 scenarios

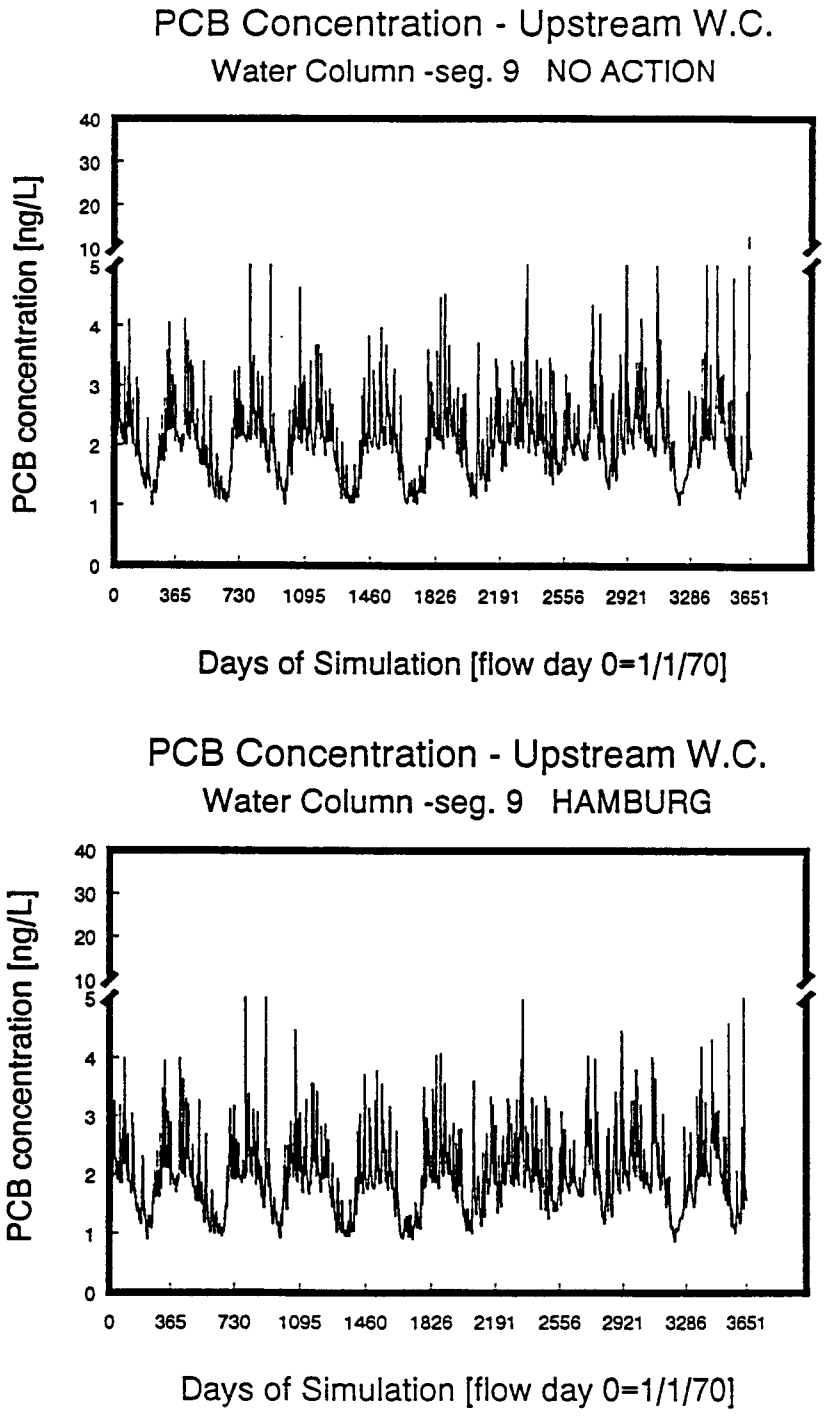


Figure 5-17. 10-year PCB upstream water column concentration in the no action and Hamburg Cove scenarios

The elimination of upstream navigational dredging in the Hamburg Cove scenario also resulted in lower levels of contaminant export to Lake Erie. Figure 5-18 shows a small-scale comparison of daily PCB export during a single event for the no action and Hamburg Cove scenarios. The peak in PCB export is slightly greater for the no action scenario during the event. As seen in figure 5-19, the cumulative event period (days starting with the high-flow event until the river returned to its average flow of 20 $m^3/s$), and maximum one-day PCB export values for the Hamburg Cove scenario are lower than those for the no action scenario during each two-year model period. The variations in the event period fluxes are the greatest due to the different contributions from resuspension in the two scenarios. The non-event periods maintain similar export patterns for the two scenarios since loading is the primary contributor of contaminants being exported. The differences in contaminant export are greater during the two-year model periods with a greater number and/or magnitude of events (years 3-4, 7-8, 9-10). Figures 5-20 and 5-21 show the cumulative two-year export fluxes for PCBs and lead, respectively. The greatest differences between the no action and Hamburg Cove scenarios occur during the last two model periods which were both high-flow periods with numerous events.

Contaminant cumulative export levels are very similar for the no action and environmental dredging scenarios as seen in figures 5-13 to 5-16. Differences in water column contamination from resuspension are minimal for the two scenarios as well. The erosional sediment concentrations are practically the same for the two scenarios and the resuspension effect is likewise similar. This shows the relative insignificance of nearshore depositional sediments on water column exposure and export.

Even though the environmental dredging scenario significantly reduces the contaminant levels in these depositional areas, their resuspension contribution is so small (due to low resuspension rates and small sediment-water interfacial areas) that they have very little impact on water column levels. The close similarities in export between the environmental dredging and no action scenarios can be seen on a 2-year basis in figures 5-20 to 5-21.

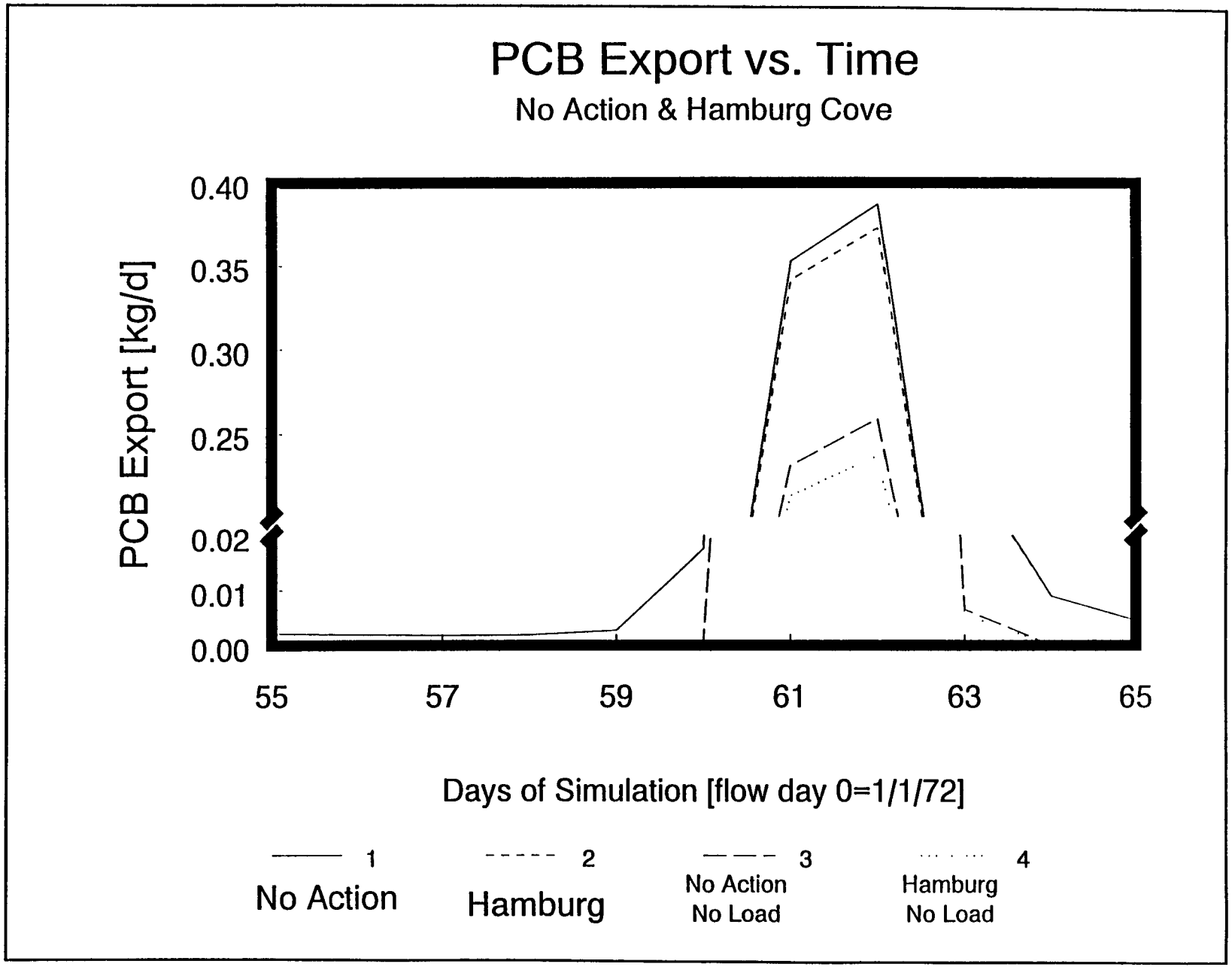


Figure 5-18. Daily PCB export during a single event for 4 scenarios

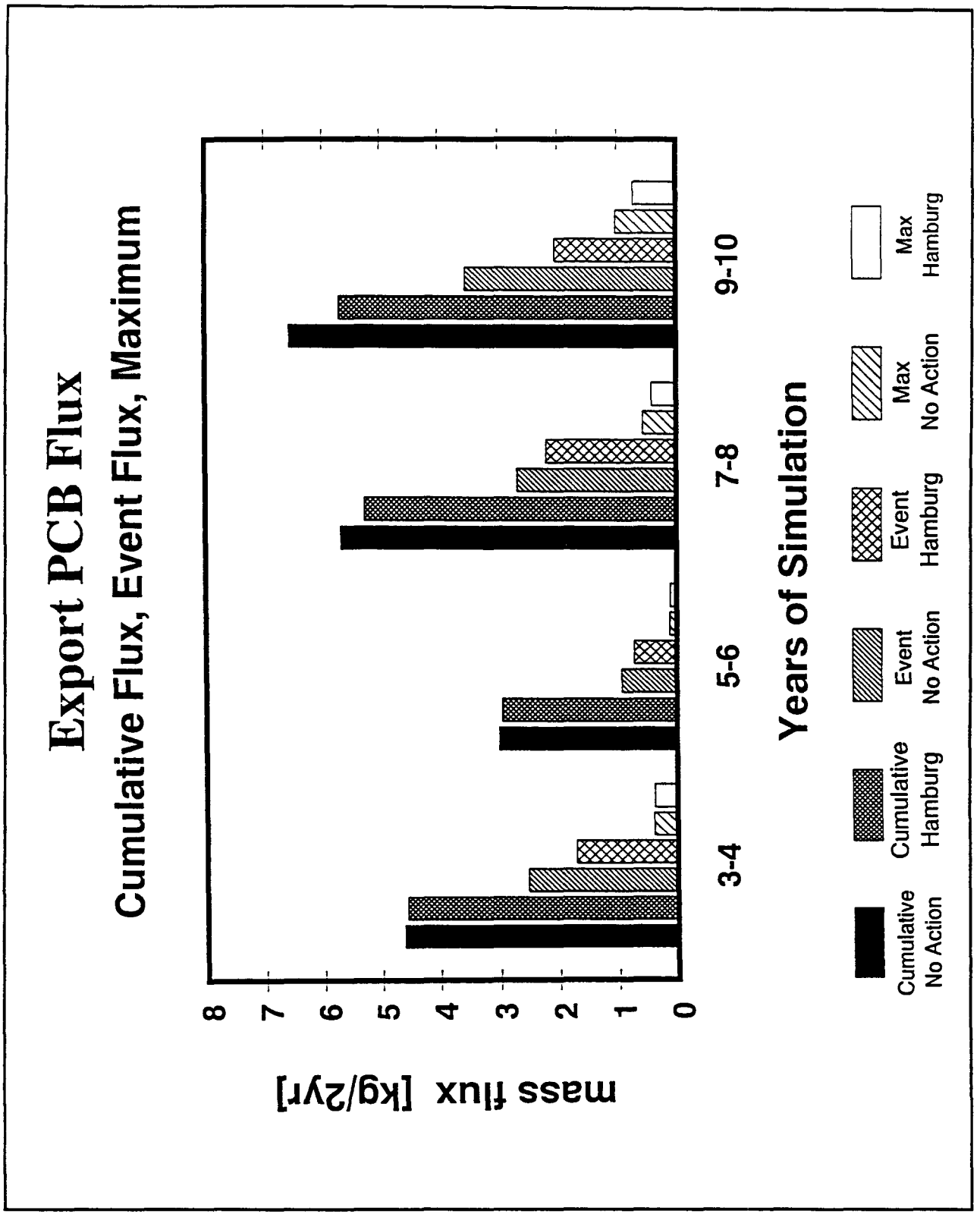


Figure 5-19. 2-year cumulative event period and maximum daily export PCB fluxes for the no action and Hamburg Cove scenarios

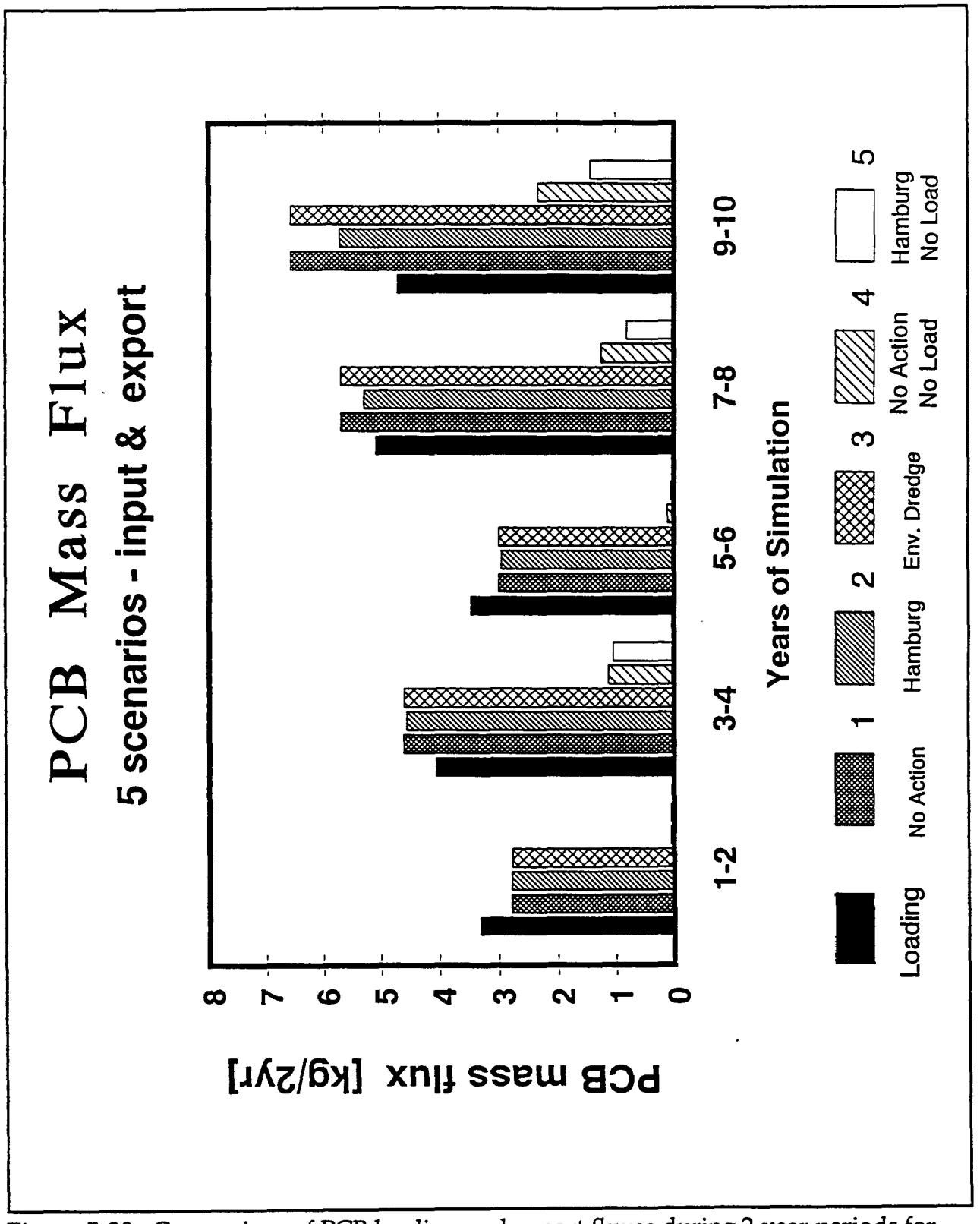


Figure 5-20. Comparison of PCB loading and export fluxes during 2-year periods for scenarios 1-5

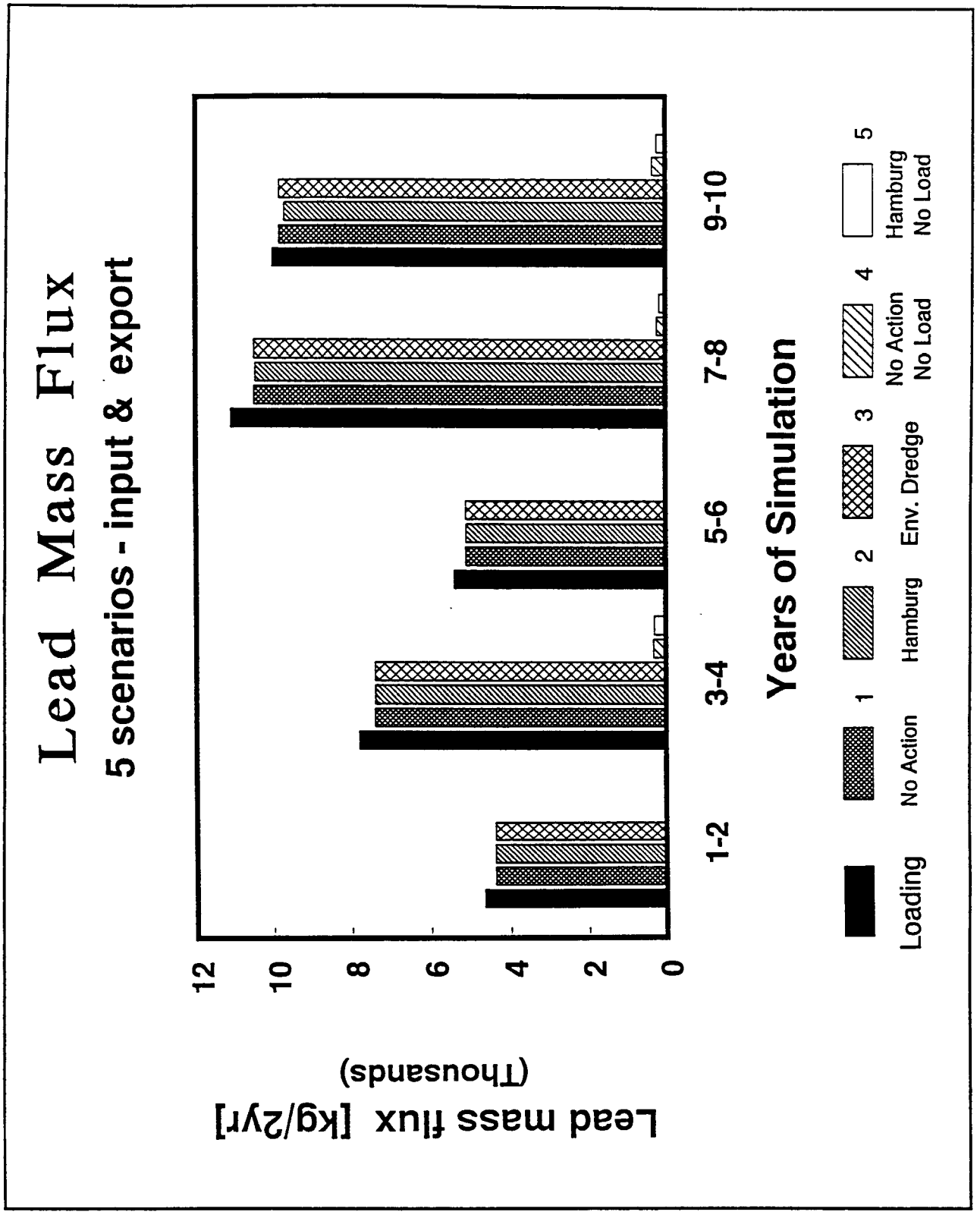


Figure 5-21. Comparison of lead loading and export fluxes during 2-year periods for scenarios 1-5

The zero initial conditions scenario is similar to the environmental dredging scenario, except that the initial conditions in the top two layers of both depositional and erosional sediments were set to zero at the beginning of the simulation. This scenario was run to see the effect on PCB water column contamination with external loading as the sole source.

The 10-year PCB cumulative export for the zero initial conditions scenario was included in Figure 5-12 (instead of the environmental dredging scenario, which was nearly identical to the no action scenario). The trend for the zero initial conditions scenario was similar to the no action and Hamburg Cove scenarios with cumulative export levels slightly lower than both scenarios. This shows that the overall impact on export of eliminating sediments as a water column contaminant source is relatively minor. The decrease in 10-year cumulative export for the zero initial conditions scenario is only a 9.2% reduction from the no action scenario. Based on this, it is apparent that sediment remediation will not reduce the water column contamination levels significantly. These results are further evidence that external loadings dominate the Buffalo River system.

Scenario #4 was a simulation of the no action scenario with no contaminant loading. Comparisons with the no action scenario (Scenario #1) show the relative impact of contaminant loading on the Buffalo River system. Without the contribution of loadings, contamination in the water column for this scenario is solely the result of resuspended sediments.

Water column concentrations are reduced significantly because of the absence of contaminant loading (see figure 5-22). Water column contaminant concentrations are nearly zero in non-event periods. The influence of the Lake Erie boundary condition can be seen in the bottom graph of figure 5-22; during summer low flow periods longitudinal dispersion can even influence upstream segments. During event periods, the water column concentrations rise sharply due to resuspension from the sediments and then decline just as fast on the downward curve of the hydrograph. As seen in the cumulative export plots (figures 5-12 to 5-16), export fluxes for the non-loading scenarios show dramatic decreases compared to the no action scenario with contaminant loadings.

Figure 5-18 shows a comparison of daily export during a single high flow event for the no action scenario with and without loadings. The variation in export between these two

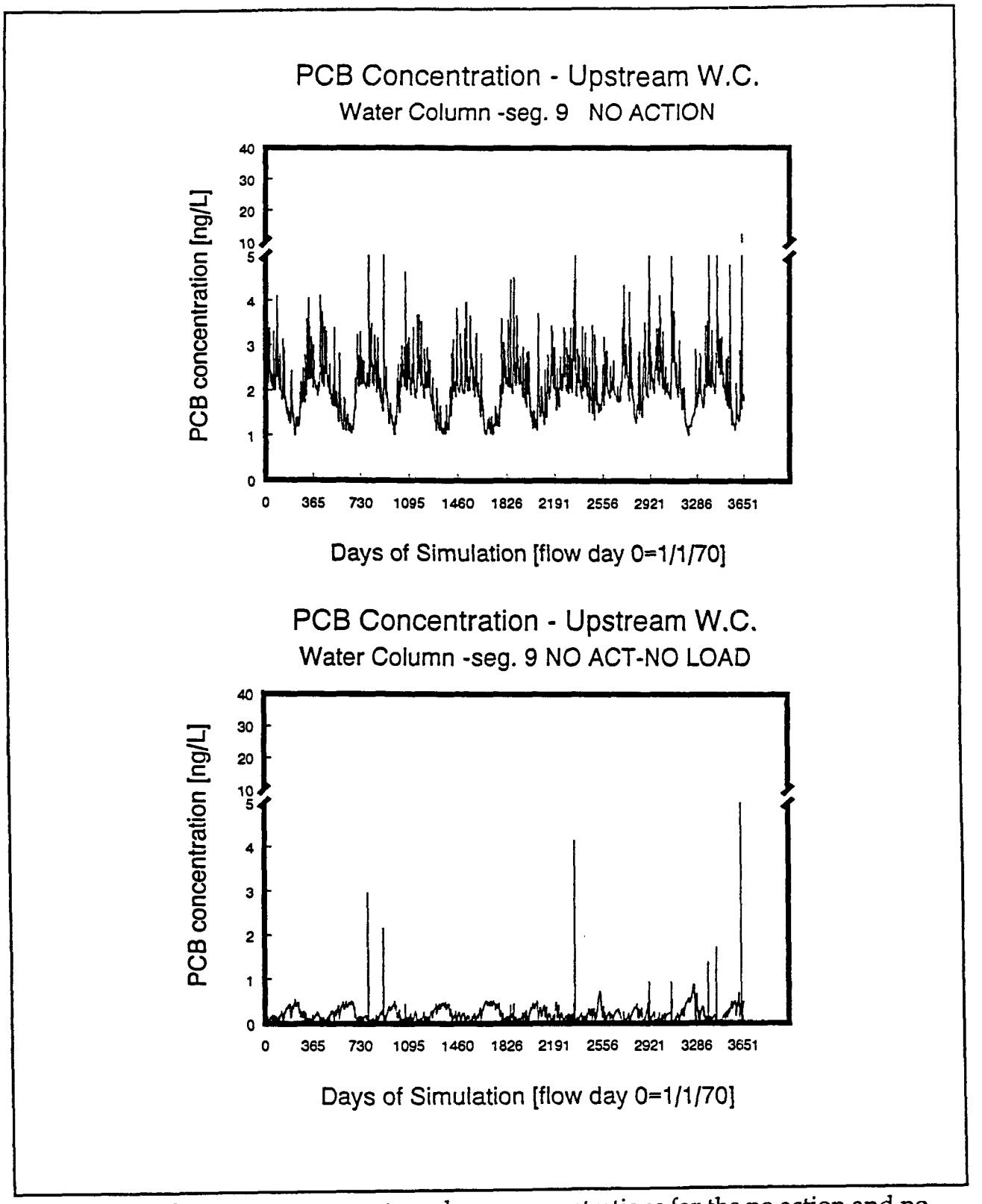


Figure 5-22. 10-year upstream water column concentrations for the no action and no action-no loading scenarios

scenarios is due to the difference in loadings. As shown, the difference due to loading is much greater than the difference between the export fluxes of the no action and Hamburg Cove scenarios. As seen in figures 5-20:21, 2-year contaminant mass fluxes for scenario #4 are much smaller than those for the scenarios with contaminant loadings. The export fluxes for the last two 2-year periods are greater since these were high-flow periods with a greater contribution from resuspension.

The importance of the selected flows used in the models was examined in the flow switching scenario. Flows from the first 2-year period (1970-71 flows), having no high-flow events, and the last 2-year period (1978-79 flows), with several high-flow events, were switched with each other for the no action scenario. PCBs were the only contaminant modeled for this scenario.

As seen in the PCB cumulative export for the no action scenario (figure 5-23), the results were affected by rearranging the flows. In the original no action scenario, the highest flow in the 10-year period occurred in the last few days of 1979. In the flow switched scenario, this event occurred at nearly 2 years into the simulation. With the high-flow period at the start of the 10 years, the cumulative export rose faster than with the previous event chronology. The cumulative export profile rises quicker in the flow switched scenario since a number of high flow events occur in the first 2 years while there are none for the original no action scenario. However, the 10-year cumulative PCB export fluxes are approximatly equal for the two scenarios. The 10-year cumulative PCB export for the flow switched scenario showed only a 5.5% decrease relative to the export in the no action scenario.

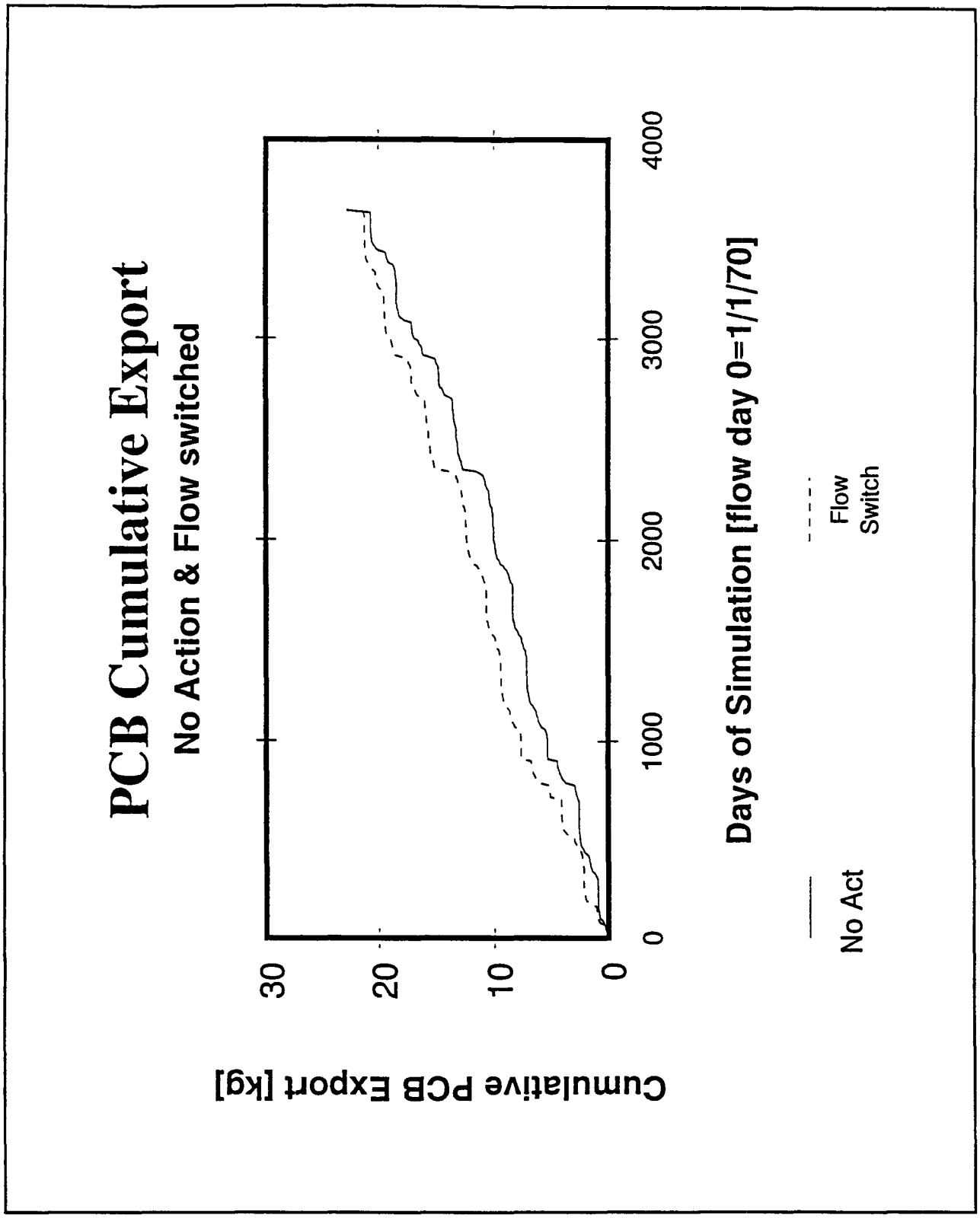


Figure 5-23. Ten-year cumulative PCB export for the no action and flow switched scenarios

**Sediment Concentrations**

Erosional sediment contaminant concentrations are nearly identical for the no action, environmental dredging and no action - no loading scenarios. Nearshore sediment remediation through environmental dredging does not significantly affect the erosional sediments of the midchannel. Elimination of contaminant loading also does not greatly affect the erosional sediment concentrations as seen for PCBs in figure 5-24. This occurs since the PCB loading is in relative equilibrium with the existing sediment concentrations on a μg PCB/g TSS basis. However, erosional sediment concentrations are strongly affected by the lack of upstream navigational dredging in this scenario.

Due to the absence of dredging, upstream erosional sediment contaminant concentrations are much lower in the Hamburg Cove scenario than those in the no action scenario. Figure 5-25 shows a comparison of the upstream erosional sediment concentrations for the top layer between the no action and Hamburg Cove scenarios. In the Hamburg Cove scenario, upstream erosional sediments do not get the boost in concentration levels due to reinitialization in the dredging process every two years. Therefore, the erosional sediment concentration levels show a gradual decline in this scenario as cleaner solids settle on the top sediment layer.

As seen in figure 5-26, the differences in the downstream erosional sediment contaminant concentrations are relatively minor compared to the no action scenario. Since the navigational dredging approach was applied downstream in both scenarios, the results were nearly the same. Downstream erosional sediment concentrations in the Hamburg Cove scenario are very slightly lower than those in the no action scenario. This is due to a smaller contribution from contaminants that resettle downstream after being resuspended in the upstream portion of the river.

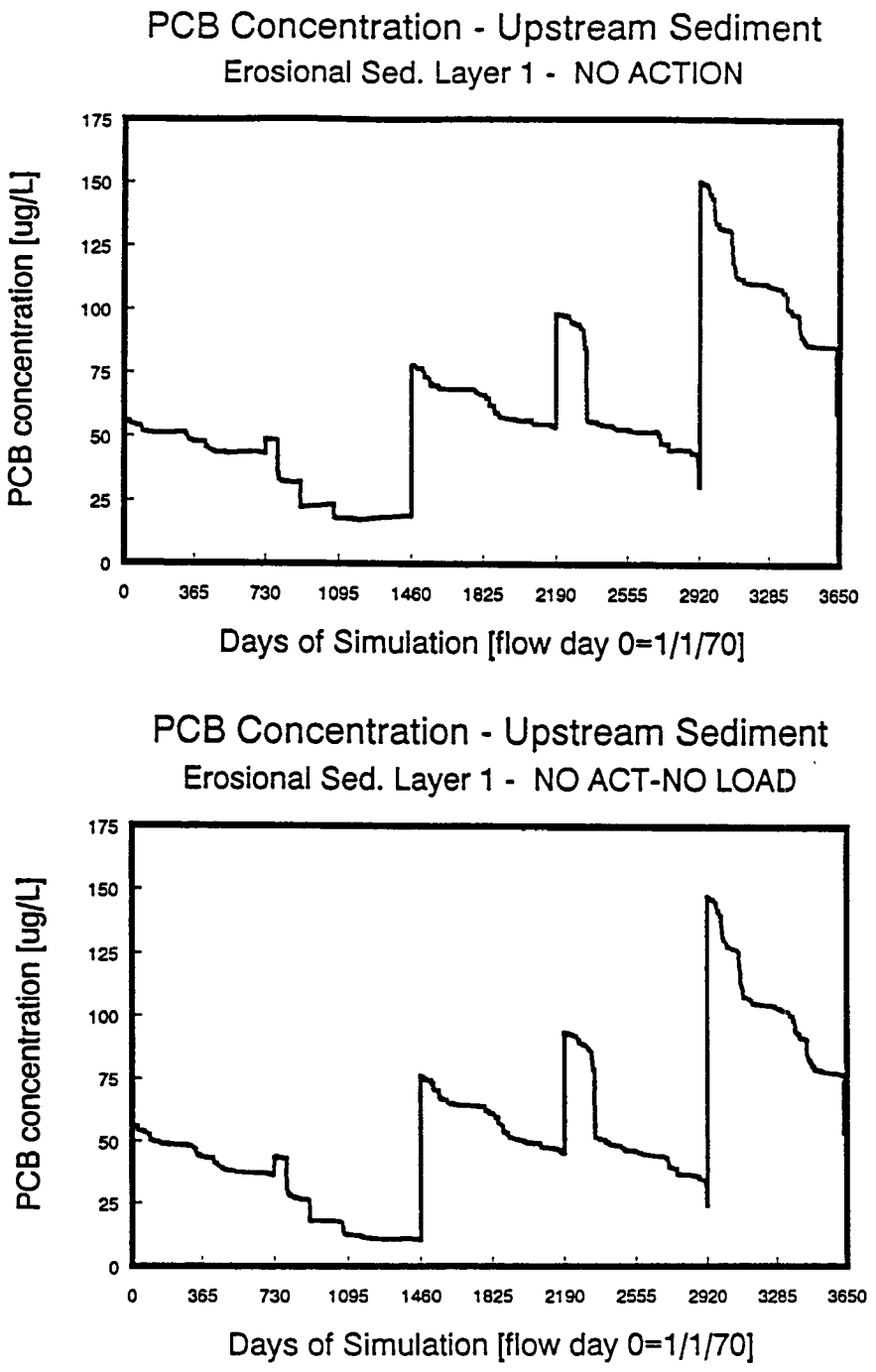


Figure 5-24. Ten-year PCBs concentrations in the upstream erosional sediments for the no action and no action - no loading scenarios

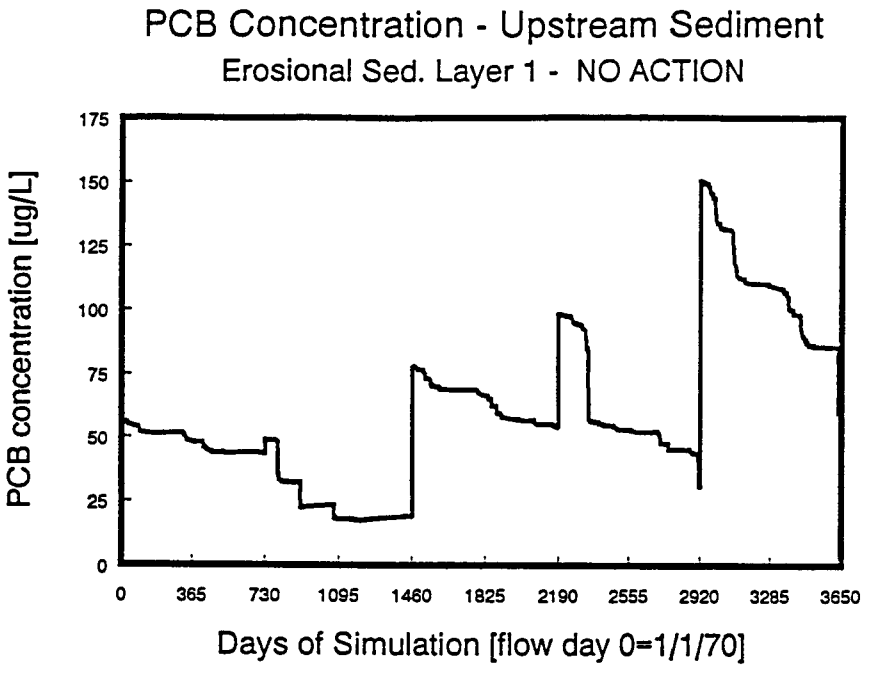


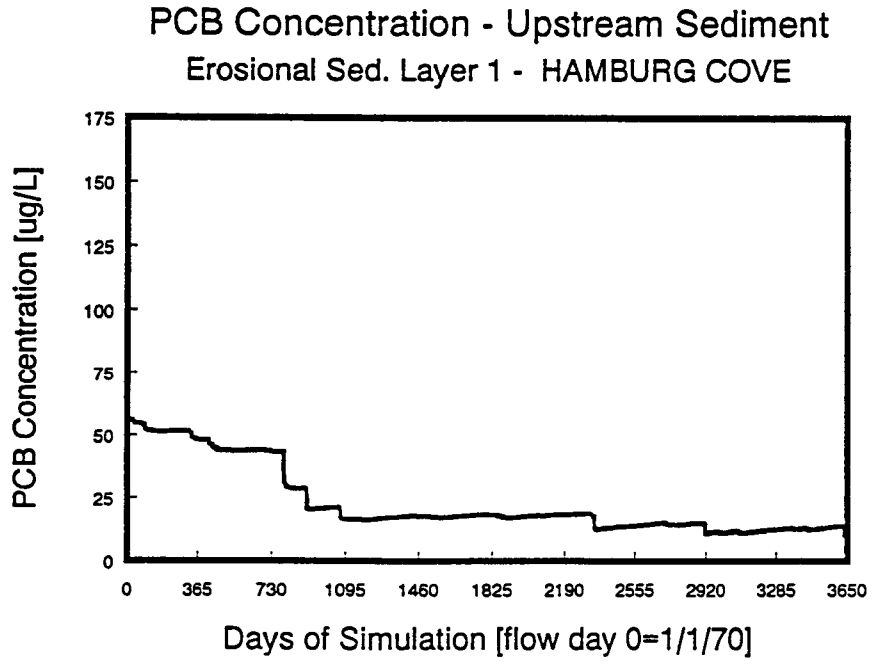


Figure 5-25. Ten-year PCB upstream erosional sediment concentrations in the no action and Hamburg Cove scenarios

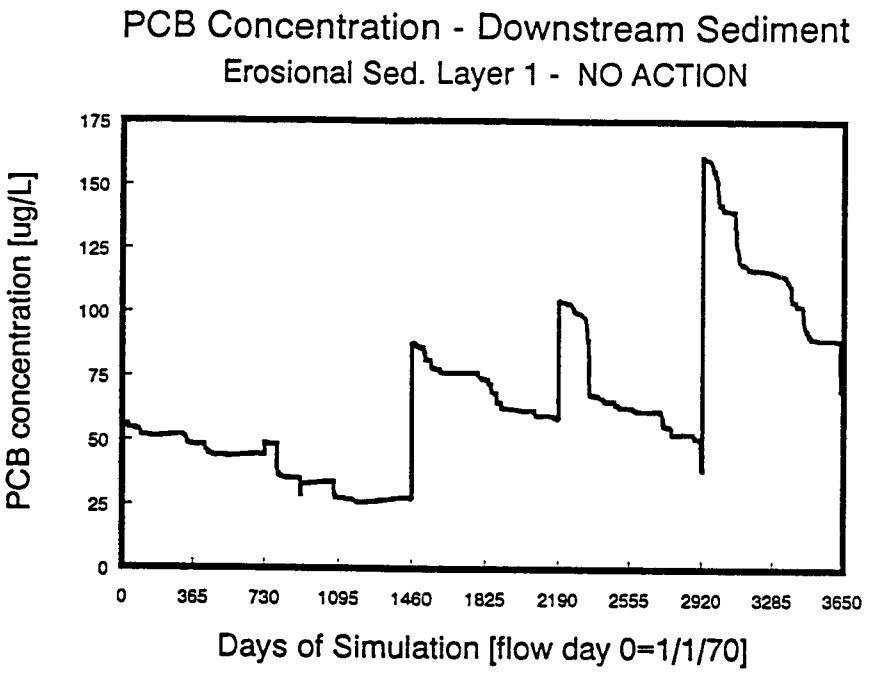


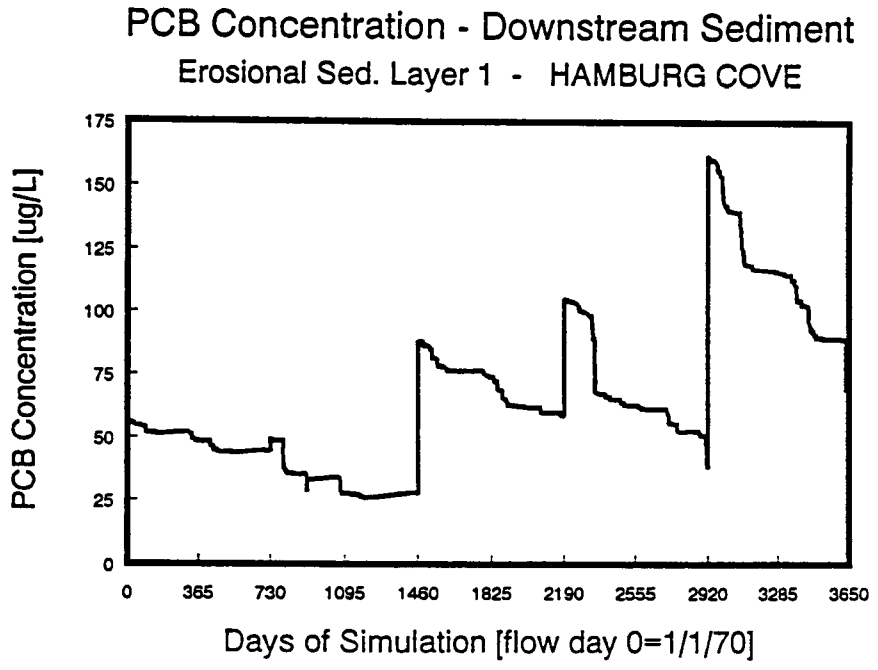


Figure 5-26. Ten-year PCB downstream erosional sediment concentrations in the no action and Hamburg Cove scenarios

Depositional sediment contaminant concentrations in the four remediation scenarios (scenarios 2-5) do not show much variation from the no action scenario, with the exception of the environmental dredging scenario. Changes in navigational dredging do not affect the nearshore depositional sediments as concentrations are nearly identical for the no action and Hamburg Cove scenarios. Without contaminant loading, the depositional sediment segments show a steady decline throughout the 10-year period similar to the no action scenario but at slightly lower concentration levels (see figure 5-27). Only minor decreases occur since PCB (and other contaminants) loadings and the depositional sediment concentrations are assumed to be in relative equilibrium on a weight contaminant per weight solid basis (similar to the erosional sediments).

In the environmental dredging scenario, the top two layers of depositional sediment segments were given uniform initial conditions equal to zero at the start of the 10-year simulation. Throughout the 10-year period, concentrations in the depositional sediment segments gradually increase in the environmental dredging scenario (see figure 5-28). The accumulation of contaminants in the top two depositional sediment layers occurs through deposition of upstream loadings which, although low in PCBs, had particulate concentrations greater than zero.

As these upstream loadings accumulate in the depositional areas, sediment concentrations for the environmental dredging scenario approach those for the no action scenario concentrations after several years (Compare final concentrations for the two scenarios in Figure 5-18).

## 5.3 SUMMARY

Based on the results of the contaminant model simulations, it was found that the geometry and hydraulics of the lower Buffalo River are such that sediment resuspension only contributes a significant amount of contaminants to the water column during major high flow events. On days of average or low flow, resuspension of contaminated sediments is not a factor in influencing water column concentrations. The primary source of water column contamination was determined to be loading from upstream of the area of concern. Current upstream loading

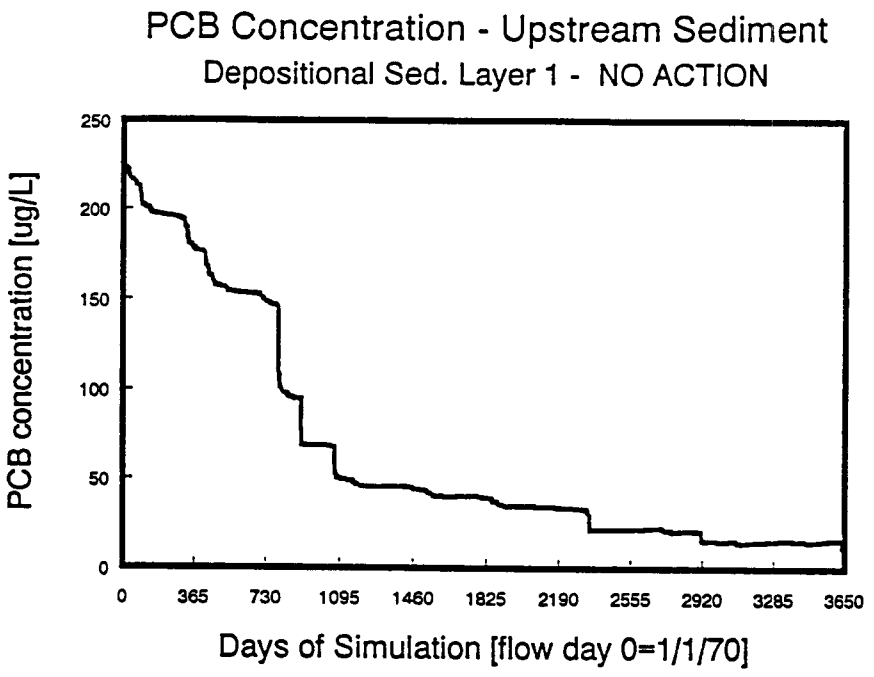


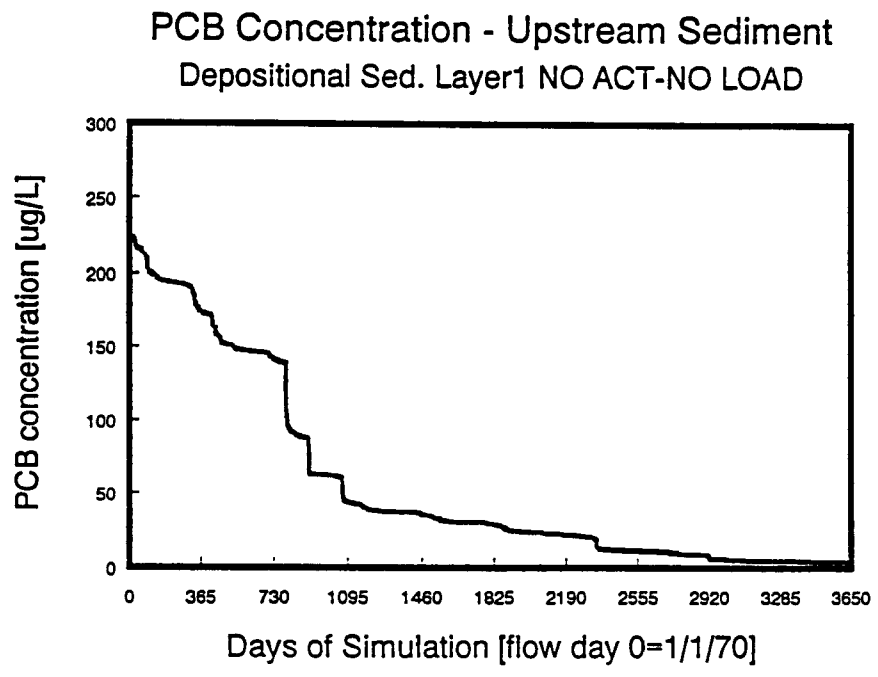


Figure 5-27. 10-year PCBs concentrations in the depositional sediment for the no action and no action-no loading scenarios

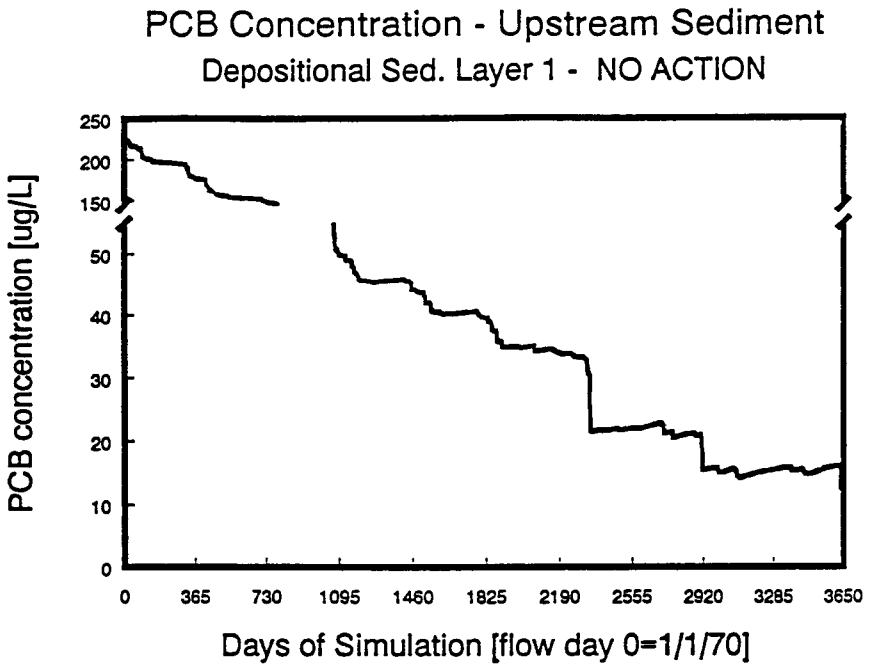


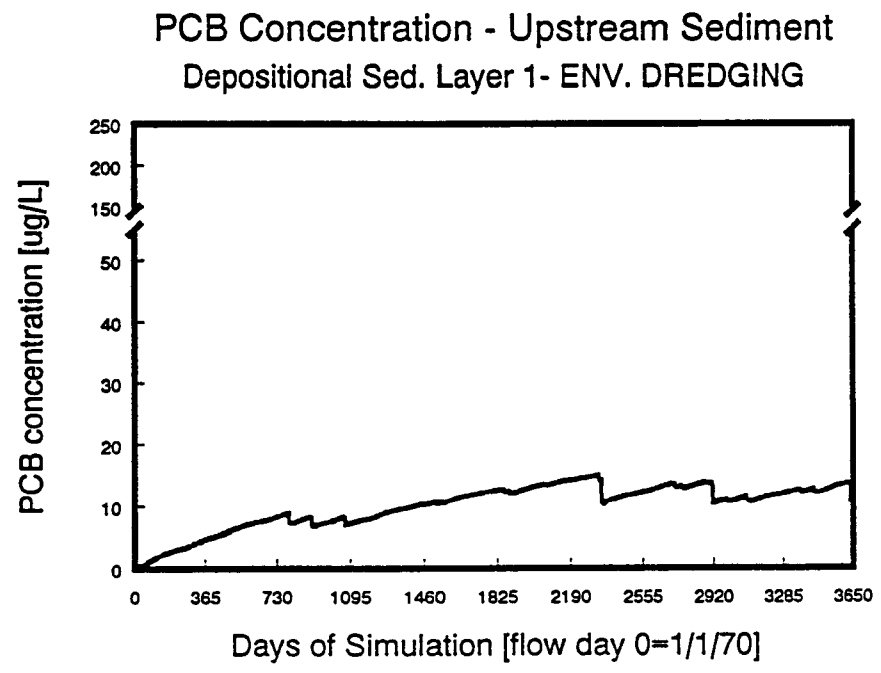


Figure 5-28. 10-year PCBs concentrations in the upstream depositional sediments for the no action and environmental dredging scenarios

of contaminants overwhelms sediment contributions to water column exposure and contaminant export to Lake Erie. CSO, industrial and groundwater pollutant loadings are all relatively insignificant compared to upstream loadings.

The 10-year export fluxes of every contaminant in each management alternative are summarized in figure 5-29 (note: values of lead and copper are divided by 1000). The two scenarios without contaminant loading (no action - no loading and Hamburg Cove - no loading) showed a 75% and 99% decrease, respectively, in contaminant export fluxes relative to the no action scenario. The sediment remediation scenarios with contaminant loading (Hamburg Cove and environmental dredging) produced declines in export of less than 10%. External loading is clearly the dominant source for water column contamination based on these results.

Based on these results, we may conclude that sediment remediation in the Buffalo River will not have a significant impact on reducing water column contaminant exposure. Environmental or full dredging of bottom sediments will not alleviate water column concerns. Also, the potential to exacerbate the water column problem still exists with these dredging options, if deeper, more contaminated sediments are exposed. However, sediment remediation will be a potentially important action for reducing direct sediment exposure, especially in "hot spots". Environmental dredging of nearshore "hot spots" could be beneficial to the benthic community and corresponding food web (See next section)..

As noted in Section 3, the navigational dredging approach that was implemented in these model simulations has the potential for overestimating the sediment contribution to water column contamination. However, even if this approach is a worst case scenario, the upstream loading contribution is still significantly larger than the impact from resuspension.

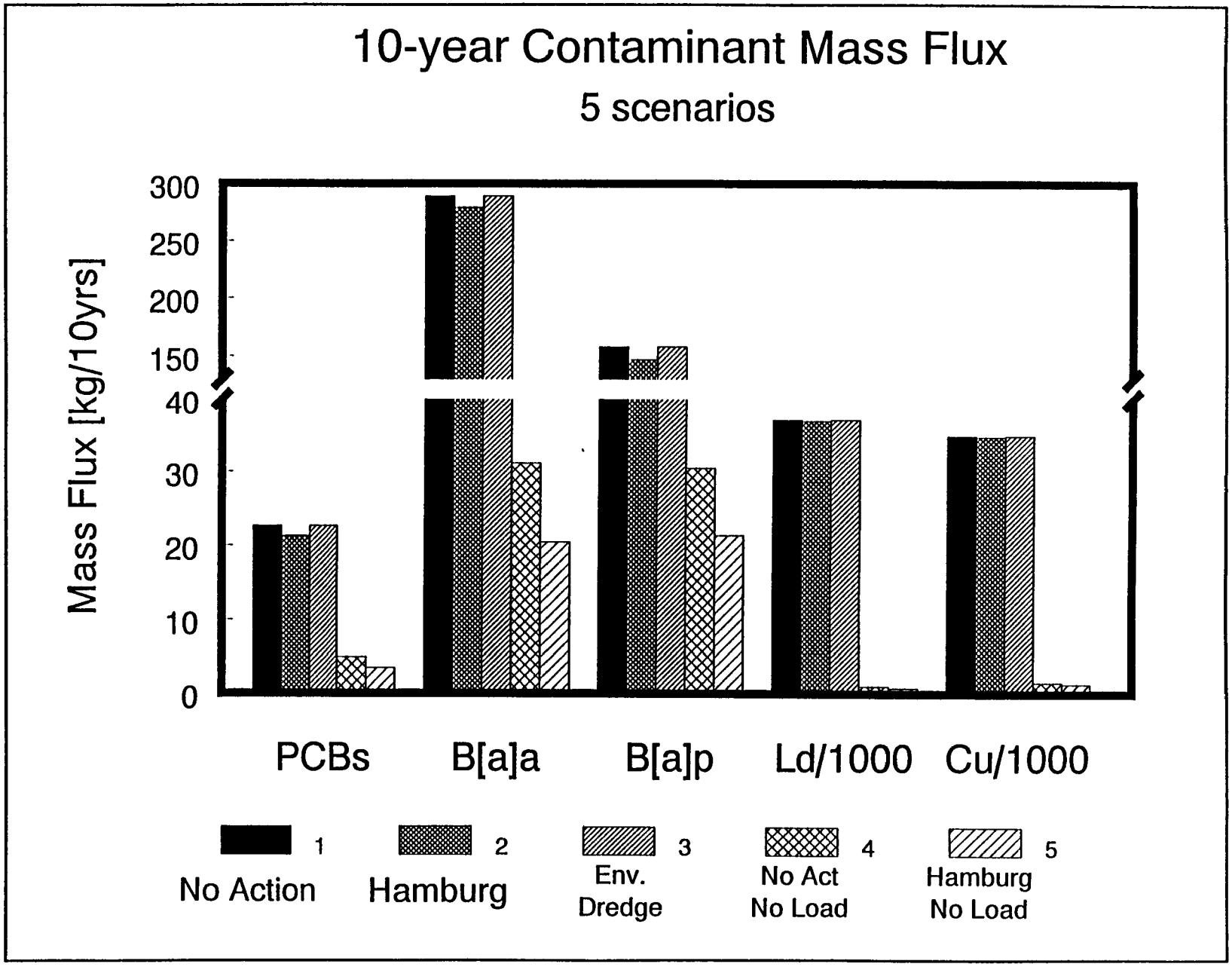


Figure 5-29. 10-year contaminant mass flux for 5 scenarios

# SECTION 6

# BIOACCUMULATION MODELING

## 6.1 INTRODUCTION

The main objective of this section was to further evaluate the remediation scenarios by analyzing their impact on PCB accumulation by carp in the Buffalo River. The same five remediation scenarios are evaluated here with respect to their impact on PCB bioaccumulation in carp of the Buffalo River: (1) no action scenario, (2) Hamburg Cove scenario, (3) environmental dredging scenario, (4) no action/no load scenario, and (5) Hamburg Cove/no load scenario (see Section 3.2 for a more complete description of these scenarios). In addition to assessing the impacts of various sediment remediations on benthic food chain bioaccumulation, these data are being used in the comparative human health risk assessment for this site.

## 6.2 MODEL DESCRIPTION

Bioaccumulation of a contaminant by an aquatic organism is, in general, the cumulative effect of bioconcentration (direct uptake from the water) and food chain transfer (uptake from food consumption). Therefore, the calculation of a chemical's concentration in an organism at a given trohpic level requires specification of the exposure concentration of that chemical in the water column, sediments, and organisms on which the target organism feeds. The modified WASP4/TOXI4 model, the application of which is presented in the previous sections, provides the water column and sediment exposure regime for the bioaccumulation calculation. The model framework used for the calculation of PCB bioaccumulation in carp in the Buffalo River is adapted from the model (FDCHN4) of Connolly, *et al.* (1992) on Green Bay. Since carp is the target species, the food chain definition for this application includes only two levels: benthic organsims, which reside and feed in the bottom sediments; and carp, which feed on benthic organisms. Presented below in this subsection is a description of this modeling framework.

Chemical uptake and bioaccumulation in benthic invertebrates can be viewed as the result of an equilibrium partitioning of the chemical between the lipids of the organism, the organic

carbon fraction of the sediment, and the interstitial water (Gobas, 1992; Bierman, 1994).

Uptake of chemicals in fish is achieved mainly through transport across the gills and through the consumption of food, i.e. transport across the gastrointestinal tract (Gobas, 1992). More specifically, accumulation of a contaminant by an aquatic animal includes the following processes (Connolly et al., 1992):

- uptake and loss across the gill membrane
- uptake and loss across the gut wall
- hepatic and/or renal excretion
- non-hepatic metabolism, and
- growth dilution.

These processes are taken into account by developing a chemical mass balance on a given "average" organism. Equation 6-1 is applied to all organisms in the food chain:

$$\frac{dv}{dt} = K_u c_d + \alpha C v_p - (K + G) v \qquad (6\text{-}1)$$

where

v = concentration of contaminant in animal [ug/g wet]
$v_p$ = concentration of contaminant in prey [ug/g wet]
$K_u$ = uptake rate from water [L/g/d]
$c_d$ = concentration of contaminant in water [ug/L]
$\alpha$ = assimilation efficiency of contaminant in food
C = consumption rate of food [g/g/d]
K = excretion rate [1/d]
G = net growth rate of the animal [g/g/d].

Direct uptake of contaminant by the animal from water is represented by the first term in equation 6-1. The second term represents the flux of contaminant into the animal through feeding. The third term is the loss of contaminant due to excretion and desorption plus the change in concentration due to growth. Water column dissolved contaminant and sediment dissolved and particulate contaminant concentrations are the driving forces behind the calculation of equation 6-1.

Figure 6-1 shows a three compartment animal consisting of a lipid compartment and a no-lipid or aqueous compartment interacting with a gut compartment. Contaminants are assumed to

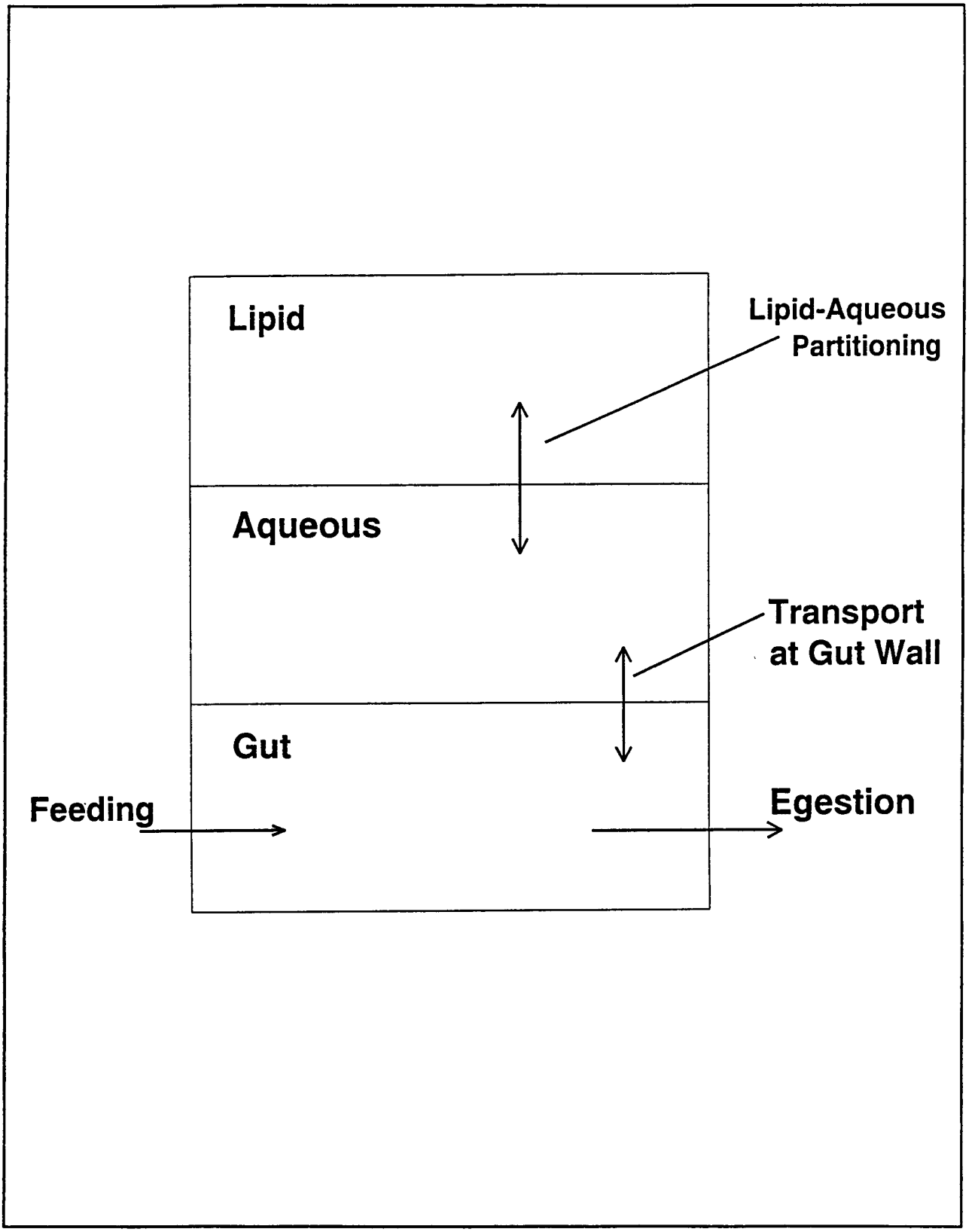


Figure 6-1. Schematic of a Three Compartment Aquatic Animal (Connolly et al., 1992)

transfer between the lipid and aqueous compartments, the aqueous and gut compartments, and the aqueous compartment and the water column through diffusion. Contaminants are taken up into the body and enter the gut through feeding and leave the gut through egestion.

## Contaminant Uptake Rate

Referring back to equation 6-1, the rate constant, $K_u$, parameterizes the transport of chemical across the gill to the blood. It can be calculated from the respiration rate of the animal if the mass transfer coefficient for the contaminant and oxygen ratio is known. The equation for $K_u$ is:

$$K_u = \frac{k_{gl}\, r}{k_{gl\,o_2}\, c_{o_2}} \tag{6-2}$$

where

$k_{gl}$ - mass transfer coefficient
$k_{glO2}$ - mass transfer rate constant at the gill
r - respiration rate in units of $gO_2/g(w)$-d
$c_{O2}$ - oxygen concentration of water.

Expressions relating these coefficients have been developed in other studies with the conclusion being that various resistances, which limit gill transfer, describe the contaminant oxygen efficiency ratio. These resistances are: 1) gill ventilation; 2) diffusion through aqueous boundary layers; 3) diffusion through the epithelial cells of the gill membrane; and 4) blood perfusion. The respiration rate, r, in equation 6-2 can be calculated using Thurston and Goerke's allometric equation:

$$r = 1.32\, w^{-0.195T}\, 0.29_e\, ^{0.035T} \tag{6-3}$$

where r is the respiration rate in units of mg $O_2$ g $wet^{-1}d^{-1}$ and w and T are the wet weight in grams and temperature in degrees C, respectively.

## Excretion Rate

Elimination of contaminant from the body is both a combination of the growth rate and the

excretion rate. The excretion rate is defined as the sum of two processes: (1) the loss rate from the gill and (2) the fraction of contaminant loss rate from the whole body to the gut that contributes to excretion (Connolly, 1992). Earlier it was stated that uptake of chemicals occurs mainly at the gills. The gills are also the major site for depuration of most organic chemicals (Gobas, 1992). Therefore, the excretion rate , or whole body loss rate, K, can be described by the gill elimination rate, $K_1$, given by equation 6-4:

$$K_1 = \frac{K_w \rho_a}{x_a + \pi_L x_L} \qquad (6\text{-}4)$$

where

$\rho_a$ = aqueous density (g/ml)
$x_a$ = weight fraction of whole body that is aqueous
$\prod_L$ = partition coefficient between aqueous and lipid phases
$x_L$ = weight fraction of whole body that is lipid.

Note that $x_a + x_L = 1$.

For higher chlorinated PCBs, the excretion rate decreases and growth becomes the more dominant factor for concentration reduction in the species (Connolly, 1991).

## Assimilation Efficiency

The ratio of the transfer rate from the gut to the animal to the total transfer rate out of the gut is called the assimilation efficiency, $\alpha$. It is dependent upon the gut mass transfer coefficient, the surface area of the gut, the aqueous fraction of contaminant in the gut and the egestion rate. Equation 6-5 is used to calculate $\alpha$:

$$\alpha = \frac{K_g f_{ga} \rho_{ga}}{K_g f_{ga} \rho_{ga} + E'} \qquad (6\text{-}5)$$

where

$K_g$ = mass transfer rate across the gut (cm/d)
$f_{ga}$ = inverse of summation of gut contents that are lipid and non-lipid
$\rho_{ga}$ = gut aqueous density (g/ml)
E' = egestion rate (g gut contents/day/weight).

Recent research shows that the assimilation efficiency of hydrophobic contaminants is closely related to dietary assimilation of lipids (VanVeld, 1990). This indicates that contaminant uptake is most likely influenced by factors influencing lipid digestion/absorption.

Other factors influencing the assimilation efficiency may be diet quality and temperature. Diet quality may indirectly influence this parameter by inducing enzymes which augment metabolic transformations of contaminants, underestimating the true assimilation efficiency. Temperature affects membrane diffusion coefficients.

## Consumption Rate

The consumption rate of food, C, is calculated from the rate of energy usage by the animal. The rates of production and metabolism of body tissue by the animal determine the energy rate, which are calculated from the growth rate, G, and the respiration rate, R, respectively. The energy usage rate, P, is:

$$P = \lambda (R + G) \tag{6-6}$$

where $\lambda$ is the caloric density of the animal's tissue in units of cal/g(w). The rate of energy intake by the animal is found by dividing P by the assimilation efficiency of food, a. Dividing this quantity by the caloric density of prey, $\lambda_p$, yields the consumption rate of food:

$$C = \frac{\lambda}{\lambda_p} \frac{(R + G)}{a} \tag{6-7}$$

For those animals feeding on sediment, the equation is the same except that the caloric density is ignored and the food assimilation efficiency, a, is taken as the fraction of ingested carbon that is assimilated. P would be expressed as gC/g(w)/d.

## Respiration and Growth Rates

The respiration rate, R, is described by a weight and temperature dependent equation of the form:

$$R = \beta W^{\gamma} e^{\rho T} \tag{6-8}$$

where

R = respiration rate [g wet/g wet/d]
T = temperature in degrees C
$\beta$, $\gamma$, and $\rho$ = respiration relationships.

The net growth rate , G, of the animal is determined from weight-age relationships determined from field data. From these data, the growth rate is calculated by the following first-order exponential model:

$$W = W_o e^{G*age} \quad (6\text{-}9)$$

where W is weight(g), $W_o$ is the initial weight and G is the growth rate($age^{-1}$). The higher the growth rate, the "greater the effect of dilution" of chemical in the carp. As carp age, they tend to have a lower growth rate than other fish species which could be a partial explanation for their high PCB body burdens.

## 6.3 INPUT DATA

Configuration of the Connolly FDCHN4 model to the Buffalo River carp bioaccumulation problem required specification of input data for the following categories:

- Number of Species
- Compound Related Parameters
- Steady-State Species Parameters
- Age Dependent Species Parameters
- Migrating Species Parameters
- Setup of Spatial Compartments
- Integration Information
- Exposure Concentrations

Following is the description of the development of each of these input data along with the source of the information.

### Number of Species

The model consists of carp as the age dependent species for which concentrations are calculated and benthics as the species for which steady-state concentrations are calculated. Eleven age classes of carp are modeled using available data on PCB concentrations in carp in the Buffalo River (Sikka et al., 1992). From these data (refer to Table 6-1), the eleven age classes

are broken up into a young age class (age classes 1-4), a middle age class (age classes 5-9), and an old age class (age classes 10 and 11). Figure 6-2 shows the food chain used for the model.

Phytoplankton are not included in the food chain because their contribution to the accumulation of chemicals in the benthic food chain of the Buffalo River is assumed to be relatively insignificant for this project. This project focuses attention on PCB accumulation in carp due to sediment contamination. Since carp are primarily a benthic-feeding fish, accumulation of PCBs is the direct result of this feeding.

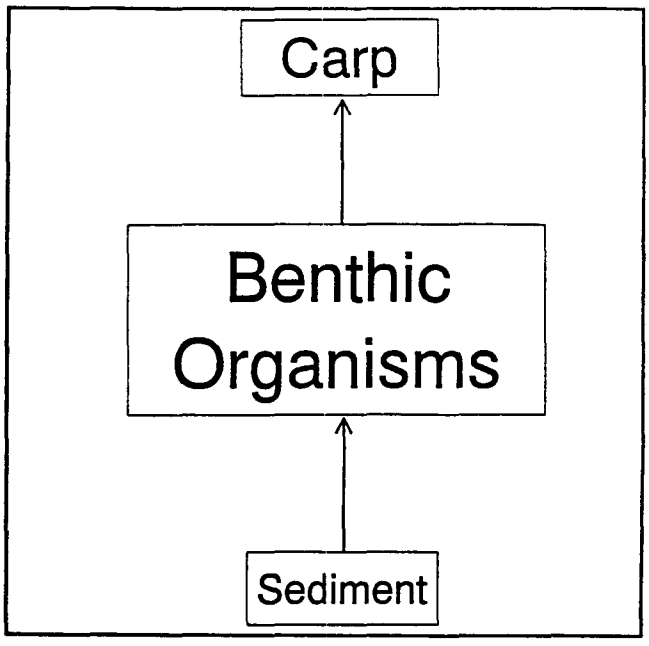


**Figure 6-2.** Food Chain Diagram for Buffalo River carp PCB bioaccumulation model.

**Compound Related Parameters**

In this section of the input data, a phytoplankton partition coefficient (bioconcentration factor) and a log $K_{ow}$ value are specified. These values are 55.4 L/g wet weight and 6.4, respectively. The phytoplankton partition coefficient was obtained from the Green Bay Model (Connolly et al., 1992) and the log $K_{ow}$ value was obtained from Buffalo River data. The partition coefficient would be used to calculate the contaminant concentrations in phytoplankton from the water column dissolved concentrations if phytoplankton were included in the food chain.

**Steady-State Species Parameters**

The steady-state species in the model are the benthic organisms. Justification for using a S-S approach for modeling these species comes from their rapid uptake and excretion rates, and their lack of any major change in diet throughout their lifespan. These factors combined allow the organisms to reach equilibrium with the contaminant very quickly (Thomann and Connolly, 1984). No particular benthic organism is modeled here, such as the previously mentioned chironomids, because it is believed that species within the same trophic level exhibit very similar bioenergetics, such as growth and metabolic rates, and accumulate toxics equally (Thomann and Connolly,

**Table 6-2.** Age Class Data on Carp in the Buffalo River (Each age class has three groups associated with it, each group containing 5 fish. Values shown are average values for the 5 fish. Sikka et al., 1992)

| | Age, Years | Wet Weight (kg) | PCB Concentration (ug/g wet wgt) |
|---|---|---|---|
| YOUNG AGE CLASS | | | |
| BRF Y W-1 | 4.2 | 0.944 | 1.89 |
| BRF Y W-2 | 4.0 | 0.972 | 1.8 |
| BRF Y W-3 | 4.6 | 0.927 | 2.2 |
| AVERAGE | 4.3 | 0.948 | 1.96 |
| MIDDLE AGE CLASS | | | |
| BRF M W-1 | 6.4 | 1.633 | 2.76 |
| BRF M W-2 | 6.0 | 1.667 | 2.34 |
| BRF M W-3 | 5.4 | 1.61 | 3.7 |
| AVERAGE | 5.9 | 1.637 | 2.93 |
| OLD AGE CLASS | | | |
| BRF O W-1 | 10.0 | 4.552 | 5.9 |
| BRF O W-2 | 10.8 | 4.257 | 3.1 |
| BRF O W-3 | 10.0 | 4.45 | 3.4 |
| AVERAGE | 10.3 | 4.42 | 4.13 |

1984).

The bioenergetic parameters for the benthic organisms include: the respiration rate, growth rate, food assimilation efficiency, fraction dry weight, coefficient for temperature dependence of species respiration, and fraction dry weight that is lipid (see Table 6-2). A bioconcentration factor is also entered here from which the excretion rate is calculated. Lack of available data on benthic organisms in the Buffalo River lead to the use of the same values for these parameters used in Green Bay (Connolly et al., 1992).

**Table 6-2.** Species Bioenergetic Parameters used for Buffalo River FDCHN4 model.

| Benthic Organism Parameters | Value |
|---|---|
| Respiration Rate (g/g/day) | 0.02 |
| Growth Rate (1/d) | 0.01 |
| Food Assimilation Efficiency | 0.30 |
| Fraction Dry Weight | 0.15 |
| Coefficient for Temperature Dependence on Benthic Respiration | 0.00 |
| Fraction of Wet Weight Lipid | 0.02 |
| Ratio of Gill Permeability to Permeability of Oxygen | 1.00 |
| Toxicant Assimilation Efficiency | 0.30 |
| Bioconcentration Factor (L/g wet) | 50.2 |
| Carp Bioenergetic Parameters | |
| Respiration Coefficients: | |
| Beta | 0.0034 |
| Gamma | 0.237 |
| Rho | 0.069 |
| Food Assimilation Efficiency | 0.8 |
| Fraction Dry Weight | 0.25 |
| Ratio of Gill Permeability to Permeability of Oxygen | 0.6 |
| Toxicant Assimilation Efficiency | 0.4 |

Other parameters entered in this section were the ratio of gill permeability of the chemical to the permeability of oxygen, and the toxicant assimilation efficiency of the species. The values used here were also the same as those derived for benthic organisms in Green Bay (Connolly et al., 1992).

**Age Dependent Species Parameters**

For the age dependent carp, parameterization was more involved than for the benthic organisms. It is specified here that the species is pelagic and that a bioconcentration factor will be entered. Also, the number of age classes of carp and the length of time of each age class is specified.

Bioenergetic parameters included the following respiration coefficients: a respiration coefficient for carp, $\beta$, a respiration weight exponent $\gamma$, and an exponential coefficient for temperature dependence of carp respiration, $\rho$. Refer to equation 6-8. Values for these

parameters are shown in Table 6-2.

Also in Table 6-2 are the food assimilation efficiency, the fraction dry weight of the carp, the ratio of gill permeability of chemical to permeability of oxygen, and the toxicant assimilation efficiency. These parameters were found from derived values from carp in Green Bay (Connolly, *et al.* 1992).

The model asks for the weight and the fraction of the wet weight that is lipid for each age class. PCBs are a highly lipophilic compound, so lipid content is an important factor in accumulation of this compound. Triglycerides act as the primary storage lipid in fish (Connolly et al., 1992). The carp weight information for various age classes was collected from the **Handbook of Freshwater Fishery Biology** (Carlander, 1970). The lipid data was derived from available Buffalo River data (Sikka et al., 1992). Plotting the lipid content vs. weight, a regression analysis was performed using a power function and a best fit curve was drawn from the existing data (Figure 6-3). This curve was used to find the lipid content for the different age classes used in the model. Equation 6-10 shows the power function used in the regression analysis:

$$y = a b^{x} \tag{6-10}$$

where:

a, b - regression constants

x - weight (kg)

y - lipid content.

The correlation coefficient for this regression was 0.96. Values found for each age class can be found in Table 6-3.

**Migratory Species Parameters**

In our model, we assumed that the carp do not migrate meaning that they are in the river throughout the year (USFWS), so this data group was not necessary. It was also assumed that they are a spawning fish as opposed to being stocked.

**Setup of Spatial Compartments**

The Buffalo River was separated into 2 spatial compartments. The first compartment is

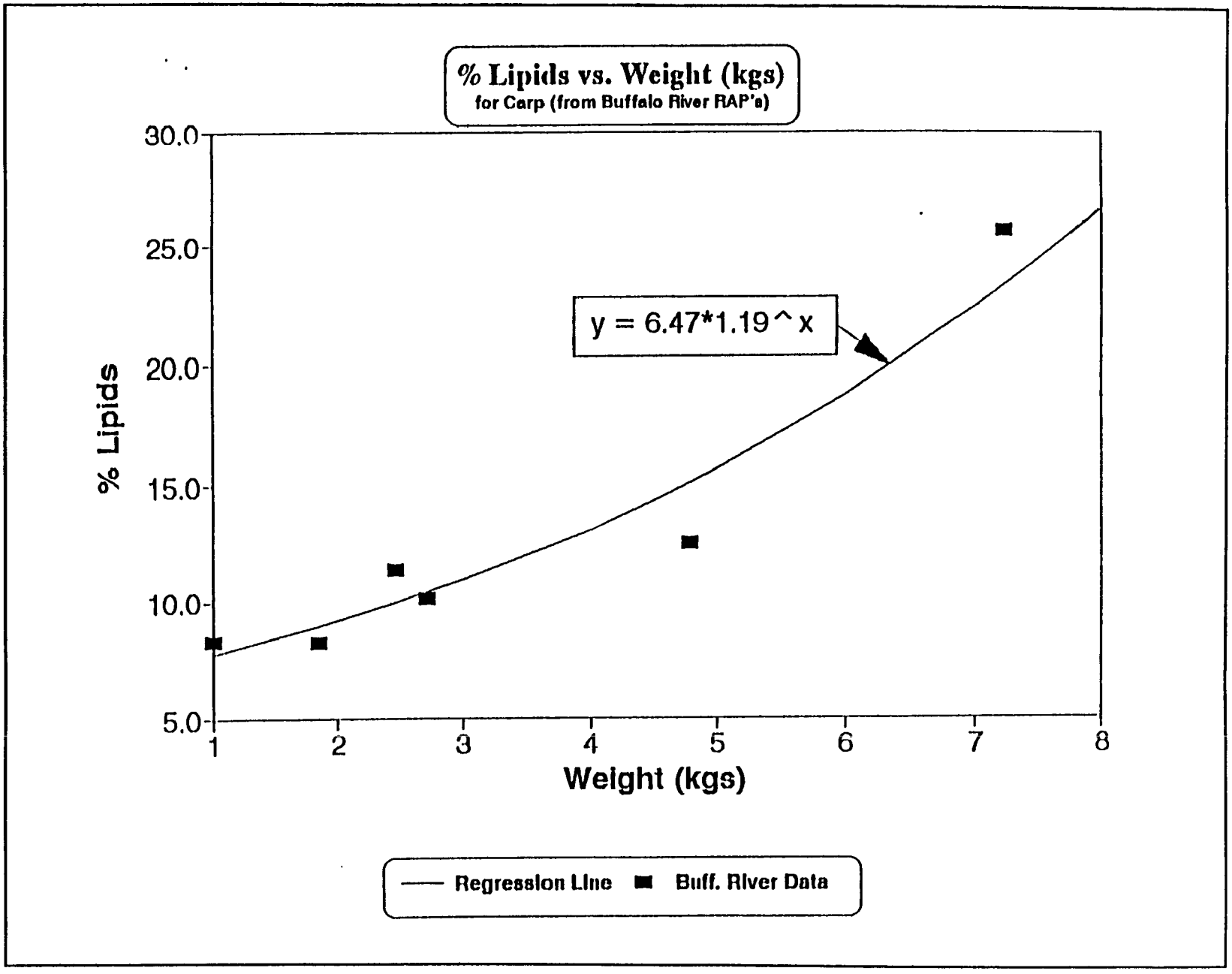


Figure 6-3. Best-fit regression line for carp lipid data.

**Table 6-3.** Ranges for weight and lipid content for each age class used in the model. Values are from regression analysis.

| Age Class | Weight Range (kg) | % Lipid Range (Best Fit) |
|---|---|---|
| 1 | 0.032 - 0.077 | 6.51 - 6.56 |
| 2 | 0.077 - 0.340 | 6.56 - 6.87 |
| 3 | 0.340 - 0.703 | 6.87 - 7.33 |
| 4 | 0.703 - 1.116 | 7.33 - 7.88 |
| 5 | 1.116 - 1.561 | 7.88 - 8.53 |
| 6 | 1.561 - 1.928 | 8.53 - 9.10 |
| 7 | 1.928 - 2.917 | 9.10 - 10.84 |
| 8 | 2.917 - 3.810 | 10.84 - 12.69 |
| 9 | 3.810 - 4.672 | 12.69 - 14.78 |
| 10 | 4.672 - 4.990 | 14.78 - 15.63 |
| 11 | 4.990 - 5.670 | 15.63 - 17.63 |

upstream of Hamburg Cove (see Figure 1-1) and the second is downstream of this area. Each compartment has a water column and sediment layer associated with it.

An annual temperature profile was developed for each compartment. Average monthly values from 1991 Buffalo River temperature data were used in the development of this profile (Anderson and Singer, 1992). It was assumed that the temperature profile for both upstream and downstream compartments was the same.

The species in each compartment consisted of carp and benthic organisms. The initial concentration of PCBs in carp in the Buffalo River varied depending on the age class (Sikka et al., 1992). Concentrations of 2, 3, and 4 ug/g wet were used for the young (0-4 yrs), middle (5-9 yrs), and old(10-11 yrs) age classes, respectively (see Table 6-1). Initial PCB concentrations in the benthic organisms was assumed to be the same as in the sediments (Gobas, 1992).

For each age class, it was necessary to define the prey for the species. The benthic organisms were assumed to be feeding on organic carbon in the sediment. Organic carbon is also where the hydrophobic PCBs adhere to. The sediment particulate contaminant concentrations define the base of the benthic food chain (Connolly et al., 1992).

**Integration Information**

This data input section included information telling the model how long to run, what

timestep to use, what time period to print concentrations for, and when to start printing. The model was run for 10 years using the results from the physical-chemical mass balance model mentioned earlier. PCB body burdens on carp were printed out semi-annually. A timestep of 10 days was used. Decreasing the timestep further resulted in longer run times with little change in results.

**Exposure Concentrations**

For each compartment in the model, it was necessary to input dissolved chemical (ug/L) and adsorbed chemical (ug/g carbon) concentrations of PCBs for both water column and sediment. The physical-chemical mass balance model output results in previously defined segments of the river. Representative segments were chosen for this model (see Figures 2-2 and 2-3). For the upstream compartment, segment 9 was chosen as the representative water column compartment with segments 48 and 49 being the upper sediment layer depositional(nearshore) and erosional(mid-channel) zones respectively. For the downstream compartment, segment 25 was chosen for the water column compartment having segments 80 and 81 as the upper sediment depositional and erosional layers, respectively.

From a project sponsored by the USFWS (United States Fish and Wildlife Service) entitled, **Buffalo River Fisheries Assessment** (Kozuchowski et al., 1993), it was observed that carp spend nearly half of their time nearshore and the other half mid-channel. Based on this information, the sediment depositional and erosional PCB concentrations were averaged and used as input for the model.

## 6.4 MODEL APPLICATION

This section presents the bioaccumulation modeling results for the five scenarios used for the Buffalo River remediation analysis: (1) no action scenario, (2) Hamburg Cove scenario, (3) environmental dredging scenario, (4) no action/no load scenario, and (5) Hamburg Cove/no load scenario. Although the model computes PCB concentrations in phytoplankton, benthos, and each age class of carp in both the upstream and downstream reaches of the river, we will focus on the age-class average concentration in carp assuming exposure to upstream and downstream water and sediment concentrations.

## Model Calibration

Sensitivty analysis (presented later in this section) has shown that the simulation of PCB concentrations in carp is quite sensitive to carp food assimilation efficiency and chemical assimilation efficiency. Therefore, the model calibration focused on adjustment of these two parameters until the model simulated the measured PCB levels in carp using the existing water column and sediment exposure concentrations. All other models parameters were taken from the FDCHN4 applications to Green Bay and the Detroit River (Connolly, *et al.* 1992; Parkerton and Connolly, 1992). We arrived at a value of 0.8 for the food assimilation efficiency and 0.4 for the chemical assimilation efficiency. The food assimilation efficiency of 0.8 was suggested by Ursin (1979) and used by Parkerton and Connolly (1992) in their Detroit River benthic food chain model. A chemical assimilation efficiency of 0.4 is not unusual for hydrophobic chemicals like PCB (Connolly, 1991; Thomann and Connolly, 1984).

## Comparison of Remediation Scenarios

Results for each of the five basic remediation scenarios are shown in Figures 6-4 and 6-5 for upstream and downstream compartments, respectively. Values shown are average values for PCB concentrations in carp from the 11 age classes used in the model calculated at 6 month intervals during a 10-year run of the model. The input for these runs was the output for the ten-year remediation scenarios run with the modified TOXI4 mass balance model presented in Section 5. Therefore, the differences in PCB concentrations in carp seen in these runs are the result of the differences in PCB water column and sediment concentrations that resulted from the five scenarios we evaluated. For purposes of discussion, we present in Table 6-4 the sediment concentrations predicted for upstream and downstream in the river during the ten-year simulations for each of the five scenarios.

**No Action Scenario.** This scenario represented the Buffalo River as it is with current navigational dredging taking place and no additional remediation action taken. As expected this scenario led to the highest PCB concentration in the carp. Note in Table 6-4 that the sediment concentration in the downstream compartment is much higher than in the upstream compartment

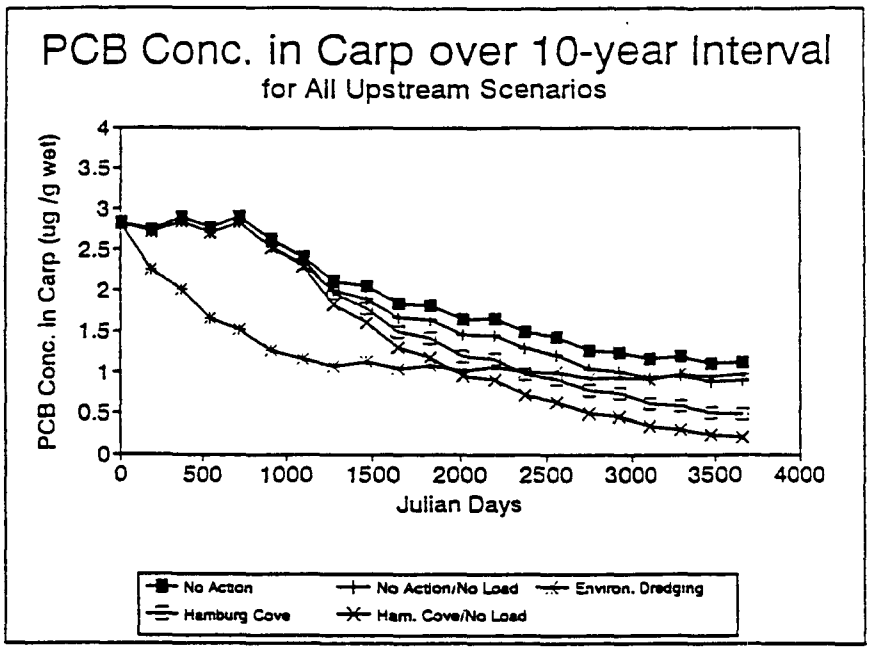


**Figure 5-1.** Average PCB Concentration in Carp for the Upstream Compartment

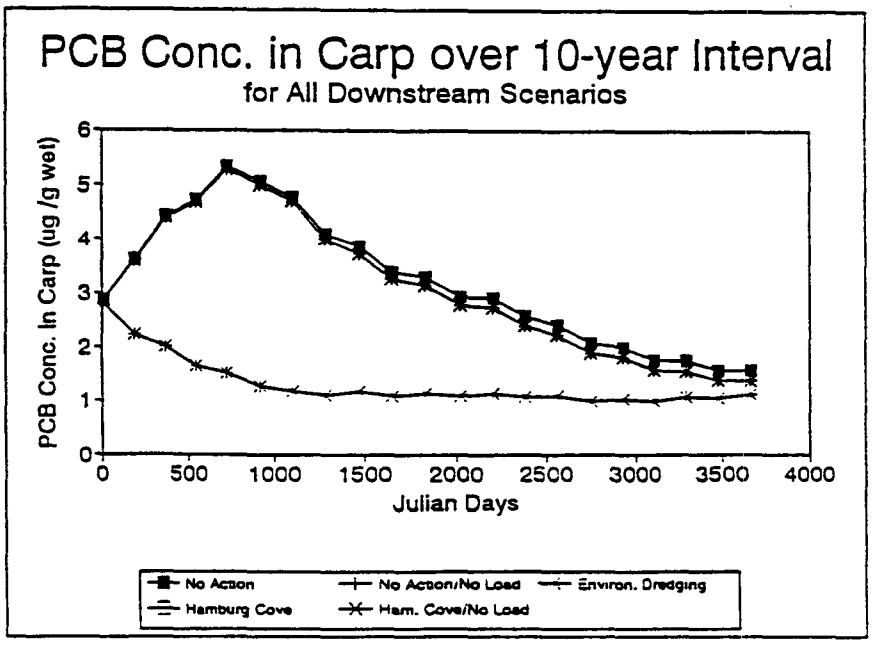


**Figure 5-2.** Average PCB Concentration in Carp for the Downstream Compartment

**Figures 6-4 and 6-5.** Average PCB concentrations in carp for upstream and downstream reaches for five sediment remediation scenarios.

**Table 6-4.** Bottom Sediment Particulate Concentrations (ug/g carbon) derived from mass balance model.

| | Day | No Action | No Action/ No Load | Environ-mental Dredging | Hamburg Cove | Hamburg Cove/ No Load |
|---|---|---|---|---|---|---|
| Upstream | 790 | 15.2 | 14.7 | 3.52 | 15.2 | 14.7 |
| | 800 | 14.1 | 13.4 | 3.67 | 13.95 | 13.2 |
| | 905 | 10.0 | 9.30 | 2.98 | 9.77 | 8.91 |
| | 910 | 8.61 | 7.80 | 2.67 | 8.38 | 7.47 |
| | 1065 | 6.63 | 5.91 | 2.11 | 6.46 | 5.66 |
| | 1085 | 6.12 | 5.33 | 2.03 | 5.96 | 5.12 |
| | 2330 | 7.10 | 5.96 | 5.41 | 3.72 | 2.24 |
| | 2356 | 7.30 | 6.10 | 6.25 | 3.05 | 1.4 |
| | 2920 | 4.83 | 3.57 | 4.22 | 2.37 | 0.883 |
| | 2925 | 3.34 | 2.16 | 2.98 | 1.88 | 0.562 |
| | 3441 | 5.72 | 4.59 | 5.43 | 1.80 | 0.461 |
| | 3647 | 5.03 | 3.96 | 4.90 | 1.53 | 0.303 |
| | 3660 | 4.86 | 3.83 | 4.74 | 1.49 | 0.310 |
| Average | Day | 7.61 | 6.66 | 3.92 | 5.81 | 4.71 |
| Std. Deviation | | 3.59 | 3.77 | 1.36 | 4.74 | 5.02 |
| Downstream | 790 | 36.0 | 35.5 | 3.55 | 36.0 | 35.5 |
| | 800 | 32.5 | 31.9 | 3.71 | 32.5 | 31.9 |
| | 905 | 23.8 | 23.1 | 3.24 | 23.8 | 23.1 |
| | 910 | 20.7 | 19.9 | 2.97 | 20.7 | 19.9 |
| | 1065 | 17.0 | 16.3 | 2.66 | 17.0 | 16.3 |
| | 1085 | 15.7 | 14.9 | 2.83 | 15.6 | 14.9 |
| | 2330 | 11.4 | 10.5 | 5.92 | 11.4 | 10.5 |
| | 2356 | 10.1 | 9.05 | 6.74 | 10.1 | 9.03 |
| | 2920 | 6.96 | 5.83 | 4.87 | 6.92 | 5.79 |
| | 2925 | 4.87 | 3.76 | 3.57 | 4.83 | 3.73 |
| | 3441 | 6.99 | 5.96 | 5.97 | 6.96 | 5.93 |
| | 3647 | 6.80 | 5.82 | 6.33 | 6.70 | 5.70 |
| | 3660 | 6.95 | 6.01 | 6.50 | 6.83 | 5.88 |
| Average | | 15.4 | 14.5 | 4.53 | 15.3 | 14.5 |
| Std. Deviation | | 10.3 | 10.4 | 1.56 | 10.3 | 10.5 |

for four of the five scenarios, especially the initial sediment concentration at the beginning of the 10-year run. This explains the initial increase in PCB concentration in carp in the downstream

reach for the first two years of the run. The PCB concentration in carp was approaching equilibrium with the high initial PCB concentration in the sediment.

**Hamburg Cove Scenario.** Navigational dredging was discontinued upstream of Hamburg Cove in this scenario. Discontinuing dredging allowed "cleaner" sediments to accumulate in the upstream reach over time instead of being removed by periodic dredging. Noticeable results started to occur after approximately three and a half years when it was observed that the PCB concentration in carp were lower in this scenario than in the no action scenario for the upstream compartment. The cleaner sediment decreased benthic exposure which in turn meant lower exposure in carp.

In the downstream compartment, both the no action and Hamburg Cove scenarios had virtually the same result. This is because the sediment concentrations used from the physical-chemical mass balance model were nearly the same for these two scenarios. The conclusion drawn here is that ceasing upstream dredging had virtually no effect on downstream surface sediment PCB levels.

**No Action/No Load Scenario.** This scenario is the no action scenario but without any external contaminant loading to the system, including upstream inputs of PCBs. As expected, this scenario led to PCB concentrations in carp relative to the no action scenario. This result was noticeable after a half year in both compartments. Although the average PCB concentration in carp for the 10-year run did decreas, the reductions were not very significant. One may conclude from this result that eliminating upstream contaminant loads has much more impact on water column exposure than on sediment exposure, especially under continued navigational dredging which periodically removes the recently deposited cleaner sediments.

**Hamburg Cove/No Load Scenario.** In addition to discontinuing navigational dredging upstream, it was also assumed in this scenario that there was no external or upstream loading of PCBs. As expected, the concentrations in carp in the upstream compartment were decreased further due to the decreased concentration of PCBs in the sediment and the cleaner sediment being deposited over time. The 10-year average PCB concentration was 26% lower than in the no action scenario.

In the downstream compartment, again there was virtually no difference between the no action scenario without loading and this scenario because the sediment concentrations from the physical-chemical mass balance model were virtually the same.

**Environmental Dredging.** For the environmental dredging scenario, initial conditions in the depositional sediment segments were set equal to zero in an attempt to represent nearshore dredging. Full navigational dredging was maintained in the channel (erosional sediments). As previously mentioned, depositional and erosional sediment concentrations were averaged for both the upstream and downstream compartments. With the depositional sediment concentrations being set equal to zero, this averaging reduced sediment PCB exposure significantly in this scenario.

In both upstream and downstream compartments, there was an immediate response to the reduced exposure, as the PCB concentration in carp rapidly decreased for the first three and a half years of the 10-year run before leveling off at approximately 1.0 ug/g (wet wgt). This scenario led to the lowest 10-year average PCB concentration in carp for any of the five scenarios. There is a 34% reduction in the 10-year average PCB concentration in the upstream reach and approximately a 58% reduction in the downstream reach. The biggest improvement was in the downstream because the "hot spots" were removed in nearshore sediments in this compartment.

## Sensitivity Analysis

In addition to evaluating the sensitivity of PCB bioaccumulation in carp to food assimilation efficiency and chemical assimilation efficiency, we also evaluated the model sensitivity to:

1. depositional versus erosional sediment feeding;
2. selectivity of feeding on benthos versus sedimenting detritus;
3. octanol-water partition coefficient, $K_{ow}$, for PCB.

All three of these model configuration parameters produced significant variation in model output when adjusted relative to the calibration conditions. Of the three factors above, the model output was most sensitive to where the carp were feeding and to the partitioning of the PCBs to the sediments in that area. We have a reasonable certainty regarding the $K_{ow}$ for the contaminants of

interest, but there is a great deal of uncertainty regarding the time spent by carp feeding in the nearshore depositional areas (where the hotspots are located) versus in the deeper erosional sediments of the channel.

# SECTION 7

# CONCLUSIONS

1. Prior to this investigation, it was hypothesized that resuspension from contaminated sediments was the primary source of water column contamination. This notion was found to be incorrect when the results of the contaminant model simulations were analyzed. The geometry and hydraulics of the lower Buffalo River are such that sediment resuspension only contributes a significant amount of contaminants to the water column during major high flow events. On days of average or low flow, resuspension of contaminated sediments is not a significant factor in water column concentrations.

2. Since contaminated sediments were not found to be the primary source of water column contamination, another source(s) must be responsible. This source was determined to be loading from upstream of the modeled section of the river. Current upstream loading of contaminants overwhelms sediment contributions to water column exposure and contaminant export to Lake Erie. CSO, industrial, and groundwater pollutant loadings within the modeled section are also relatively insignificant compared to upstream loadings.

3. Based on the management scenarios selected for this study, sediment remediation will not have a significant impact on reducing water column contaminant exposure. Environmental or full dredging of bottom sediments will not alleviate water column concerns for the five chemicals included in this report. Also, the potential to exacerbate the water column problem still exists with these dredging options by exposing higher contaminated sediments in deeper layers.

4. Sediment remediation will be a potentially important action for reducing direct sediment exposure, especially in "hot spots". Environmental dredging of nearshore "hot spots" could be beneficial to the benthic community and corresponding food web.

5. The contaminant body burdens of bottom-dwelling and bottom-feeding organisms, such as carp, will improve in response to sediment remediation actions. On a river-wide basis environmental dredging in the nearshore depositional areas lead to the most significant improvement in carp PCB body burdens. However, the cessation of navigational dredging above

Hamburg Cove proved to be the best alternative for that portion of the modeled river.

# SECTION 8

# RECOMMENDATIONS

The following recommendations are offered to improve model performance, data collection and model development efforts in the future:

1. The contaminant model for this system was very sensitive to upstream loadings. Loading estimates for model input were based on numerical regressions of available data (especially TSS data). Year-round TSS data were not available. Of more importance was the lack of data during high-flow events, which could easily influence the regressions and reduce the need for extrapolation. To improve contaminant model results, it is essential to gather more data, especially during high flow events, to adequately define upstream loadings.
2. Uniform sample collection and analytical protocols should be applied by all groups involved with data collection. Handling of the Below Detection Limit (BDL) data should be discussed clearly in the reports provided. Full QA/QC procedures are important to assure the accuracy and precision of the sample data.
3. Surficial sediment data are very important for accurate modeling of resuspension. Finer resolution of vertical profiles in sediment cores would be valuable. Also, a more uniform distribution of the horizontal location of sediment cores would improve quantification of initial conditions for model runs.
4. A more accurate description of erosional/depositional areas of the river would enhance the model simulation. A possibility, which would greatly improve input file creation, is to coordinate efforts with a Geographic-based Information System (GIS). Segment morphometry would be much easier to define and more accurate than current practices.
5. In order to better characterize sediment transport in the Buffalo River, it would be beneficial to measure deposition rates and other physical and chemical properties of resuspended and upstream sediments as a function of flow.
6. Studies regarding the effect of navigational dredging on reinitializing contaminant levels

in surface sediments are recommended. The effect of sediment sloughing following dredging is potentially important for establishing a modeling approach for navigational dredging. Profiles of sediment concentration data before and after dredging would be valuable.

## SECTION 9

## REFERENCES


Ambrose, R. B.; T. A. Wool; J. P. Connolly and R. W. Schanz. (1988) WASP4, a Hydrodynamic and Water Quality Model -- Model Theory, User's Manual, and Programmer's Guide. U. S. Environmental Protection Agency. Athens, GA. EPA / 600 / 3-87 / 039.

Atkinson, J. F.; and S. H. Blair. (1990) Application of Laser Anemometry in Sediment Flows. Great Lakes Program, Occassional paper series, number 90-9. State University of New York at Buffalo, Buffalo, NY.

Atkinson, J. F.; T. Bajak; M. M. Morgante; S. Marshall and J. V. DePinto. (1993) Model Data Requirements and Mass Loading Estimates for the Buffalo River Mass Balance Study (ARCS/RAM Program). Great Lakes Program. State University of New York at Buffalo. Buffalo, NY.

Bierman, V. J.; J. V. DePinto; T. C. Young, P. W. Rodgers, S. C. Martin, and R. K. Raghunathan. (1992) Development and Validation of an Integrated Exposure Model for Toxic Chemicals in Green Bay, Lake Michigan. Report to US EPA Office of Research and Development, ERL-Duluth. Large Lakes Research Station, Grosse Ile, MI. Cooperative Agreement CR-814885.

Carlander, K. D. (1970). Handbook of Fresh Water Fishery Biology, Volume One, The Iowa State University Press, Ames, Iowa.

Chapra, P. D. and K. H. Reckhow. (1983) Engineering Approaches for Lake Management, Volume 2: Mechanistic Modeling. Butterworth Publishers, Boston, MA.

Connolly, J. P.; T. F. Parkerton; J. D. Quadrini; S. T. Taylor and A. J. Thumann. (1992) Development and Application of a Model of PCBs in the Green Bay, Lake Michigan Walleye and Brown Trout and Their Food Webs. Report to US EPA Office of Research and Development, ERL-Duluth. Large Lakes Research Station, Grosse Ile, MI. Cooperative Agreement CR-815396

Endicott, D. D.; W. L. Richardson; T. F. Parkerton and D. M. DiToro. (1991) A Steady State Mass Balance and Bioaccumulation Model for Toxic Chemicals in Lake Ontario. Final Report to the Lake Ontario Fate of Toxics Committee. US EPA ERL-Duluth, LLRS, Grosse Ile, MI.

Endicott, D. D.; M. Velleux and K. Freeman. (1992) Development and Calibration of a Mass Balance Model for Estimating the Export of In-place Pollutants from the Lower Fox River to Green Bay. Report to US EPA Office of Research and Development, ERL-Duluth. Large Lakes Research Station, Grosse Ile, MI.

Fisher, H. B.; E. J. List; R. C. Y. Koh; J. Imberger and N. H. Brooks. (1979) Mixing in Inland and Coastal Waters. Academic Press, New York, NY.

Freeman, K. A.; and D. D. Endicott. (1990) Changes to WASP4, TOXI, W4DIS, and FCHNONLY implemented by LLRS. US EPA Large Lakes Research Station, Grosse Ile, MI.

Freeman, K. A.; F. D. Mitchell; M. Velleux and D. D. Endicott. (1992) Changes to the LLRS implementations of WASP4 and TOXI specific to the Lower Fox River Application. US EPA Large Lakes Research Station, Grosse Ile, MI.

Gailani, J.; C. K. Ziegler and W. Lick. (1991) The Transport of Suspended Solids in the Lower Fox River. *Journal of Great Lakes Research*, 17(4):479-494.

Gobas, F. A. P. C.; J. A. McCorquodale. (1992) Chemical Dynamics in Fresh Water Ecosystems. Lewis Publishers, Chelsea, MI.

Guan, W. (1993) TIN program in ARC/INFO package.

Havlicek, L. L. and R. D. Crain. (1988) Practical Statistics for the Physical Sciences. American Chem. Soc., Washington, DC.

Irvine, K. N.; E. J. Pratt and S. Marshall. (1993) Estimate of Combined Sewer Overflow Discharges to the Buffalo River Area of Concern. Report to the US EPA, Great Lakes National Program Office.

Kozuchowski, E.; A. Poole and C. Lowie. (1993) Buffalo River Fisheries Assessment. Administrative Report 93-03, United States Fish and Wildlife Service (USFWS), Lower Great Lakes Fishery Resources Office, Maherst, NY.

Linsley, R. K. and J. B. Franzini. (1979) Water Resources Engineering. McGraw-Hill Book Co. New York, NY.

Marshall, S. (1993) Contaminant Loading to the Buffalo River from Combined Sewer Overflows. M. Eng. project.

Mills, W. B.; J. D. Dean; D. B. Porcella; S. A. Gherini; R. J. M. Hudson; W. E. Frick; G. L. Rupp and G. L. Bowie. (1982) Water Quality Assessment: a Screening Procedure for Toxic and Conventional Pollutants, Part I. Tetra Tech, Inc. US EPA, Athens, GA. EPA / 600 / 6-82 / 004a.

Newman, M. C. (1993) Regression analyses of log-transformed data: Statistical Bias and its Correction. *Environmental Tech. Chem.* 12, 1129-1133.

NYSDEC. (1989) Buffalo River Remedial Action Plan. Water Division, Buffalo Office.

O' Connor, D. J. and W. E. Dobbins. (1958) Mechanism of Reaeration in Natural Streams. *Transactions of the American Society of Civil Engineers*, 123:655.

O' Connor, D. J. (1988) Modeling of Fate and Effects of Toxic Substances in Surface and Ground Waters. Manhattan College Summer Institute in Water Pollution Control, Manhattan College, Bronx, NY.

Rathbun, R. E. (1990) Prediction of Stream Volatization Coefficients. *Journal of Environmental Engineering*, ASCE, 116(3):615-631.

Smith, J. H.; D. C. Bomberger Jr. and D. L. Haynes. (1981) Volatilization rates of intermediate and low volatility chemicals from water. *Chemosphere*, 19:281-289.

Tateya, S.; S. Tanabe and R. Tatsukawa. (1988) PCBs on the Globe: Possible Trend of Future Levels in the Open Ocean Environment. In Toxic Contamination in Large Lakes, Vol. III. Ed., N. W. Schmidtke. pp. 237-282. Lewis Publishers, Inc., Chelsea, MI.

Thomann, R. V. (1972) Systems Analysis and Water Quality Management. McGraw-Hill Book Co., New York, NY.

Thomann, R. V. and J. A. Mueller. (1987) Principles of Surface Water Quality Modeling and Control. Harper and Row Publishers, Inc. New York, NY.

Velleux, M. (1992) An Application of the Mass Balance Approach for Estimating the Export of In-place Pollutants from Tributary Sources to Receiving Waterbodies. M. S. Thesis. Clarkson University, Potsdam, NY.



☆ U.S. GOVERNMENT PRINTING OFFICE: 1995-647-890